Analysis of ectomycorrhiza induced gene expression of selected poplar genes expressed in poplar fine roots

Dissertation

zur Erlangung des akademischen Grades eines

Doktors der Naturwissenschaften

-Dr. rer. nat.-

im Fachbereich 2 (Biologie/Chemie)

der Universität Bremen

vorgelegt von

Jana Schnakenberg

Bremen, 2020

Erster Gutachter: Prof. Dr. Uwe Nehls

Zweite Gutachterin: Prof. Dr. Rita Groß-Hardt

Datum des Kolloquiums 30.11.2020

Für Papa

Danksagung

An dieser Stelle möchte ich mich bei meinem Betreuer Prof. Dr. Uwe Nehls für die Möglichkeit und die Unterstützung bedanken meine Doktorarbeit in seiner Arbeitsgruppe durchzuführen. Danke für die vielen Diskussionen und den wissenschaftlichen Austausch und dafür, dass es immer möglich war mal gerade schnell etwas zu besprechen.

Vielen Dank auch an Prof. Dr. Rita Groß-Hardt für die Erstellung des Gutachtens und die Zeit die Sie investiert haben.

Meinen herzlichen Dank möchte ich auch Thea aussprechen für deine unkomplizierte Unterstützung bei der Kultivierung der Pilze und Vorbereitung der Mykorrhizierungsexperimente. Danke Annette, dass auch du immer deine tatkräftige Unterstützung angeboten hast. Vielen Dank Lea, dass du mir bei der Kultivierung und Vorbereitung vieler Bakterienproben für die Entwicklung der transienten Expression geholfen hast und dabei immer gute Laune versprüht hast. Jana und Anneke möchte ich für die gute Zusammenarbeit, vor allem in schwierigen Zeiten der Etablierung danken. Unsere großen AG Frühstücke zu besonderen Anlässen werden mir immer in schöner Erinnerung bleiben.

Vielen Dank an Vanessa und Malte für eure Freundschaft und euer Verständnis. Ihr wart immer da, ihr seid die Besten.

Der größte Dank für einfach alles gebührt meiner Familie, ohne euch hätte ich es nicht schaffen können. Ich danke besonders dir Mama, dass du mir immer zugehört hast und ich mich immer auf deine Unterstützung aller Art verlassen kann.

Zuletzt möchte ich meinem Partner Johann danken. Danke, dass du immer für mich da bist und wir schon so vieles zusammen durchlebt haben. Ich liebe dich.

Table of contents

Zusammenfassung

Die Ectomykorrhiza ist eine symbiotische Interaktion, die zwischen Pilzhyphen und Pflanzenwurzeln ausgebildet wird. Der Pilz versorgt die Pflanze mit mobilisierten Nährstoffen aus dem Waldboden, während die Pflanze dem Pilz Kohlenhydrate aus der Photosynthese zur Verfügung stellt. Wie frühere Untersuchungen gezeigt haben, sind während der Interaktion im Ectomykorrhiza Modelorganismus Pappel Gene, die für einen Transkriptionsfaktor *dehydration responsive element binding factor 1* (*DREB1*) sowie einen Facilitator der Genefamilie *sugar will be eventually exported transporter 1* (*SWEET1*) induziert (Nehls and Bodendiek 2012, Nehls *et al.* unpublished). SWEET1 ist ein Glukose Transporter, der bei verschiedenen biotischen Interaktionen wie pathogene Interaktionen, Knöllchen Symbiose und arbuskularer Mykorrhiza (Chen *et al.* 2010, Kryvoruchko *et al.* 2016, Manck-Götzenberger and Requena 2016, An *et al.* 2019) induziert ist, während bisher keine direkte Beteiligung des DREB1 an entsprechenden biotischen Interaktionen bekannt ist. Das *Arabidopsis* DREB1 Homolog ist an regulatorischen Prozessen der Abscisinsäure abhängigen Signalkaskaden und Glukose bezogenen Stoffwechselwegen beteiligt (Finkelstein *et al.* 1998, Huijser *et al.* 2000, Bossi *et al.* 2009, Foyer *et al.* 2012). Ziel der Arbeit war die *in vivo* Analyse von Promoter Fragmenten der genannten Gene.

Für diese Analyse sollten Promoter Reporter Konstrukte in transgenen Composite Pappeln exprimiert werden. Um transgene von nicht transgenen Wurzeln unterscheiden zu können, sollte als erstes ein zweiter, visueller Marker, der unter Kontrolle eines konstitutiven Promoters exprimiert wird, in den Pflanzentransformationsvektor integriert werden. Um dies zu erreichen, wurden verschiedene Promotoren zur Expression eines Zellkern-getargeten Td-Tomato getestet. Ein *nopaline synthase* (NOS) Promoter zeigte klare Signale in Pappelwurzeln und wurde ausgewählt. Weiterhin wurden verschiede binäre Vektorsysteme hinsichtlich ihrer Transformationseffizienz in Pappeln untersucht. Dabei zeigte der pCAMBIA-basierte Vektor pCXUN im Vergleich zu pBi121 und dem p-Green-basiertem pPLV Vektor eine deutlich höhere Transformationseffizienz. Um die Expression des zu untersuchenden Promoters abzubilden wurden kernlokalisiertes *super yellow fluorescence protein* (sYFP) und *double green fluorecence protein* (dGFP) analysiert. DGFP zeigte eine höhere Signalintensität und eine bessere Lokalisierung im Kern verglichen mit dem sYFP, daher wurde dGFP als Marker Gen im finalen binären Vektor verwendet.

Um zu untersuchen ob die Aktivität der Ectomykorrhiza induzierten Promotoren wurzelspezifisch ist, wurde ein transientes Expressionssystem in Pappelblättern etabliert. Dabei stellte sich die Infiltration der fragilen Pappelblätter als am erfolgreichsten heraus. Die transiente Expression in Pappelblättern stellte sich verglichen mit *N. benthamiana* als nicht so robust und stabile heraus, ermöglichte aber eine schnelle, transiente Expression in Pappeln.

Der neu zusammengesetzte Vektor pCXUN04NOS wurde genutzt, um die Promoter Fragmente von *DREB1* (3.2 kb) und *SWEET1* (3.4 kb) auf die Ectomykorrhiza spezifische Lokalisierung in Composite Pappeln und die Expression in Pappelblättern zu analysieren. Um die Expression in mycorrhizierten und nicht-mycorrhizierten Wurzeln vergleichen zu können, wurden die Composite Pflanzen mit den Ectomykorrhizapilzen *Pisolithus microcarpus* und *Amanita muscaria* inokuliert. Die erhaltenen Ergebnisse entsprachen nicht den Expressionsdaten (Nehls and Bodendiek 2012, Nehls *et al.* unpublished), da keine Ectomykorrhiza induzierte Expression festgestellt werden konnte. Darüber hinaus ermöglichten beide Promoter Fragmente eine Expression des Markers im Blattgewebe von *N. benthamiana* und *P. tremula x alba*. Diese Ergebnisse sprechen dafür, dass die untersuchten Promoter Fragmente die für eine Ectomykorrhiza spezifische Expression notwendigen *cis*-Elemente nicht enthalten.

Summary

Ectomycorrhiza is the symbiotic interacting between fungal hyphae and plant roots. The fungus provides the plant with nutrients mobilized from soil and the plant delivers carbohydrates from photosynthesis in exchange (Smith and Read 2010). Former studies showed an up-regulation of genes coding for the transcription factor dehydration responsive element binding factor 1 (*DREB1*) and for one facilitator of the gene family sugar will be eventually exported transporter (*SWEET1*) in the model organism poplar (Nehls and Bodendiek 2012, Nehls *et al.* unpublished). While SWEET1 was shown to be involved as glucose transporter in diverse associations like pathogenic interactions, rhizobia nodules and arbuscular mycorrhiza (Chen *et al.* 2010, Kryvoruchko *et al.* 2016, Manck-Götzenberger and Requena 2016, An *et al.* 2019), no link between DREB1 and such biotic interactions is reported. The *Arabidopsis* DREB1 homolog was shown to be involved in the regulation process of abscisic acid signaling and glucose related pathways (Finkelstein *et al.* 1998, Huijser *et al.* 2000, Bossi *et al.* 2009, Foyer *et al.* 2012). Aim of the thesis was the *in vivo* analysis of promoter fragments of the mentioned genes.

For analysis promoter reporter constructs should be expressed in transgenic composite poplar. To distinguish between transgenic and non-transgenic roots, firstly a second, visual marker under control of a constitutive promoter should be integrated into the plant transformation vector. This step was necessary, since no classical selection procedure can be performed during composite plant generation leading to transgenic and non-transgenic roots emerging from the transformed shoot. A nuclear targeted Td-Tomato under control of the nopaline synthase (NOS) promoter turned out to give clear signals in poplar roots and was chosen as visual selection marker.

Furthermore different binary vectors were tested for their transformation efficiency in composite poplar. The pCAMBIA-based vector pCXUN showed compared to pBi121 and the p-Green-based vector pPLV significantly increased transformation efficiency. To monitor expression of the promoter of interest, nuclear targeted super yellow fluorescence protein (sYFP) and double green fluorescence protein (dGFP) were analyzed. DGFP showed higher signal intensity in poplar roots and distinct localization to the nucleus in comparison to sYFP and was therefore used as marker gene in the final binary vector.

Furthermore a transient expression system for poplar leaves was established, to analyze the activity of ectomycorrhiza induced promoters for their root specificity. Different techniques were tested and the infiltration of the fragile poplar leaves turned out to be most successful. The transient expression in poplar turned out to be not as robust as the infiltration of model organism *N. benthamiana*, but it enables a fast, transient expression in poplar.

The newly composed vector pCXUN04NOS was used to analyze promoter fragments of *DREB1* (3.2 kb) and *SWEET1* (3.4 kb) for ectomycorrhiza dependent expression localization in composite poplar and expression in leaf tissue. To compare expression in mycorrhized and non-mycorrhized roots, composite plants were mycorrhized using the ectomycorrhiza fungi *Pisolithus microcarpus* and *Amanita muscaria*. The generated results stand in contrasted to previous expression data (Nehls and Bodendiek 2012, Nehls *et al.* unpublished), since no ectomycorrhiza induced expression could be detected. Furthermore both fragments showed expression in leaf tissue of *N. benthamiana* and *P. tremula x alba*. These results indicate that the investigated promoter fragments did not contain all *cis*-elements important for ectomycorrhiza specific expression.

1 Introduction

1.1 Mycorrhiza

The term mycorrhiza is composed of the Greek words 'mycos' and 'rhiza' and means fungal root (Smith and Read 2010). Together plant roots and fungal hyphae form an organ in order to exchange carbohydrates for soil based nutrients and water. Additionally, the tolerance of the plant partner against biotic and abiotic stresses is increased by this interaction (Smith and Read 2010). Such mutualistic interaction can be found in all climatic zones of the world (Tedersoo *et al.* 2010). It is estimated that these types of interactions have been occurring for 460 million years and was one of the reasons that plants were able to colonize terrestrial habitats (Nicolson 1975, Pirozynski and Malloch 1975).

90 % of all plants form some type of mycorrhizal interaction (Hibbett *et al.* 2000). Seven different types of mycorrhizal interactions can be defined: arbuscular mycorrhiza, ectomycorrhiza, ectoendomycorrhiza, orchid mycorrhiza, ericoide mycorrhiza, monotropoide mycorrhiza and arbutoide mycorrhiza (Smith and Read 2010). In the following only ectomycorrhiza (ECM) will be further introduced.

1.1.1 Ecological meaning of ectomycorrhiza

Most trees in the Northern Hemisphere form ectomycorrhiza, a symbiotic interaction of plant fine roots with fungal hyphae and ECM fungal hyphae can form up to 80 % of the fungal biomass in forest soil (Högberg and Högberg 2002). This type of symbiosis is mainly formed by fungi belonging to the homobasidiomycetes and far less by ascomycetes and zygomycetes (Smith and Read 2010). On the plant side ECM can be formed by conifers and multiple clades of angiosperms (Smith and Read 2010). The six families of highest ecological importance are Betulaceae, Dipterocarpaceae, Fagaceae, Myrtaceae, Pinaceae and Salicaceae (Hibbett *et al.* 2000). In forests of the Northern Hemisphere and alpine regions members of the Pinaceae are highly abundant, while plants of the Fagaceae are dominant in the Southern Hemisphere and tropical forests (Smith and Read 2010).

The ECM symbiosis evolved in a polyphyletic way from both plant and fungal side and is still a dynamic process (Hibbett *et al.* 2000). Thereby the transition of homobasidiomycetes occurs between mutualist and free-living forms, but not between mutualist and parasite. While few ECM fungi and plants reveal a high host specificity, the majority shows low host specificity (Bruns *et al.* 2002). Low host specificity is also observed in other mutualistic interactions e. g. nodule symbiosis, but is rare in parasitic systems where high host

specificities are common (Borowicz and Juliano 1991). In ECM not only low host specificity is observed, but plants are also able to form ECM with different fungi at the same time and the other way around (Hibbett *et al.* 2000, Bruns *et al.* 2002). Within this complex interaction, different plants are frequently linked by the interaction with one fungus and vice versa resulting in a high impact of ECM on the whole ecosystem (Bruns *et al.* 2002).

The growth of soil fungi depends on the presence of simple carbohydrates, which are rare in forest soils (Wainwright 1993). Plants are restricted in their ability to mobilize inorganic nutrients from complex forest soils, but they can overcome this limitation by interaction with ECM fungi (Nehls *et al.* 2007). Thereby together these organisms can colonize nutrient limited regions, where they could not survive separately (Nehls and Bodendiek 2012). However, the nutrition of the fungus with soluble sugars and organic acids can cost the plant up to one third of its photosynthesis products (Finlay and Söderström 1992). Although fungal and plant partner could benefit from each other, both grow separately under optimal nutritional conditions (Bruns *et al.* 2002, Nehls 2008).

1.1.2 Structure and function of ectomycorrhiza

The initiation sites of ectomycorrhizas are newly formed plant fine roots, which become infected (**Figure 1 a**). At the fungal site ectomycorrhizas are defined by the formation of three distinct structures (**Figure 1 b**): a hyphae mantle covering the root, a highly branched extraradical mycelium and a highly branched intraradical mycelium, the so called Hartig net (Smith and Read 2010). The hyphae of the intraradical mycelium are restricted to the rhizodermis and in some other cases to the whole cortex of the root, but never penetrate the endodermis (**Figure 1 b**) (Lepage *et al.* 1997, Smith and Read 2010). A particular feature of ECM symbiosis is that the fungal hyphae grow exclusively within the apoplast of plant cells and never penetrate into symplast (Smith and Read 2010).

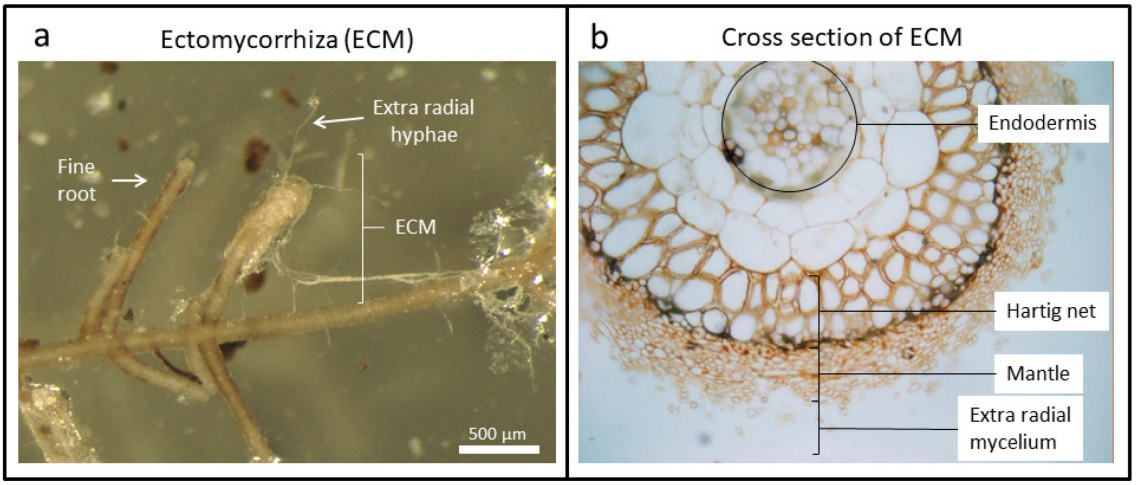

Figure 1: Structure of ectomycorrhiza. a) Overview of an ectomycorrhiza structure (ECM) formed by poplar and *Pisolithus microcarpus*. b) Cross section of a wildtype beech ECM (Uwe Nehls).

The formation is initiated by the fungus recognizing an emerging plant fine root. Fungal hyphal growth is directed to the emerging plant fine root, resulting in an attachment of hyphae to the surface of the root (Martin *et al.* 2001). The detailed recognition process is not known, but it is supposed that the composition of the plant root exudates is important and fungus-derived phytohormones are involved (Nehls and Martin 1995, Smith and Read 2010). During ECM formation the fungal mycelia frequently cover the complete root, which lead to the formation of the fungal mantle. The mantle isolates the root from the surrounding soil and dissolved nutrients and water have to pass fungal hyphae prior to reaching the root surface (Blasius *et al.* 1986). Furthermore the root hair formation is suppressed by ECM formation (Nehls *et al.* 2007). The fungal mantle serves as intermediate storage for nutrients delivered by soil hyphae and carbohydrates taken up from the symbiotic interface (Jordy *et al.* 1998).

To provide the plant with nutrients, the fungal hyphae form a large and highly branched extraradical mycelium in the soil, building up a large interaction surface, which can spread over several square meters (Smith and Read 2010). Extraradical fungal hyphae mobilize inorganic and organic nutrients (nitrogen, phosphate) from complex forest soil and need to transport them to the symbiotic interface.

The symbiotic interface between plant and fungus is formed by the intraradical hyphae growing in apoplastic space of the plant fine root. The Hartig net allows the exchange of plant-delivered carbohydrates for fungal nutrients (Kottke and Oberwinkler 1987, Smith and Read 2010, Nehls and Bodendiek 2012). The fungal sugar support makes between 8 – 17 % of plant photo assimilates (Hobbie and Hobbie 2006), but it is, however, not clear which carbon source is delivered to the fungus. To allow such high supply of photosynthetic

products to the fungus, the photosynthetic efficiency of ECM plants is increased (Vodnik and Gogala 1994, Wright *et al.* 2000). To avoid fungal parasitism plants have to regulate the carbohydrate flux towards the fungus (Nehls 2008). However, detailed mechanisms are unknown, but regulatory effects on the metabolism, enzyme activity and gene expression of both partners in ECM were shown e. g. (Nehls *et al.* 2001, Grunze *et al.* 2004, Duplessis *et al.* 2005, Nehls *et al.* 2007).

1.2 Model organisms in ectomycorrhizal research

The work with models always raises the question of transferability of obtained results to other organisms. Furthermore, such results are frequently generated under laboratory conditions and need thus to be proven under field conditions. In addition, ECM has polyphyletic origins at the plant and fungal sites (Hibbett *et al.* 2000). Therefore many details of the interaction may differ between particular partners and may make a general interpretation of obtained results difficult. To allow a broader interpretation of results the analysis of different fungal models of selected families is thus necessary.

1.2.1 The plant model: *Populus spec.*

Poplar is a wide spread woody plant in the northern hemisphere and thereby important for the conservation of different ecosystems (Dickmann 2001). Similar to many other forest trees poplar roots undergo ECM formation.

The approximate 40 poplar species belong to the family Salicaceae in the order Malpighiales in the Eurosid I clade (Cronk 2005) (APG, 2012). Since poplar are inter fertile, a large number of natural hybrids exist (Cronk 2005). These hybrids are often characterized by a faster growth rate and are therefore frequently used for wood production in paper industry (De Boever *et al.* 2007). In 2006 the genome of *Populus trichocarpa* was fully sequenced as the first genome of a wood forming plant (Tuskan *et al.* 2006). The approximate 45 000 genes are spread over 19 chromosomes (2n = 38) (Tuskan *et al.* 2006). Moreover, it was found that poplar is paleopolyploid, which means that the current genome evolved from one or two genome duplications, which is indicated by the size of gene families found in *P. trichocarpa* (Brunner *et al.* 2000).

Under laboratory conditions *P. trichocarpa* is difficult to handle, but hybrids like *P. tremula x tremuloides* and *P. tremula x alba* are easy to cultivate (personal communication, Uwe Nehls). Furthermore, hybrids are able to form ectomycorrhiza in closed petri dish systems, within four to six month indicating ECM investigation as a highly time consuming process (personal communication, Uwe Nehls).

Poplar was also the first woody plant, which was transformed (Fillatti *et al.* 1987). Since the generation of entirely transgenic poplar plants is time consuming and last at least eight months, a protocol for the generation of so called composite plants under sterile laboratory conditions was established (Neb *et al.* 2017). The generation of composite poplar is possible within weeks and thereby represents a big advantage over classical stable transformation (Veena and Taylor 2007). Composite plants consist of a wild type shoot carrying transgenic roots and can be generated within six to eight weeks. Such transgenic plants are especially interesting for studying root-based processes (Alpizar *et al.* 2006). The main disadvantage of composite plants is that the morphology of transgenic roots has been changed, making determination of changed phenotypes impossible. Main roots of composite plants grow gravitation independently, form many more root hairs and root systems are more branched (Veena and Taylor 2007). Nevertheless composite plants were successfully used to carry out sub-cellular protein localization, RNAi silencing, promoter analysis and interaction studies with microorganisms, like ECM (Collier *et al.* 2005, Veena and Taylor 2007).

1.2.2 *Amanita muscaria* as fungal partner

Amanita muscaria, more commonly known as fly agaric, is part of the family Amanitaceae of the phylum Basidiomycota (Trappe 1962). The native habitats of *A. muscaria* are boreal forests, where it forms ECM with birch and pine. Due to the world-wide distribution of its native host trees *A. muscaria* is nowadays not only found in Northern, but also Southern Hemispheres like Australian pine plantations as well as in association with *Eucalyptus* (Sawyer *et al.* 2001, Robinson 2010). *A. muscaria* forms associations with at least 23 species of Betulaceae, Fagaceae, Pinaceae and Salicaceae and thereby has a low host specificity (Trappe 1962, Hibbett *et al.* 2000).

A. muscaria can be easily cultivated under sterile laboratory conditions and is furthermore able to form ECM with *Populus* in closed petri dish systems (Zhang *et al.* 2005).

1.2.3 *Pisolithus microcarpus* as fungal partner

Pisolithus microcarpus belongs to the family Sclerodermataceae in the phylum Basidiomycota (Trappe 1962). *P. microcarpus* is an ectomycorrhizal fungus, native to Australian forests, where it is often associated with *Eucalyptus* (Macdonald and Westerman 1979, Martin *et al.* 2002). Industrial usage of its natural host plants in the Northern Hemisphere have led to migration of *P. microcarpus* to regions outside of the Southern Hemisphere. Today, isolates of *P. microcarpus* can be found all over the world (e.g. Brazil,

China, Morocco, Portugal, Senegal, South Africa) in plantations of eucalypts and acacias (Martin *et al.* 2002).

P. microcarpus is cultivated as model organism under laboratory conditions and forms ECM with *Eucalyptus* not only in nature but also under laboratory conditions e.g. (Plett *et al.* 2015). Furthermore ECM formation of *P. microcarpus* can be observed with *Populus* under laboratory conditions (personal communication, Uwe Nehls).

1.3 Plant transformation

To transform plants, different strategies can be applied. Techniques can be divided in transient and stable expression systems. Both can be achieved by direct transfer of DNA or *Agrobacterium*-mediated transformation (Newell 2000). To find the most efficient method to investigate biological questions the specific advantages and disadvantages of the transformation procedures have to be considered.

1.3.1 Principles of plant transformation

Transient expression is characterized by the time limited expression of introduced DNA. Expression can be detected after a few days of incubation, which enables a fast generation of results (Hernandez-Garcia and Finer 2014). Since the DNA is not integrated into the plant genome, but is expressed extrachromosomal, gene expression is limited to days (Newell 2000). Leaf infiltration with transgenic *Agrobacteria* is one of the most widely used assays for transient expression and is suitable e. g. for sub-cellular localization or promoter analysis experiments (Yang *et al.* 2000, Wroblewski *et al.* 2005). Since transient expression is limited to the transformed organ, only organ specific results can be generated.

During stable transformation the introduced DNA is integrated into the plant genome (Newell 2000). Stable transformation is more time consuming compared to transient expression, since in case of wood forming plants the generation of entire transgenic plants needs several months (Alpizar *et al.* 2006). Even if stable transformation is more time consuming than transient expression, it is the only way to perform experiments over longer time periods.

One special form of stable transformed plants are composite plants. Transgenic roots emerge after transformation with *Agrobacterium rhizogenes* from wild type shoots (Alpizar *et al.* 2006). The generation of transgenic roots is possible in about four weeks and is thereby faster than the generation of entire transgenic plants in case of wood forming plants (Veena and Taylor 2007). Composite plants can be used to study processes in the

root system over a longer period of time and are therefore suitable for interaction studies (Veena and Taylor 2007). Furthermore localization of gene expression or promoter analysis can be performed in a root specific manner (Collier *et al.* 2005).

Transient expression as well as stable transformation can be carried out by direct transformation or *Agrobacterium*-mediated transformation (Newell 2000). The direct transformation implies a direct transfer of the DNA of interest into the plant cell. Plant tissues can be transformed by particle bombardment with DNA-coated particles or protoplasts can be transformed with plasmid DNA by electro-proration or polyethylene glycol treatment (Newell 2000).

1.3.2 *Agrobacterium*-mediated plant transformation

Agrobacteria are gram negative soil bacteria, which are able to transfer parts of their extrachromosomal DNA, named transfer DNA (T-DNA) into the host cell, where it usually integrate, it into the plant genome (McCullen and Binns 2006). The infection causes diseases, which are dependent on the agrobacterial species. *Agrobacterium tumefaciens* cause tumor formation in the plant host, whereas *Agrobacterium rhizogenes* causes the so called "hairy roots" disease (Gelvin 2003). The *Agrobacteria* carry large plasmids, the tumor inducing plasmid (Ti plasmid, *A. tumefaciens*) or root inducing plasmid (Ri plasmid, *A. rhizogenes*), which harboring the T-DNA, flanked by 23 base pair long boarder repeats (McCullen and Binns 2006). The introduction of the T-DNA into the plant's genome leads to the expression of novel amino acid-sugar conjugates (opines), serving as a carbon and nitrogen source for the *Agrobacteria* (McCullen and Binns 2006). The ability of *Agrobacteria* to transfer any DNA cloned into the T-DNA region into a host plant genome, provides a great tool for plant transformation. Furthermore *Agrobacteria* were shown to transfer DNA not only into plants, but also to other bacteria, fungi and even some mammalian cells (Lacroix *et al.* 2006).

The transport process of the T-DNA into the plant cells is mediated by the virulence genes (*vir*-genes), which are encoded on the Ti or Ri plasmid. It was shown that the *vir*-genes and the T-DNA can be functionally encoded by different plasmids in the same *Agrobacterium* (Lee and Gelvin 2008). For the use in biotechnology the tumor inducing genes of the T-DNA of *A. tumefaciens* were deleted to form "disarmed" strains that, allow the regeneration of transgenic plants without tumor formation. Those stable transformed plants can pass their modified genome onto the next generation allowing investigation of mutants over several generations (Hooykaas and Schilperoort 1992, Newell 2000). In contrast to *A. tumefaciens*,

A. rhizogenes strains cannot be disarmed, since the root inducing genes (*rol* genes) are needed. The *rol* genes induce root formation on transformed shoots, leading to the formation of roots showing untypical root hair allocation, a high number of branching points and gravity independent growth (Veena and Taylor 2007). The induction of transgenic roots can be used to generate composite plants consisting of a wild type shoot carrying transgenic roots (Hansen *et al.* 1989). Upon transformation T-DNAs of the native Ri plasmid (riT-DNA) and a binary vector (biT-DNA) are transferred into plant cells upon the formation of transgenic roots (Alpizar *et al.* 2006).

1.3.3 Plant transformation vectors: The binary system

In the binary vector system the expression of the *vir*-genes and the T-DNA are separated on two different plasmids (Lee and Gelvin 2008). The plant transformation vector, referred to as binary vector is characterizes by different properties (**Figure 2**) with two regions; the vector backbone and the T-DNA region. The binary vector has to be replicated in *E. coli* and *Agrobacterium*. The plasmids can carry one *origin of replication* (*ori*) allowing replication in *E. coli* and *Agrobacteria* or two different *ori*s. For selection purpose the vector backbone harbors a selection marker gene that can be expressed in both bacteria. Further characteristics of a binary vector are the left and right border repeats flanking the T-DNA, a multiple cloning site (MCS) for introduction of DNA fragments by endonucleases restriction sites, a bacterial selection marker encoded on the vector backbone (often antibiotic resistance) and a plant selection marker encoded in the T-DNA region (Lee and Gelvin 2008). In addition marker genes like florescence proteins can be encoded within the T-DNA region. Several plant transformation vectors are available. In the following three different vector families will be introduced.

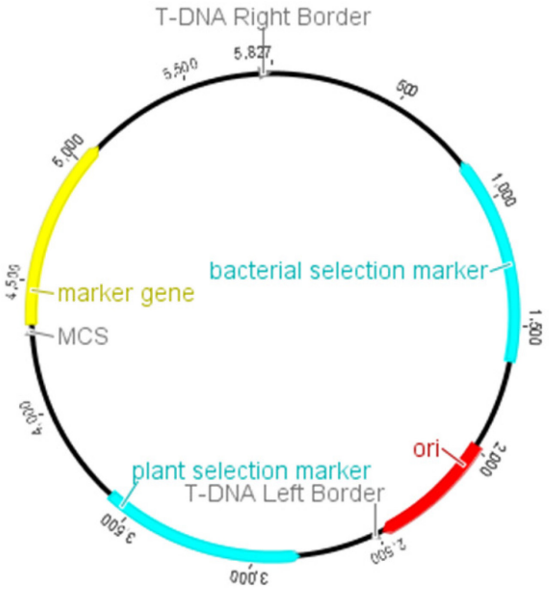

Figure 2: Scheme of a typical binary plant transformation vector. The vector map shows the basic characteristics of a binary plant transformation vector. The *origin of replication* (*ori*) is active in *E. coli* and *Agrobacteria*. In gray the multiple cloning site (MCS) and the left and right border repeats are shown. Furthermore bacterial and plant selection markers are indicated as well as a marker gene. The vector map is drawn with geneious (version 6.1.8, Biomatters, Auckland, New Zealand).

1.3.3.1 The pGreen based vector family pPLV

The pPLV is a binary vector family based on the pGreen vector, which was generated from the pBluescript (Hellens *et al.* 2000, De Rybel *et al.* 2011). The pPLV vector harbors the *pColE1-ori* responsible for the very high copy number of the plasmid in *E. coli*. The high copy number and its relatively small size of 3 kb make pPLV easy to handle for cloning purpose (De Rybel *et al.* 2011). In *Agrobacteria* the replication is started from the *pSA-ori*. Usually, the proteins necessary for initiation of replication are encoded on the vector backbone, but in the case of pPLV the requested *pSA-repA* gene was removed from the vector backbone to reduce the size of the vector (Hellens *et al.* 2000). Therefore the introduction of helper plasmids is essential for replication in many bacterial strains. However, some agrobacterial strains harbor the *repABC* operon and are thereby able to replicate the vector without helper plasmids. *A. tumefaciens* strains C58 and GV3101 need the respective helper plasmid pSOUP for successful replication, while *A. rhizogenes* strain K599 does not need a helper plasmid (Cevallos *et al.* 2008).

1.3.3.2 The pBIN19 based vector pBI121

The pBI121 vector was constructed on the basis of pBIN19 (Bevan 1984, Chen *et al.* 2003). The widely used plant transformation vector has a total size of 12.8 kb and is therefore comparatively large (Chen *et al.* 2003). The plasmid harbors the *ori-V* for replication in *E. coli* and *Agrobacteria* that enables only a low copy number. On the vector backbone the *trfA* genes are encoded, which are important for promotion of replication (Frisch *et al.* 1995).

1.3.3.3 The pCAMBIA based vector pCXUN

The pCXUN vector belongs to the pCAMBIA vector family, which backbone was derived from pPZP (Hajdukiewicz *et al.* 1994, Leclercq *et al.* 2015). With 6 kb the vector is larger than the pPLV, but smaller than the pBI121 vector. The two different *oris ColE1-ori* and *pVS1-ori* are present on the vector backbone to guarantee replication of the plasmid in *E. coli* and *Agrobacteria*, respectively (Hajdukiewicz *et al.* 1994). Those *oris* lead to a high copy number in *E. coli* and a good stability in *Agrobacteria* (Leclercq *et al.* 2015). The genes necessary for initiation of replication are encoded on the vector backbone.

1.4 Promoters: key players in transcriptional regulation

Gen regulation appears on different levels and is characterized in transcriptional, post-transcriptional and post-translational regulation (Hernandez-Garcia and Finer 2014). Transcriptional regulation is coordinated by the promoter sequence, which harbors information under which conditions a gene is expressed (Zuo and Li 2011). Regulatory processes are important to coordinate gene expression during development, organ function or in response to changed abiotic or biotic conditions (Hernandez-Garcia and Finer 2014).

1.4.1 Promoter elements involved in transcriptional regulation

The promoter is usually localized upstream of the coding region and contains various *cis*-acting elements involved in regulation. The *cis*-acting elements function as binding sites for transcription factors (Hernandez-Garcia and Finer 2014). The basic transcriptional machinery assembles prior to transcription and binds to the TATA box to initiates transcription (Burley and Roeder 1996). This region is defined as the core promoter. The transcription initiation is performed by RNA polymerase II and is started by open complex formation. Promoter regions have a lower stability around -35 to -25 bp, related to the TATA-box motif to facilitate melting of the DNA (Kanhere and Bansal 2005). Plant promoters may contain a sequence motif 45 bp to 25 bp upstream of the transcriptional start site (TSS) named TATA box (**Figure 3**) (Molina and Grotewold 2005). However, 50 to 70 % of all promoters do not contain a TATA box motif e. g. housekeeping genes and photosynthesis genes (Shahmuradov *et al.* 2005). Those TATA-less promoters contain alternative sites to control transcription initiation, such as the transcription initiation region (Inr) or the downstream promoter element (DPE) 30 bp downstream of the TSS (Shahmuradov *et al.* 2005)

The proximal promoter is located 200 to 300 bp upstream of the core promoter and contains *cis*-acting elements (**Figure 3**) as well as the distal promoter, which is localized upstream of the proximal promoter (Shahmuradov *et al.* 2005).

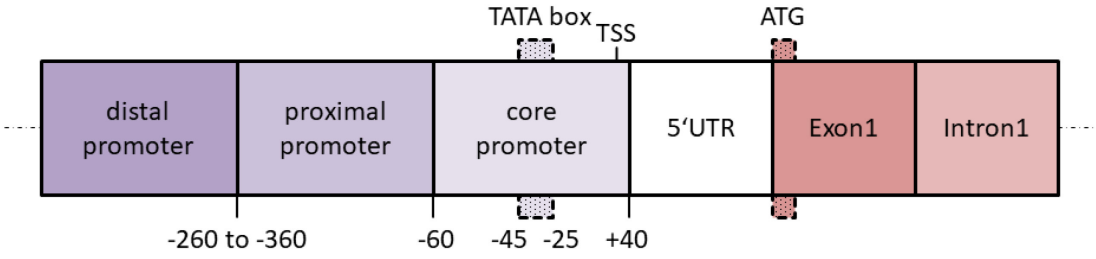

Figure 3: Schematic structure of a plant promoter. The approximate positions of the distal, proximal and core promoter regions upstream of the 5' untranslated region (5'UTR) are given. Furthermore the first exon and intron are shown. Key positons as the transcriptional start site (TSS), the TATA box and the ATG are also marked.

The bending capacity influences the ability of the DNA to form 3D structures guiding transcription factors to the TSS (Zuo and Li 2011). Therefore, *cis*-acting elements of the distal promoter can be located several kb upstream of the TSS can influence gene expression. Furthermore, the access to the DNA is regulated by chromatin structure and histone composition, which has an impacted on transcriptional regulation as well (Hernandez-Garcia and Finer 2014).

Next to the promoter structure gene expression is affected by the availability of active transcription factors, which is related to the state of the organism (Zuo and Li 2011). The transcription factors can activate or suppress gene expression, by interacting with the transcriptional machinery bound to the core promoter (Lee and Young 2000). In the end the level of gene expression is the result of all involved factors.

1.4.2 Promoter types

According to their regulatory role in gene expression, promoters can be categorized in different classes: constitutive, spatiotemporal and inducible promoters (Peremarti *et al.* 2010).

Promoters permitting constitutive gene expression enable comparable mRNA levels in all tissues during the entire life cycle of the plant and are often based on plant virus or plant housekeeping genes. Viral promoters achieve their constitutive expression profile by additive effects of multiple tissue specific elements (Lam *et al.* 1989). One of the most widely used examples is the CaMV35S promoter isolated from the cauliflower mosaic virus (Odell *et al.* 1985, Benfey and Chua 1990). Promoters of plant housekeeping genes contain non-specific elements, which are considered to be highly efficient in the recruitment of

proteins important for transcription (Hernandez-Garcia and Finer 2014). Classical examples are the promoter regions of actin, tubulin and some ubiquitin genes (Peremarti *et al.* 2010). Even if constitutive promoters are defined as active in all tissues at all times, many promoters show stronger expression in meristematic tissues or the vascular system compared to other tissues (Hernandez-Garcia and Finer 2014).

The activity of spatiotemporal promoters is restricted to cells, tissues, organs or developmental stages. But the expression can also be leaky, meaning weak expression in regions were no signal would be expected (Hernandez-Garcia and Finer 2014). Promoters of genes involved in seed development as well as pollen-specific promoters are classical examples (Peremarti *et al.* 2010).

The class of inducible promoters responds to endogenous signals (e. g. plant hormones), external physical stimuli like biotic (e. g. interaction with another organism) and abiotic stresses (e. g. heat) or external chemical stimuli (e. g. herbicides) (Peremarti *et al.* 2010, Hernandez-Garcia and Finer 2014). The wound-inducible promoter of *Agrobacterium tumefaciens* nopaline synthase (NOS) is a widely-used example for an inducible promoter active in a variety of plant organs (An *et al.* 1990). The activity of the NOS promoter can be further induced by auxin addition, but also un-wounded or non-induced leaf tissue can show basal expression of the NOS promoter (An *et al.* 1990). This basal expression level is common for inducible promoters, however the expression level is highly increased under stimulating conditions (Hernandez-Garcia and Finer 2014).

1.5 Promoter analysis

In a first step, potential promoter regions are often analyzed using *in silico* methods. The potential promoter sequence is investigated for specific sequence motifs by promoter prediction programs. The database of those programs is based on results generated with other model organisms, like *Arabidopsis* for dicotyledonous plants and is thus very often highly speculative.

For a functional analysis, the predicted promoter region is separated from its native environment and fused to a reporter gene e. g. luciferase, β-glucuronidase or fluorescence proteins (Ow *et al.* 1986, Jefferson *et al.* 1987, De Rybel *et al.* 2011). The position of *cis*-elements is frequently determined by 5'truncation studies. By the amount of formed reporter, the expression strength of the promoter is monitored.

1.5.1 Limitations of functional promoter analysis *in planta*

Promoter expression *in planta* can be analyzed using transient or stable transformation. In transient transformation high DNA amounts often leads to high extrachromosomal expression levels that could result in an overload of the regulatory machinery and gene silencing (Hernandez-Garcia and Finer 2014). Furthermore very high initial levels of gene expression can be reached compared to stable transformation (Hernandez-Garcia and Finer 2014). Transient expression studies are usually performed in organs of model plants that are easy to transform. Further frequently used systems are promoter analysis using cell cultures or protoplasts transformation, with which high transformation rates can be reached, but no organ or tissue specific gene expression can be investigated (Newell 2000). On the other hand transient expression using *Agrobacterium* infiltration is often performed in leaves, which can only give results over the promoter activity in leaf tissue.

But also stable transformation can produce tissue specific results. Since the generation of entire stable transformed plants often lasts several months up to a year, often generation of composite plants carrying hairy roots are performed (Alpizar *et al.* 2006). The advantages are no chlorophyll auto-fluorescence and the generation of results within weeks (Veena and Taylor 2007). The integration of the DNA into the plant genome can cause position effects, which lead to variation of gene expression (Vaucheret *et al.* 1998). Furthermore, the copy number of integrated DNA copies can influence gene expression levels (Hernandez-Garcia and Finer 2014).

In addition, chromatin based regulation cannot be detected in artificial systems, since the native environment of the promoter is changed in transient and stable transformation (Hernandez-Garcia and Finer 2014). In the case of the usage of heterologous model systems, the situation can be even more difficult, since the transcription factors important for promoter regulation might be missing (Hernandez-Garcia and Finer 2014).

1.5.2 Fluorescence proteins as reporter genes

Compared to enzymatic-based assays for promoter analysis with e. g. luciferase, fluorescence proteins allow only a less sensitive detection, but have the advantage of *in vivo* visualization without exogenous intervention (Chudakov *et al.* 2010). Furthermore different promoters can be investigated at the same time by using different fluorescence marker genes.

The discovery and development of the first fluorescence marker the green fluorescent protein (GFP) received the Nobel Prize of Chemistry in 2008 (Ehrenberg 2008). The original

GFP was isolated from jellyfish *Aequorea victoria* in 1962 and successfully expressed in *E. coli* and *C. elegans* without the need of external factors in 1994 (Shimomura *et al.* 1962, Chalfie *et al.* 1994). Because of high potential of fluorophores regarding the study of biomolecular processes in living cells, tissues and organisms, a whole research field focuses on the optimization of fluorophores for biotechnological usage.

The structure of the GFP was described as 11-stranded β-barrel with an α-helix running through the center (Pakhomov and Martynov 2008). The chromophore is formed by a post-translational cyclisation of the tripeptide X65-Tyr66-Gly67 in the cell without the need of external factors (Pakhomov and Martynov 2008). While position 66 and 67 are highly conserved within the natural occurring GFP-like proteins, position 65 can vary (Chudakov *et al.* 2010). The chromophore is located in the center of the β-barrel, which protects it against influences of the surrounding substances. Color, intensity and stability of the GFP are influenced by the surrounding amino acid side chains within the β-barrel (Chudakov *et al.* 2010). By mutation of the surrounding amino acid's properties, the fluorophore can be altered, which brought up a large family of fluorescent proteins with different characteristics.

The naturally occurring GFP was biotechnologically engineered to achieve brighter signal intensity leading to the so called enhanced GFP (EGFP) (Heim *et al.* 1995). EGFP has an excitation maximum of 489 nm and an emission maximum of 509 nm (Patterson *et al.* 1997). To further increase signal intensity a genetic fusion of three EGFP gene copies was created by Takada and Jürgens in 2007 and successfully used for promoter analysis in the model plant *Arabidopsis*. The created tripleGFP contains a nuclear targeting signal and has a size of app. 81 kDa (Takada and Jürgens 2007, Morris *et al.* 2010).

The super yellow fluorescence protein sYFP was generated by directed mutagenizes from EYFP and has a size of app. 27 kDa (Kremers *et al.* 2006). The protein showed an improved brightness and more efficient folding compared to the previous variant. The excitation and emission maxima of sYFP are 490 nm and 527 nm, respectively (Kremers *et al.* 2006). The sYFP was cloned in a series of pPLV vectors designed for promoter analysis and was successfully used in *Arabidopsis* and poplar (De Rybel *et al.* 2011, Neb 2017).

Td-Tomato is derived from a monomeric mutant of dsRed by several rounds of directed mutagenesis (Shaner *et al.* 2004). Two gene copies of dTomato were genetically fused to improve the brightness of the fluorophore (Campbell *et al.* 2002). The resulting protein forms an intramolecular dimer and thereby behaves like a monomer with a size of app.

54 kDa (Shaner *et al.* 2004, Morris *et al.* 2010). Td-Tomato has an excitation maximum of 554 nm and an emission maximum of 581 nm (Shaner *et al.* 2004). With a nuclear target it was successfully used as a promoter reporter gene (e. g. (De Rybel *et al.* 2011)).

1.6 The dehydration-responsive element-binding protein

Plants are exposed to different environmental stresses like drought, high salt concentration in the soil or low temperatures. To survive stress periods, selected genes are upregulated in response to given environmental stresses. Those stress responses are mediated by specific groups of transcription factors (TF). The dehydration-responsive element binding (DREB) proteins are TFs, belonging to the gene family of APETALA 2/ethylene responsive element binding protein (AP2/EREBP)-like proteins. The gene family of the AP2/EREBP like proteins is plant specific and all members harbor the highly conserved AP2/ethylene responsive factor (AP2/ERF) DNA binding domain (Riechmann and Meyerowitz 1998). The domain consists of 50 to 60 amino acids forming three β-sheets and one α-helix at the N-terminus (Wang *et al.* 2011, Chen *et al.* 2013). The transcription factors recognize the dehydration responsive element with the core motif A/GCCGAC or the GCC box motif AGCCGCC (Liu *et al.* 1998, Sakuma *et al.* 2002). AP2/EREBP like proteins are involved in developmental and adaptive processes in plants, particularly in response to biotic and abiotic stresses (Chen *et al.* 2013). This family is one of the largest gene families of transcription factors *in planta* and can be further divided into four subfamilies.

Genes of the AP2/EREBP family are divided into four subfamilies according to their number and type of DNA-binding domains. The AP2 subfamily is characterized by the presence of two AP2/ERF domains and was shown to be mainly involved in developmental processes (Elliott *et al.* 1996, Chuck *et al.* 1998, Boutilier *et al.* 2002). In addition to one AP2/ERF domain, TFs of the RAV (Related to ABI3/VP1) subfamily harbor a second DNA-binding domain called B3 (Cao *et al.* 2015). RAVs respond to ethylene or brassinosteroids and thus are involved in biotic and abiotic stress response (Alonso *et al.* 2003, Hu *et al.* 2004, Sohn *et al.* 2006). Only one AP2/ERF domain was found in the ERF subfamily (Agarwal and Jha 2010). ERFs mainly recognize the GCC box motif, which is located in pathogenesis-related genes (Ohme-Takagi and Shinshi 1995, Fujimoto *et al.* 2000). Like ERFs, DREBs also harbor only one AP2/ERF domain, but it was stated that DREBs bind primarily to CRT (C-Repeat) or dehydration responsive element (DRE) motifs (Sakuma *et al.* 2002, Mizoi *et al.* 2012). DREBs are known to be involved in abiotic stress response (Lata and Prasad 2011).

1.6.1 DREB proteins: a subfamily with subgroups

The subfamily of DREBs can further be classified into six subgroups A1 to A6 according to sequence similarities of the DNA-binding domains (Sakuma *et al.* 2002). The gene distribution over the subgroups for *Arabidopsis* and *P. trichocarpa* is shown in **Table 1** (Cao *et al.* 2015). The subgroups A1 and A2 were analyzed more broadly and it was shown that genes of the subgroup A1 and A2 bind to the DRE/CRT motif (Sakuma *et al.* 2002). For the binding process of the DRE/CRT motif, the amino acid valine in position 14 was shown to be crucial (Sakuma *et al.* 2002). All of the subgroup members harbor a conserved valine14, but detailed binding specificities of subgroups A3 to A6 are unknown.

Table 1: Comparison of DREB gene distribution in *A. thaliana* and *P. trichocarpa*. The gene numbers of DREBs (dehydration-responsive element-binding) belonging to the six subgroups A1 to A6 are given. The numbers occurring in *A. thaliana* and *P. trichocarpa* are compared (Cao *et al.* 2015).

Subgroup	Genes in *A. thaliana*	Genes in *P. trichocarpa*
A1 DREB1/CBF gene family	6 genes	6 genes
A2 DREB2 gene family	8 genes	8 genes
A3 ABI4	1 gene	2 genes
A4 TINY	16 genes	26 genes
A5 RAP2.1, 2.9 and 2.10	16 genes	14 genes
A6 RAP2.4	10 genes	11 genes

1.6.2 Subgroup A3: ABI4 and PtrDREB1

In *Arabidopsis* one member of the DREB subfamily was found, which is known as Abscisic acid insensitive 4 (ABI4) (Finkelstein *et al.* 1998, Sakuma *et al.* 2002). ABI4 was shown to be important for signal cascades of the phytohormone abscisic acid (ABA) during seed development and germination (Finkelstein *et al.* 1998). Further functions are lipid mobilization in the embryo, chloroplast retrograde signaling and glucose response (Arenas-Huertero *et al.* 2000, Huijser *et al.* 2000, Laby *et al.* 2000, Penfield *et al.* 2006, Koussevitzky *et al.* 2007). Expression of ABI4 in *Arabidopsis* is mainly present during seed maturation and in seedlings shortly after germination (Finkelstein *et al.* 1998, Söderman *et al.* 2000, Arroyo *et al.* 2003). The expression is high in seeds, however is not seed specific (Finkelstein *et al.* 1998). In later developmental stages the expression of ABI4 is low, but detectable (Söderman *et al.* 2000, Arroyo *et al.* 2003). ABI4 can function as both a transcriptional activator as well as repressor and therefore has a dual function in modulation gene expression (Bossi *et al.* 2009). Furthermore, a self-regulatory function as a positive regulator was shown in development related, ABA related and sugar signaling responses

(Bossi *et al.* 2009). In maize the DRE *cis*-acting element CACCG was identified as a binding site for ABI4 and found in genes of ABA- and sugar-related pathways (Niu *et al.* 2002). An important regulatory function of ABI4 in glucose related pathways is published several times (Huijser *et al.* 2000, Niu *et al.* 2002, Foyer *et al.* 2012).

In *Populus trichocarpa* two members of the A3 subgroup were found and named as *PtrDREB1* and *PtrDREB2* (Chen *et al.* 2013). The nomenclature of Chen *et al.* 2013 can be misleading, since the two genes were grouped with the *Arabidopsis* ABI4 gene and does not belong to the DREB1/CBF and DREB2 families of subgroups A1 and A2. *PtrDREB1* is located on chromosome 8 (Chen *et al.* 2013) and is suspected to form a soluble protein (Hirokawa *et al.* 1998, Das 2018). Sub-cellular localization experiments in *Nicotiana benthamiana* leaves have shown a nuclear localization of PtrDREB1 (Das 2018). The expression of *PtrDREB1* is root specific and induced in an ectomycorrhiza specific way (Nehls *et al.* unpublished). Functional information about DREB1 in poplar is unknown.

1.7 The sugar will eventually be exported transporters

A new family of sugar transporters in plants was identified 2010 by Chen *et al.*, named sugar will eventually be exported transporters (SWEETs). Homologs were found to be wide spread in all eukaryotic kingdoms animals, fungi and plants (Chen *et al.* 2015). SWEETs are involved in cellular sugar uptake as well as sugar efflux (Chen *et al.* 2010, Chen 2014). *In planta* SWEETs were shown to be involved in phloem unloading, pollen nutrition, embryo development and nectar secretion (Chen *et al.* 2010, Chen *et al.* 2012, Lin *et al.* 2014, Chen *et al.* 2015). Furthermore, it was shown that fungal and bacterial pathogens can induces gene expression of different SWEET genes in *Arabidopsis* and rice to improve nutrition by manipulated sugar excretion (Ferrari *et al.* 2007, Chen *et al.* 2010). Inducing effects on *SWEET* expression were also found for interactions with beneficial microbes in *S. tuberosum*, *M. truncatula*, soy bean and *P. trichocarpa* (Kryvoruchko *et al.* 2016, Manck-Götzenberger and Requena 2016, An *et al.* 2019, Zhao *et al.* 2019, Nehls *et al.* unpublished).

1.7.1 Protein structure and evolution

Proteins of the SWEET family were found to be small proteins with 7 transmembrane domains (TMDs) and extracellular N-terminus (Chen *et al.* 2010, Chen *et al.* 2015) The cytosolic C-terminus contains multiple phosphorylation sites and is comparatively long (~ 45 aa), which may be potential sites of post-translational modifications and binding of other (regulatory) proteins (Chen *et al.* 2015). In prokaryotes smaller SWEETs containing 3 TMDs called Semi-SWEETs were found. It was shown, that the TMDs of eukaryotic SWEETs

are direct repeats of the bacterial TMDs, separated by a less conserved TMD building up a 3 + 1 + 3 configuration (Chen *et al.* 2015). Therefore, an evolution of eukaryotic SWEETs from prokaryotic SWEETs by gene duplication and fusion is likely and was observed for other transporters before (e. g. ABC-transporters). The crystal structure of Semi-SWEETs was determined by Chen *et al.* 2015 and supports findings that Semi-SWEETs need to form dimers to build up a functional complex (Xuan *et al.* 2013). Even if eukaryotic monomers should be sufficient to form functional pores, there are indications that functional oligomer formation also exists in eukaryotes (Xuan *et al.* 2013, Chen *et al.* 2015).

1.7.2 Classification of SWEETs

The SWEET family is found to be conserved in different members of *planta* (**Table 2**). In dependence of similarities in protein sequence, SWEETs are categorized into four different clades, which were defined for *Arabidopsis thaliana* (Chen *et al.* 2010). SWEETs of clade I and II are specific glucose transporters (Chen *et al.* 2010), while SWEETs of clade III mainly transport sucrose (Chen *et al.* 2012). Clade IV contains fewer members compared to the other clades. The proteins are located in the tonoplast mediating vacuolar transport of fructose (Guo *et al.* 2013).

Table 2: Number of *SWEET* genes in selected plant species. The numbers of *SWEET*s (sugar will be eventually exported transporters) are compared between *A. thaliana*, *O. sativa*, *S. tuberosum*, *M. truncatula* and *P. trichocarpa*.

Organism	Number of SWEET genes	Reference
Arabidopsis thaliana	20	(Chen *et al.* 2010)
Oryza sativa	21	(Chen *et al.* 2010)
Solanum tuberosum	35	(Manck-Götzenberger and Requena 2016)
Medicago truncatula	26	(Hu *et al.* 2019)
Eucalyptus grandis	47	(Eom *et al.* 2015)
Populus trichocarpa	26	(Nehls *et al.* unpublished)

1.7.3 Role of SWEETs in plant-microbe interaction

In *Arabidopsis* leaves highly induced mRNA levels of various numbers of *SWEET*s were detected during the infection with the pathogens *Pseudomonas syringae* and *Botrytis cinerea* (Ferrari *et al.* 2007, Chen *et al.* 2010). The pathogen *Xanthomonas oryzae pv. oryzae* also induced gene expression of different *SWEETs* in rice (Chen *et al.* 2010). The induction in rice is mediated by transcriptional activator like (TAL) effectors from *Xanthomonas oryzae pv. oryzae* (Chu *et al.* 2006, Yang *et al.* 2006, Antony *et al.* 2010, Chen *et al.* 2010). TAL

effectors are secreted by the type III secretion system and were shown to directly bind to the *OsSWEET11* promoter (Chen *et al.* 2010). Loss of TAL based *SWEET* activation resulted in a limited sugar supply and reduced growth of the pathogenic bacteria (Chu *et al.* 2006, Yang *et al.* 2006). The regulation based on TAL effectors was also shown for *OsSWEET11* to *OsSWEET15*, which all belong to clade III (Streubel *et al.* 2013). But not only the *SWEET* promoters of the monocot rice, but also the dicot cassava are targets for TAL effectors of *Xanthomonas pv. manihotis* (Cohn *et al.* 2014). While it already has been shown, that TAL effectors fulfill a regulatory function in inducing gene expression of clade III *SWEETs* in rice; regulatory factors for regulation of the specific glucose transporters of clade I *SWEETs* are unknown.

1.7.4 The glucose carrier SWEET1

It is hypothesized that SWEETs are bidirectional uniporters and the transport happens along a concentration gradient, but this theory is unproven (Chen *et al.* 2015). In *Arabidopsis* the transport of glucose by SWEET1 was shown to happen pH independently with a low glucose affinity (Km ~ 9 mM) (Chen *et al.* 2010). However, these finds cannot rule out a co-transport completely and the detailed transport mechanism is still elusive (Chen *et al.* 2015).

SWEET1 belongs to clade I. The ability to transport glucose was shown for homologs of *Arabidopsis*, *M. truncatula* and *P. trichocarpa* (Chen *et al.* 2010, Nintemann 2012, An *et al.* 2019). In *Arabidopsis* the protein is located in the plasma membrane of leaves and highly expressed in flowers (Chen *et al.* 2010). Two variants of SWEET1 were found in *M. truncatula*. *MtSWEET1a* is highly expressed in flowers, while *MtSWEET1b* is induced upon arbuscular mycorrhiza formation (Benedito *et al.* 2008, An *et al.* 2019). Furthermore, it was shown that *MtSWEET1b* was highly expressed in nodules during Rhizobia interaction (Kryvoruchko *et al.* 2016). It is estimated that *Arabidopsis* has lost the second SWEET1 variant, since it is not able to form mycorrhiza or rhizobia nodules (An *et al.* 2019). In *S. tuberosum StSWEET1b* is clearly induced upon arbuscular mycorrhiza, but not mycorrhiza restricted expressed (Manck-Götzenberger and Requena 2016).

P. trichocarpa contain three genes of *SWEET1* homologs, while *P. tremuloides* contain one homolog (phytozome data base). In *P. trichocarpa SWEET1* was shown to be highly up-regulated upon ectomycorrhiza formation (Nehls and Bodendiek 2012). RNAseq data showed an exclusive expression in roots and no other vegetative organs (Nehls *et al.* unpublished). Sub-cellular localization studies showed the localization of the *P. trichocarpa* homolog to the plasma membrane of *N. benthamiana* leaf cells (Neb 2017).

1.8 Aim of the project

Based on previous studies, the promoter regions of the ECM induced genes *DREB1* and *SWEET1* will be investigated in the model organism poplar in this project. Promoter fragments will be generated and cloned upstream of a fluorescence marker gene. Results will be obtained using composite poplar plants. Expression in non-mycorrhized and mycorrhized roots will be compared using fluorescence microscopy and laser confocal microscopy. The mycorrhization will be performed with two ECM fungi *Amanita muscaria* and *Pisolithus microcarpus*. Furthermore a transient expression system in poplar leaves will be established to investigate whether the expression of *DREB1* and *SWEET1* is specific for root tissue or if expression can also be detected in leaf tissue.

During the generation of composite plants no selection procedure on transgenic roots (ri and biT-DNA or biT-DNA containing) can be performed with antibiotics like it is used in generation of entire transgenic plants, since only the roots and not the shoot become resistant. This leads to growth of transgenic and ri-transgenic roots (only riT-DNA) from the same shoot. In case of the investigation of ECM induced promoters no expression of the marker gene is expected in transgenic roots and therefore discrimination between transgenic and ri-transgenic roots before the mycorrhization procedure is not possible. Since the transformation efficiency in composite poplar formation showed high variation depending on the used plant batch, high deficiencies can occur, which would only be detectable after month of mycorrhization. To maximize time and cost efficiency, a second constitutively expressed marker was integrated into the pPLV vector system in this project. Therefore the expression of Td-Tomato driven by the CaMV35S, UBQ10 and NOS promoter will be tested. Related strategy was already successfully used, studying arbuscular mycorrhiza effects in *M. truncatula* (Kuhn *et al.* 2010).

2 Materials and Methods

2.1 Materials

2.1.1 Plasmid DNA

Table 3: Used plasmid DNA. This table gives information about the original plasmid DNA used in this project. In the first column the name of the plasmid is given. A description about the elements encoded on the plasmid is given in the second column, followed by the origin of the plasmid in the third column. Arabidopsis stock centre can be found at http://arabidopsis.info/.

Plasmid	Description	Origin
pJET1.2/blunt	Ap^R, rep (pMB1), $P_{lac}UV5$, *eco47I*, MCS, T_7 promotor.	Thermo Fisher Scientific, Waltham, Massachusetts.
Sharina 1	Kan^R, rep (Ori pSa), T-DNA [T_{35S}_*NPTII*_P_{35S}, P_{35S}_*sYFP*_T_{Nos}]	AG Nehls unpublished
Sharina 3	Kan^R, rep (Ori pSa), T-DNA [T_{35S}_*NPTII*_P_{35S}, P_{368}_*sYFP*_T_{Nos}]	AG Nehls unpublished
pBinCM_GRX1-roGFP2	Kan^R, rep (Ori V, Ori ColE1), T-DNA [P_{UBQ}_*roGFP2*_T_{OCS}, T_{NOS}_*NPTII*_P_{Nos}]	(Gutscher *et al.* 2008) Arabidopsis stock centre
pBIN19_hygII_P_{UBQ}	Kan^R, rep (Ori V, Ori ColE1), T-DNA [pAg7 (polyadenylation site)_T_*CFP*_P_{NOS}, P_{UBQ}_*NPTII*_T_{HSP18}]	Dr. Neb (RWTH Aachen, Germany)
pPLV04	Kan^R, rep (Ori pSa), T-DNA [T_{35S}_*NPTII*_P_{35S}, MCS_*3xGFP_NLS*_T_{Nos}]	(De Rybel *et al.* 2011) Arabidopsis stock centre
pPLV06	Kan^R, rep (Ori pSa), T-DNA [T_{35S}_*NPTII*_P_{35S}, MCS_*sYFP_NLS*_T_{Nos}]	(De Rybel *et al.* 2011) Arabidopsis stock centre
pPLV11	Kan^R, rep (Ori pSa), T-DNA [T_{35S}_*NPTII*_P_{35S}, *td-tomato_NLS*_T_{Nos}]	(De Rybel *et al.* 2011) Arabidopsis stock centre
pBI121	Kan^R, rep (Ori V, Ori ColE1), T-DNA [T_{NOS}_*NPTII*_P_{NOS}, P_{35S}_*gusA*_T_{Nos}]	Arabidopsis stock centre
pCXUN-FLAG	Kan^R, rep (Ori pBR, Ori pVS1), T-DNA [T_{35S}_*HPTII*_P_{35S}, T_{NOS}_FLAGtag_$P_{maize-UBQ}$]	(Chen *et al.* 2009) Arabidopsis stock centre

2.1.2 Primers

Table 4: Primers to amplify DNA fragments. Primers were synthesized by Eurofins Genomics (Ebersberg, Germany) and solved in 5 mM Tris-HCl. Solutions were stored at -20 °C. The sequences of the primers are given in this table. Included restriction sites were under lined and named. In addition the target name and the used anneling temperature I are given. T_m was calculated using the NEB T_m calculator.

Primer	Sequence (5'-3')	Restriction sites	Target	Used T_m (°C)
OCSShortBamFor	AGGATCCATGCCTGCTTTAATGAGA	*Bam*HI	T_{OCS}	60.1
OCSShortNotRev	AGCGGCCGCTACAATCAGTAAATTGAACG	*Not*I	T_{OCS}	60.1
OcsT_rev_SacI	CTGAGCTCGCTACAATCAGTAAATTGAACG	*Sac*I	T_{OCS}	62.4
NOSpXhoI_for1	AATCTCGAGGATCATGAGCGGAGAATTAA	*Xho*I	P_{NOS}	65
NOSpEcoRI_rev1	CGAGAATTCAGATCCGGTGCAGATTATTT	*Eco*RI	P_{NOS}	65
NOSpNotI_for1	ACTGCGGCCGCGATCATGAGCGGAGAATTAA	*Not*I	P_{NOS}	
Td-tomato_for_SmaI	CATCCCGGGATGACTAGTCCTAAGAAGAAG	*Sma*I	*td-tomato*	62
Td-tomatoRev	ATCCTTACTTGTACAGCT	none	*td-tomato*	62
OcsT_rev_SacI	CTGAGCTCGCTACAATCAGTAAATTGAACG	*Sac*I	T_{OCS}	59
35SP_for_NotI	ATGCGGCCGCAGATTAGCCTTTTCAATTTCAG	*Not*I	$P_{CaMV35S}$	59
UBQp_XhoI-f1	ACTCTCGAGCGACGAGTCAGTAATAAACG	*Xho*I	P_{UBQ10}	59
UBQp_EcoRI_r1	ACTGAATTCGTCTGTTAATCAGAAAAACTCAG	*Eco*RI	P_{UBQ10}	59
UBQp_NotI_f2	ACTGCGGCCGCCGACGAGTCAGTAATAAACG	*Not*I	P_{UBQ10}	59
Ptt7360Pro_f1_KpnI	GTAGGTACCGCTACCATTTAATGAATTAC	*Kpn*I	*Ptt SWEET 1*	61.7
Ptt7360Pro_r1_SmaI	GTACCCGGGCTTATCTAAACCTAACAGTTGTTAC	*Sma*I	*Ptt SWEET 1*	61.7

Ptt7360Pro_r2_SmaI	GTACCCGGGGTCTCTTACTAACCGGGAA	*Sma*I	*Ptt SWEET 1*	61.7

Table 5: Sequencing primers. Primers were synthesized by Eurofins Genomics (Ebersberg, Germany) and solved in 5 mM Tris-HCl. Solutions were stored at -20 °C. pJET1.2 primers were ordered as solution of 10 µM. The sequences of the primers are given in column 2 and the names of the vectors witch can be sequenced with the given primer are given in column 3.

Primer	Sequence (5'-3')	Target vector
pJET1.2 forward	CGACTCACTATAGGGAGAGCGGC	pJET1.2
pJET1.2 reverse	AAGAACATCGATTTTCCATGGCAG	pJET1.2
M13-seq	GTAAAACGACGGCCAGTG	pPLV, pCXUN, pBi121
M13 rev	GGAAACAGCTATGACCATG	pPLV, pCXUN, pBi121

2.1.3 Kits

Table 6: Kits used in this thesis. The purposes and companies from which the kits were ordered are given.

Kit	Purpose	Company
NucleoSpin® Gel and PCR Clean-up	Purification of DNA fragments from agarose slices	MACHEREY-NAGEL GmbH & Co. KG , Düren, Germany
NucleoSpin® Plasmid	Isolation of plasmid DNA from *E. coli* cultures	MACHEREY-NAGEL GmbH & Co. KG , Düren, Germany
Monarch® Plasmid Miniprep Kit	Isolation of plasmid DNA from *E. coli* cultures	New England Biolabs, Ipswich, Massachusetts
CloneJET™ PCR Cloning Kit	Cloning of blunt-end PCR products	Thermo Fisher Scientific, Waltham, Massachusetts

2.1.4 Media

Media were prepared with double distilled water and were autoclaved (20 minutes at 121 °C and 2 bar) or sterile filtered (pore size 0.2 µm; cellulose acetate-membrane; Sartorius, Göttingen, Germany). All chemicals had the purity equal "pro analysi".

2.1.4.1 Luria Bertani (LB) medium (Sambrook *et al.* 1989)

- 15 g/L peptone
- 5 g/L yeast extract
- 5 g/L NaCl
- for plates 18 g/L agar (Serva Kobel)

2.1.4.2 CPY medium

- 5 g/L peptone
- 5 g/L sucrose
- 1 g/L yeast extract
- 0.5 g/L $MgSO4 \times 7\ H_2O$
- for plates 15 g/L agar (Serva Kobel)

2.1.4.3 MS6 medium (Murashige and Skoog 1962)

- 2.2 g/L Murashige & Skoog medium (Duchefa, Haarlem, Netherlands)
- 4 g/L sucrose
- 6.8 g/L plant agar (Duchefa, Haarlem, Netherlands)
- pH was adjusted with potassium hydroxide to pH 5.6

2.1.4.4 MMN medium (Kottke *et al.* 1987)

- 12.28 mg/L KCl
- 15.46 mg/L H_3BO
- 8.45 mg/L $MnSO_4 \times H_2O$
- 5.75 mg/L $ZnSO_4 \times 7\ H_2O$
- 1.25 mg/L $CuSO_4 \times 5\ H_2O$
- 0.18 mg/L $(NH_4)_6Mo_7O_{24} \times 4\ H_2O$
- 25 mg/L NaCL
- 500 mg/L KH_2PO_4 (for mycorrhization 845 mg)
- 250 mg/L $(NH_4)_2HPO_4$ (for mycorrhization 50 mg)
- 50 mg/L $CaCl_2 \times 2\ H_2O$
- 150 mg/L $MgSO_4 \times 7\ H_2O$
- 1 mg/L $FeCl_3 \times 6\ H_2O$
- 20 g agar (Serva Kobel)

add after autoclaving:

- 50 or 10 mM glucose
- 0.1 mg/L Thiaminhydrochlorid (Vit.B_1)
- 1 mg/L Pyridoxinhydrochlorid (Vit. B_6)
- 1 mg/L Nicotinsäure
- 100 mg/L Myo-Inositol

2.1.4.5 MMN 1/5 N medium [modified after (Kottke *et al.* 1987)]

- see MMN medium but:
- 845 mg/L KH_2PO_4
- 50 mg/L $(NH_4)_2HPO_4$

Table 7 Antibiotics and cytostatics. The used antibiotics and cytostatics were all ordered from Duchefa, Haarlem, Netherlands. The final concentrations used in media are listed in Table 7. Stock solutions of the substances were prepared with double distilled water (or 70 % ethanol for tetracycline) and sterile filtered with a pore size of 0.2 µm.

Substance	Final concentration
Ampicillin	100 mg/L
Kanamycin	50 mg/L
Tetracyclin	5 mg/L
Carbenicillin	500 mg/L
Cefotaxime	252 mg/L

2.1.5 Buffers and solutions

All buffers were prepared in double distilled water. Components were autoclaved (20 minutes at 121 °C and 2 bar) or sterile filtered (pore size 0.2 µm; cellulose acetate-membrane; Sartorius, Göttingen, Germany). The purity of used chemicals equals "pro analysi".

2.1.5.1 CTAB extraction buffer

- 2% hexadecyltrimethyl ammoniumbromide solution (CTAB)
- 1.4 M NaCL
- 100 mM Fe (III)- Ethylendiamintetraessigsäure (EDTA)
- 100 mM Tris(hydroxymethyl)-aminomethan (Tris)
- 0.2 % (v/v) β-mercaptoethanol (add freshly)
- pH adjusted with hydrochloric acid to pH 8

2.1.5.2 Wash buffer

- 10 mM ammonium acetate
- 76 % ethanol

2.1.5.3 Tris-EDTA-buffer (TE buffer)

- 10 mM Tris
- 1 mM EDTA
- pH adjusted with hydrochloric acid to pH 7.4

2.1.5.4 Solution I

- 50 mM Tris
- 10 mM EDTA
- 0.1 mg/mL Rnasev A (add after autoclaving)
- pH adjusted with hydrochloric acid to pH 8

2.1.5.5 Solution II

- 1 % (w/v) sodium dodecyl sulfate (SDS)
- 0.2 M NaOH

2.1.5.6 Tris-buffer

- 5 mM Tris
- pH adjusted with hydrochloric acid to pH 8

2.1.5.7 Tris-acetate-EDTA-buffer (TAE buffer)

- 20 mM Tris
- 0.5 mM EDTA
- pH adjusted with pure acetic acid to pH 8

2.1.5.8 6x loading dye purple (New England Biolabs, Frankfurt am Main, Germany)

- 15 %(w/v) Ficoll-400
- 60 mM EDTA
- 19.8 mM Tris-HCl
- 0.48 % (w/v) SDS
- 0.12 % (w/v) Dye 1

- 0.006 % (w/v) Dye 2
- pH 8.0

2.1.5.9 5 x KCM buffer

- 100 mM KCl
- 30 mM $CaCl_2$
- 50 mM $MgCl_2$

2.1.5.10 RF1 Solution

- 30 mM potassium acetate
- 100 mM RbCl
- 10 mM $CaCl_2$
- 50 mM $MnCl_2$
- 15 % (v/v) glycerol
- pH adjusted with acetic acid to pH 5.8

2.1.5.11 RF2 Solution

- 10 mM 3-(N-Morpholino)propansulfonsäure
- 75 mM $CaCl_2$
- 10 mM RbCl
- 15 % (v/v) glycerol
- pH adjusted with potassium hydroxide to pH 6.5

2.1.5.12 MES-buffer

- 10 mM MES
- 10 mM $MgCl_2$
- 150 µM Acetoseringone
- pH adjusted with potassium hydroxide to pH 5.6

2.2 Methods

2.2.1 Cultivation of biological materials

2.2.1.1 *Escherichia coli*

Escherichia coli TOP10F´ cells were grown at 37 °C under aerobe conditions on LB plates or in liquid LB medium under agitation at 200 rpm and sterile conditions. *Escherichia coli* TOP10F´ (lacIqTn10 (TetR))mcrA Δ(mrr-hsdRMS-mcrBC) Φ80lacZΔM15 ΔlacX74 recA1 araD139 Δ(ara-leu)7697 galU galK rpsL endA1 nupG, ordered from Invitrogen, Groningen, Netherlands was used.

2.2.1.2 *Agrobacteria*

Three different *Agrobacteria* strains were used in this thesis: *Agrobacterium rhizogenes* K599 (Daimon *et al.* 1990), *Agrobacterium tumefaciens* C58 (Wood *et al.* 2001) and *Agrobacterium tumefaciens* GV3101 (Holsters *et al.* 1980). All three strains were grown under the same conditions; at 28 °C under aerobe conditions on CPY plates or in liquid CPY medium under agitation at 160 rpm and sterile conditions.

2.2.1.3 Fungal species

Stocks of *Amanita muscaria* (source: collected by Nehls in 2009 in Bremen, Germany) and *Pisolithus microcarpus D2* (source: Maira Pereira, INRA Nancy, France) were cultivated at 18 °C on modified Melin Norkrans medium (MMN) plates containing 50 mM or 10 mM glucose, respectively. Propagation was performed by cutting mycelium in approximately 20 mm^2 parts and transferration to fresh agar plates.

2.2.1.4 *Nicotiana benthamiana*

Plants of *Nicotiana benthamiana* (source: Prof. Dr. Hänsch, TU- Braunschweig, Germany) were seeded on soil. To enhance germination rate the seeds were covered with a glass slide for one week. After two weeks plants were pricked in single pots. All steps were performed at 25 °C with a day-night cycle of 16 h with a light intensity of 75 µmol photons m^2 s^{-1} and relative humidity of 70 %.

2.2.1.5 *Populus tremula x alba*

Populus tremula x *alba* (source: Institute de la Recherche Agronomique, INRA Nancy, France, clone no. 717.1B4) were grown in sterile preserving jars on MS6 medium. Plants were propagated by shoot cuttings. Fresh shoot cutting were transferred every four to eight weeks to fresh MS6. Plants were grown at 18 °C with a day-night cycle of 16 h with a light intensity of 80 µmol photons m^2 s^{-1}.

2.2.2 DNA extraction

2.2.2.1 Extraction of genomic DNA from poplar leaves

0.5 g fresh leave material was grinded with pre-cooled mortar and pestle under liquid nitrogen. The leave powder was transferred to a new mortar and 2.5 mL CTAB extraction buffer (preheated to 60 °C) were added step wise. The obtained suspension was splitted to three 2 mL reaction cups. After incubating the suspension at 60 °C for 30 min and gently mixing every 10 min, 600 µL chlorohorm/isoamylalcohol (24:1) were added to the sample. The sample was mixed by vortexing for 5 sec and centrifuged at 3000 rpm at RT for 10 min. The upper aqueous phase was transferred into a fresh 1.5 mL reaction cup. DNA was precipitated by adding two thirds the volume of pre-cooled isopropanol (4 °C) and gently mixing. After incubation on ice for 10 min sample was centrifuged at 13000 rpm at RT for 10 min. The supernatant was discarded and the precipitated DNA was incubated swirling at RT for 20 min. After a centrifugation step at 13000 rpm at RT for 5 min the supernatant was discarded completely and the DNA pellet was air dried for 3 min. The DNA pellet was

resuspended in 150 µL TE buffer containing RNAse (10 µg/mL) by gently flicking and incubation steps at RT for 5 min, at 50 °C for 5 min and at RT for 5 min in connection with an incubation step at 37 °C for 30 min. Afterwards lithium chloride precipitation was performed. Genomic DNA was stored at 4 °C.

2.2.2.2 Lithium chloride precipitation

1/10 volume of 4 M lithium chloride solution was added to 1 volume of DNA sample and mixed gently by flicking. Two times the volume of 100 % ethanol was added for precipitation and samples were gently mixed and incubated at RT for 1 hour. After centrifugation at 13000 rpm at RT for 10 min, the supernatant was discarded and 10 times the volume of 70 % ethanol was added to the pellet. Samples were centrifuged at 13000 rpm at RT for 10 min and pellets were air dried at 50 °C for 5 min after discarding the supernatant. Genomic DNA pellets were solved in 1 volume of TE buffer (stored at 4 °C) and plasmid DNA pellets in 1 volume of 5 mM Tris buffer (stored at -20 °C).

2.2.2.3 Plasmid preparation by alkaline lysis from *Escherichia coli* (Sambrook et al. 1989)

Single colonies of *Escherichia coli* were transferred with toothpicks in reaction tubes containing 3 mL LB medium and cultivated as descripted in 2.2.1.1. Cells were harvested from 2 mL of a freshly grown overnight culture by centrifugation for 5 min at 16 000 x g and RT. The cell pellet was resuspended in 300 µL of solution I. The addition of the same amount of solution II was followed by carefully mixing the sample by inverting 8 times and an incubation of maximal 5 min at RT. Ice cold 1.5 M potassium acetate solution pH 4.8 was added to a final concentration of 375 mM, samples were mixed 8 times by inverting and incubated for 30 min on ice. After 20 min centrifugation at 16 000 x g at 4 °C, the supernatant was transferred to a fresh 1.5 mL reaction tube. DNA was precipitated by adding 500 µL of 100 % isopropanol, incubation for 20 min on ice and centrifugation for 30 min at 16 000 x g and RT. The supernatant was discarded. 500 µL of 70 % ethanol were added and samples were inverted 8 times. After 10 min of centrifugation at 16 000 x g and RT, the supernatant was discarded and pellets were dried in a heat block for 5 min at 50 °C. Dried pellets were dissolved in 20 µL of 5 mM Tris/HCl pH 8. Plasmid DNA was stored at -20 °C.

2.2.3 Methods for DNA analysis

2.2.3.1 Agarose gel electrophoresis (Sambrook *et al.* 1989)

Agarose gel electrophoresis was performed using 1-2 % (w/v) agarose gels prepared with 0.5 x TAE buffer. Samples were combined with 6 x loading dye to a final concentration of 1 x. The gel was stacked with 0.5 x TAE buffer and samples were loaded. For samples with a fragment size larger than 600 bp Phage Lambda DNA/*Sty*I marker (Bioron, Ludwigshafen am Rhein, Germany), while for samples with a fragment size smaller than 600 bp the Gene Ruler 100 bp plus DNA ladder (Thermo Fisher Scientific, Waltham, Massachusetts) was used as size reference. Separation was performed applying 60-80 V for 40 to 60 min. For visualization gels were stained in ethidium bromide solution (0.2 % (w/v)) for 10 to 30 min and documented under UV light of 312 nm (Bachofer, Reutingen, Germany) with a camera system from peqlab biotechnology GmbH (Erlangen, Germany).

2.2.3.2 DNA treatment with restriction enzymes

Restriction analysis was performed using enzymes obtained from New England Biolabs (Ipswich, Massachusetts) or Thermo Fisher Scientific (Waltham, Massachusetts). 500 ng to 1 µg of DNA were analyzed with 2 units of restriction enzymes. The reaction was prepared using the recommended buffer in a final concentration of 1 x in a total volume of 20 µL. The results of restriction analysis were monitored by gel electrophoresis (2.2.3.1).

2.2.3.3 Spectrophotometric determination of DNA concentration

DNA concentrations were determined by photometric determination using the Nanodrop 1000 spectrophotometer (peqlab, Erlangen, Germany).

2.2.3.4 Sample preparation for sequencing

Sanger sequencing was performed by Macrogen (Amsterdam, Netherlands). The samples were prepared using 500 ng of DNA and 50 pmol of the sequencing primer filled up with nucleases free water to 10 µL. Sequencing results were analyzed using geneious (version 6.1.8, Biomatters, Auckland, New Zealand).

2.2.3.5 *In silico* tools for DNA analysis

Sequences of gDNA, plasmids and sequencing reactions were analyzed using the geneious software package (version 6.1.8, Biomatters, Auckland, New Zealand). The program was used to compare sequences using the alignment tool or find restriction sites. All cloning processes were prepared *in silico* within the software before lab performance. Also map drawing was performed with this software package.

2.2.4 Polymerase chain reactions

2.2.4.1 Amplification with Q5 polymerase

The Q5 polymerase system (New England Biolabs, Ipswich, Massachusetts) was applied to amplify from genomic DNA or plasmid DNA. Final concentrations of 200 µM dNTPs (Boehringer Ingelheim, Ingelheim am Rhein, Germany), 1.25 µM of each primer and the reaction buffer in a final concentration of 1x containing 2 nM Mg^{2+}were used. Additionally, 200 ng to 600 ng of DNA template for amplification and a final concentration of 0.02 U/µL of the Q5 polymerase were utilized. The reaction was performed in a total volume of 20 µL. For amplification a Tgradient cycler from Biometra (Jena, Germany) and the PCR program given in **Table 8** were used. PCR products were stored at -20 °C and purified using the NucleoSpinR Gel and PCR Clean-up kit (MACHEREY-NAGEL, Düren, Germany) before cloning.

Table 8: PCR program for amplification with Q5 polymerase. The annealing temperature I was calculated using the online tool Q5 Tm calculator of NEB. The extension time was calculated according to an amplification rate of 30 sec/bp.

Step	Temperature	Time	Cycles
Initial denaturation	98 °C	30 s	
Denaturation	98 °C	10 s	35 x
Annealing	Tm °C	30 s	
Extension	72 °C	Q5 30 sec/ kb	
Final extension	72 °C	10 min	

2.2.5 DNA processing in molecular cloning

2.2.5.1 Cloning into the entry vector pJET1.2

The pJET1.2 cloning kit from Thermo Fisher Scientific (Waltham, Massachusetts) was used. Ligation mixture was set up on ice. The components were unfrozen on ice and carefully mixed before use. 2 x reaction buffer was used in a final concentration of 1 x. 50 ng of the pJET1.2 vector were used for ligation. PCR products were cloned in a molar ratio of 1:3 (vector : insert). The reaction mix was filled up to 19 µL with ddH_2O and 1 µL ligase was added at last followed by brief vortexing of 3-5 sec. The reaction was incubated for 5 to 30 min at 22 °C in a PCR machine and was either directly used for transformation or stored at -20 °C.

2.2.5.2 Blunting of DNA

The reaction was prepared on ice and all components were carefully mixed. The blunting reaction was prepared using 10 x fast digest buffer (Thermo Fisher Scientific, Waltham,

Massachusetts) in a final concentration of 1 x and the respective dNTPs (Boehringer Ingelheim, Ingelheim am Rhein, Germany) in a final concentration of 1 mM each. 1 unit of the klenow enzyme (Thermo Fisher Scientific, Waltham, Massachusetts) was used to blunt DNA amounts between 500 ng to 1 µg and reaction was filled up with ddH_2O to 20 µL. The reaction was incubated for 15 min at 37 °C and was stopped by adding EDTA in a final concentration of 20 mM followed by a heat inactivation for 10 min at 65 °C. DNA was directly used for downstream applications or was stored at -80 °C.

2.2.5.3 Dephosphorylation of DNA

Single digested vectors and blunted vectors were dephosphorylated before use in ligation reactions. The reaction was prepared with 10 x cutsmart buffer (New England Biolabs, Ipswich, Massachusetts) used in a final concentration of 1 x. 1 unit of the shrimp alkaline phosphatase (New England Biolabs, Ipswich, Massachusetts) was used to dephosphorylate DNA amounts of 500 ng. The reaction was filled up with ddH_2O to 20 µL and carefully mixed. Dephosphorylation was incubated for 30 min at 37 °C and heat inactivated for 5 min at 65 °C. DNA was directly used for downstream applications or was stored at -80 °C.

2.2.5.4 Ligation reaction

Ligation was performed using ligase from NEB. The 10 x T4 DNA ligase buffer (New England Biolabs, Ipswich, Massachusetts) was unfrozen on ice and resuspended at RT shortly before preparation of the reaction. T4 DNA ligase buffer was used in a final concentration of 1 x. 50 ng of the vector were used for ligation and a molar ratio of 1:3 of vector to insert was used. The reaction was filled up to 20 µL with ddH2O and the T4 DNA ligase (New England Biolabs, Ipswich, Massachusetts) was added at last. The reaction was carefully mixed by pipetting up and down and spined down. For sticky end ligations ligation was incubated 10 min at 22 °C or overnight at 18 °C. Blunt end ligations were incubated 2 h at 22 °C or overnight at 18 °C. Ligation reactions were heat inactivated for 10 min at 65 °C and directly used for transformation or stored at -20 °C.

2.2.6 Transformation of bacterial cells

2.2.6.1 Preparation of chemical competent *Escherichia coli* TOP'10 cells (Hanahan 1983)

A pre-culture of *E. coli* TOP'10 cells was grown overnight in 3 mL LB medium shaking at 200 rpm at 37 °C. The main-culture was prepared with 50 mL LB medium in a 100 mL flask using 500 µL of the overnight culture for inoculation and grown under aggregation at

200 rpm at 37 °C till an OD_{600} of 0.7 was reached. After an incubation of 10 min on ice, cells were pelleted by centrifugation for 15 min at 2000 x g and 4 °C. The cell pellet was resuspended in 18 mL RF1 solution shaking carefully on ice bath, followed by incubation for 30 min on ice. In the next step cells were pelleted by centrifugation for 15 min at 2000 x g and 4 °C. 4 mL of RF2 solution were used to resuspend cells carefully by shaking on ice bath. The cell suspension was frozen as 100 µL aliquots in liquid nitrogen and stored at -80 °C.

2.2.6.2 Transformation of *Escherichia coli* TOP'10 (Sambrook *et al.* 1989)

Chemical competent *E. coli* TOP'10 cells of a competence of 2 x 10^7 till 1 x 10^8 CFU/µg DNA were used. A 100 µL aliquot of competent cells was unfrozen on ice for 10 min. A mixture of 1 x KCM buffer with DNA amounts between 60 and 80 ng was prepared and added to the cells, followed by 20 min incubation on ice. The cells were heat shocked for exactly 2 min at 42 °C. After 1 min incubation on ice, 600 µL of LB medium were added and cells were incubated 1 h at 37 °C under aggregation. The cells were centrifuged down for 3 min at 8 000 x g and RT. The cell pellet was resuspended in 100 µL LB medium. 10 µL and 90 µL of the cell suspension were plated on selective LB medium and incubated over night at 37 °C.

2.2.6.3 Preparation of chemical competent *Agrobacteria*

To prepare chemical competent *A. rhizogenes K599*, *A. tumefaciens C58* or *A. tumefaciens GV3101* cells, 20 mL CPY medium in a 100 mL flask were inoculated with a single colony. The pre-culture was incubated overnight under agitation at 140 rpm and 28 °C. For the main-culture 50 mL of CPY medium in a 300 mL flask were inoculated with the pre-culture to a final OD_{600} of 0.1 and incubated under agitation at 140 rpm at 28 °C until an OD_{600} of 0.5 to 0.8 was reached. 10 min incubation on ice was followed by a centrifugation for 10 min at 4000 rpm and 4 °C. The pelleted cells were resuspended in 20 mL 150 mM NaCl on ice and centrifuged again for 10 min at 4000 rpm and 4 °C. 2 mL 20 mM $CaCl_2$ were used for resuspension and cell suspension was frozen as 100 µL aliquots in liquid nitrogen and stored at -80 °C.

2.2.6.4 Transformation of *Agrobacteria* (Holsters *et al.* 1978)

Self-made chemical competent *A. rhizogenes K599*, *A. tumefaciens C58* or *A. tumefaciens GV3101* cells were used. A 100 µL aliquot of competent cells was unfrozen for 1 h on ice. 1 µg plasmid DNA was added to the unfrozen cells and incubated for 10 min on ice. Thereafter cells were frozen for 5 min in liquid nitrogen, followed by an incubation of 5 min at 37 °C. 800 µL of CPY medium were added directly for cell regeneration and cells were incubated

for 4 h at 28 °C. Cells were pelleted for 3 min at 3000 x g at RT and resuspended in 100 µL CPY medium. Cells were plated on selective CPY medium and grown at 28 °C for one week.

2.2.7 Expression methods *in planta*

2.2.7.1 Infiltration of *Nicotiana benthamiana* leaves

Transgenic *Agrobacteria* were cultivated in 20 mL CPY medium with selective antibiotic overnight under aggregation of 160 rpm at 28 °C. The cells were harvested by centrifugation for 20 min at 3000 g at RT. The pellet was resuspended in MES-buffer and the OD_{600} was adjusted to 0.3. The bacterial suspension was incubated for 2 h under aggregation at 160 rpm and 28 °C. Leaves of four to six weeks old plants were infiltrated with the bacterial suspension using a syringe without a needle. Results were analyzed after three to five days of incubation at 25 °C with a day-night cycle of 16 h with a light intensity of 75 µmol photons m^2 s^{-1} and relative humidity of 70 %. If not otherwise stated, infiltration was performed using three different plants and two to three leaves of each plant.

2.2.7.2 *Agrobacteria*-mediated transformation of *Populus tremula x alba* leaves

Transgenic *Agrobacteria* from strain *A. tumefaciens C58* were cultivated in 20 mL CPY medium with selective antibiotics overnight under aggregation of 160 rpm at 28 °C. The cells were harvested by centrifugation for 20 min at 3000 x g at RT. The pellet was resuspended in MES-buffer and the OD_{600} was adjusted to 0.3. The bacterial suspension was incubated for 2 h under aggregation at 160 rpm at 28 °C. For transformation leaves of *Populus tremula x alba* were used. Leaves were removed from plant and infiltrated with the bacterial suspension under sterile conditions. The infiltrated leaves were incubated on MS6 agar plates for 3 to 7 days at 22 °C with a day-night cycle of 16 h with a light intensity of 80 µmol photons m^2 s^{-1}. If not otherwise stated, infiltration was performed using three different plants and three to four leaves of each plant.

2.2.7.3 Generation of composite poplar plants with transgenic roots (Neb *et al.* 2017)

Fresh shoot cuttings of *Populus tremula x alba* containing two to three leaves were used for transformation. Cuttings were prepared using a scalpel with a fresh blade under sterile conditions. The shoot cuttings were inoculated with transgenic *A. rhizogenes* on the cutting site. Bacteria were freshly cultivated on CPY plates containing selective antibiotics and 200 µM acetoseringone for two days at 28 °C before plant transformation. The inoculated shoots were inserted into MS6 medium and incubated for 3 days at 22 °C with 48 µmol

photons m^{-2} s^{-1} illumination and 16 h day-night rhythm. After 3 days the shoots were transferred to fresh MS6 medium containing 1.18 mM carbenicillin and 0.52 mM cefotaxime, to soak excess humidity two cotton rolls were placed within the petri dish. Plants were cultivated for three to six weeks under described conditions. Experiments were performed using a minimum of ten plants per batch and were repeated three times with plants for independent cultured plant batches.

2.2.8 Mycorrhization of *Populus tremula x alba* (Fründ & Nehls unpublished)

Composite poplar plants (2.2.7.3) were used three to four weeks after transformation for mycorrhization. As fungi partner *Amanita muscaria* or *Pisolithus microcarpus D2* were used. Both fungi were cultured as described in 2.2.1.3 for three to four weeks. Before mycorrhization small parts of the mycelium of the fungi were transferred onto fresh MMN plates covered with foil and were pre-cultured two to three weeks at 22 °C. The mycorrhization was performed on MMN 1/5 N medium in square petri dishes. Firstly, half of the medium was removed with a sterile scalpel and the pre-cultivated fungi were transferred with the cellophane foil to the mycorrhization plate, in way that the agar is covered completely. Next the poplar plants were taken out of the petri dish and the remaining agar is removed with sterile forceps. Three to four plants can be transferred to one plate for mycorrhization. The fungal mycelia and plant roots were covered with a sterile substrate with equal parts of vermiculite, clay and coconut fiber (presoaked with MMN medium). To soak excess humidity three cotton rolls were placed within the petri dish. The petri dish systems were closed with pressure-sensitive adhesive tape and incubated for two to four month at 22 °C with 48 µmol photons m^{-2} s^{-1} illumination and 16 h day-night rhythm.

2.2.9 Analysis of plant material

2.2.9.1 Generation of root cuttings

Roots were embedded in 4 % agarose before sectioning. Solidified agarose blocks were fixated on vibratome fixation plate using 4 % agarose. Root cuttings with a thickness between 50 µm and 80 µm were prepared using a vibratome (VT1000S, Leica Microsystems, Wetzlar, Germany). For inspection samples were placed on slides in a water drop covered by a cover slip.

2.2.9.2 Analysis of plant material with a binocular

Prepared plant samples were analyzed using a binocular (Mz10F, Leica Microsystems, Wetzlar, Germany). As UV-light source Lej LQ-HXP 120 (Leistungselektronik JENA GmbH, Jena, Germany) was used. Information about the used filter sets are given in **Table 9**. For documentation a Leica camera (DFC425C, Leica Microsystems, Wetzlar, Germany) was used.

Table 9: Properties of different fluorescence filters. The described filters were ordered from Leica Microsystems (Wetzlar, Germany). The extension and emission spectra are given in this table.

Filter name	Extension	Emission
GFP	450 – 490 nm	500 – 550 nm
YFP	500 – 520 nm	540 – 580 nm
RFP	510 – 560 nm	590 – 650 nm

2.2.9.3 Analysis of plant material using a fluorescence microscope

Prepared plant samples were analyzed using Leica DMRB microscope (Leica Microsystems, Wetzlar, Germany). As UV-light source a Lej LQ-HXP 120 (Leistungselektronik JENA GmbH, Jena, Germany) was used. Information about the used filter sets are given in **Table 10**. For documentation the Leica camera (DFC425C, Leica Microsystems, Wetzlar, Germany) was used.

Table 10: Properties of different fluorescence filters. The described filters were ordered from Leica Microsystems (Wetzlar, Germany). The extension and emission spectra are given in this table.

Filter name	Extension	Emission
GFP	450 – 490 nm	500 – 550 nm
YFP	490 – 510 nm	520 – 550 nm
RFP	540 – 580 nm	595 – 635 nm

2.2.9.4 Confocal laser scanning microscopy (cLSM)

Prepared leaf or root samples were investigated using cLSM 880 (Zeiss, Oberkochen, Germany). For excitation of the different fluorescence proteins an argon laser (488 nm) or a helium neon laser (543 nm) was used. In case of the simultaneous use of both lasers at the same time a beam splitter avoided light detection between 540 and 548 nm. The emission light was sensed by PMT detector. The used laser intensities are given in the figure descriptions. For all pictures the 20x objective with a numeric aperture of 0.8 was used (20er Plan appopromata20er/0.8 M27, Zeiss).

3 Results

3.1 Vector construction and testing for promoter analysis in poplar

In entire transgenic plants, that are regenerated from single transformed cells, a dominate selection marker is requested to prevent non-transgenic cells to grow. Such a strategy is, however not successful for composite plants, as only the roots but not the shoot would become resistant. One problem of *A. rhizogenes* based composite plants is that transgenic roots always contain the T-DNA of the Ri-plasmid, but not necessarily the T-DNA of the binary vector (biT-DNA). As the transformation efficiency concerning the integration of the biT-DNA can vary a lot, a selection marker for roots harboring both T-DNAs would be rather helpful. One possibility is the introduction of a second constitutively expressed fluorescence marker, into the biT-DNA.

3.1.1 Construction and establishment of a constitutively expressed red fluorescence marker cassette in poplar

For constitutive expression of a given gene in transgenic poplar roots, different promoters were tested. In a former PhD thesis a 368 bp large DNA fragment from a promoter region from *P. trichocarpa* was found to give strong signals in non-mycorrhized roots (Neb 2017). In addition to this *P. trichocarpa* promoter, the cauliflower mosaic virus 35S (CaMV35S) promoter, the ubiquitin 10 (UBQ10) promoter from *Arabidopsis* and nopaline synthase (NOS) promoter from *Agrobacterium tumefaciens* were tested. As terminator the octopine synthase (OCS) terminator was chosen. The assembly of the marker cassettes was performed in the pPLV vector system.

3.1.1.1 Construction of a marker cassette containing a nuclear targeted Td-Tomato and a 368 bp fragment of a *P. trichocarpa* promoter

To avoid repetitive homologous sequences within the biT-DNA the NOS terminator was exchanged with the OCS terminator. The OCS terminator was amplified from the plasmid pBinCM_GRX1-roGFP2 (Gutscher *et al.* 2008) with *Bam*HI and *Not*I overhangs (**Sup. Figure 1**) and cloned into the entry vector pJET1.2. The insertion of the OCS terminator was verified by restriction digestion and sequencing (**Sup. Figure 1**).

OCS terminator was released with *Bam*HI and *Not*I and inserted into the *Bam*HI / *Not*I digested vector Sharina 3 (Neb *et al.* 2017). By integration into Sharina 3, a cassette carrying the 368 bp promoter fragment and the OCS terminator with a unique *Bam*HI site in between was created (Sharina_P_{368}_T_{OCS}, **Figure 4 A**). The correct integration of the OCS terminator was verified using *Bam*HI / *Not*I double digestion and sequencing (**Sup. Figure 2 A**).

A fragment containing a Td-Tomato coding sequence harboring a N-terminal nuclear targeting signal was generated from pPLV11 (De Rybel *et al.* 2011) by *Bam*HI digestion. The fragment was integrated into the *Bam*HI linearized and dephosphorylated Sharina_P_{368}_T_{OCS} vector (**Figure 4 B**). Positive clones were identified by *Bam*HI digestion (**Figure 4 B**) and further analyzed by *Nco*I and *Nco*I/*Sac*I digestion, to determine the orientation of the *td-tomato* DNA (data not shown). The DNA of a clone containing *td-tomato* inserted in forward direction was verified by sequencing (**Sup. Figure 2 B**).

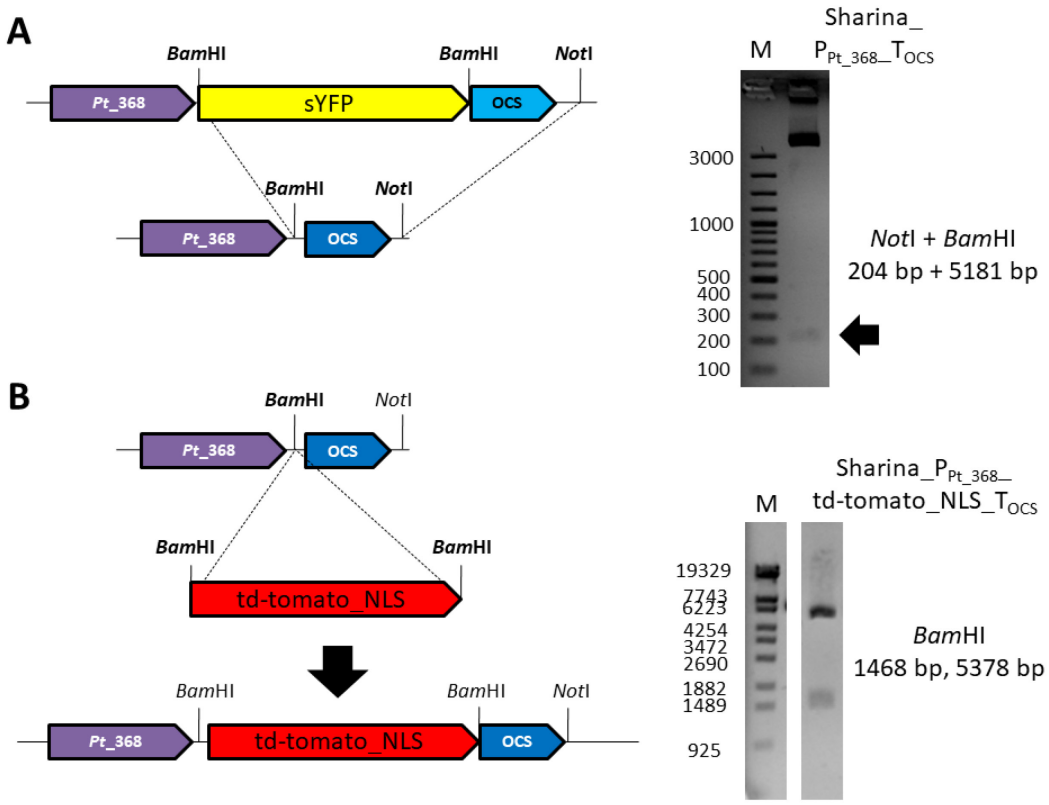

Figure 4: Construction of a *td-tomato_NLS* marker cassette. The figure shows at the left side the construction scheme of the marker cassette consisting of the *P. trichocarpa* promoter (*Pt_368*) and the coding sequence of a Td-Tomato with nuclear localization signal (NLS), and the octopine synthase terminator (OCS) At the right site corresponding agarose gels are shown. A) Exchange of the OCS terminator by *Bam*HI and *Not*I and integration of a *Bam*HI and *Not*I fragment. As marker 3 µL Gene Ruler 100 bp plus DNA ladder (Thermo Fisher Scientific, Waltham, Massachusetts) was used on 2 % agarose gel. B) The integration of the Td-Tomato_NLS coding sequence into Sharina 3 and verification with *Bam*HI digestion on 1 % agarose gel with Phage Lambda DNA/*Sty*I marker (Bioron, Ludwigshafen am Rhein, Germany) is given.

After poplar transformation with Sharina_P_{368}_td-tomato_NLS_T_{OCS}, no Td-Tomato fluorescent signal was detected in roots. Therefore the *Agrobacteria* strain with the original P_{368} construct (Neb 2017) harboring the 368 bp long fragment from *P. trichocarpa* in front of a sYFP were tested (data not shown), but also failed to reproduce fluorescent protein expression. The respective promoter fragment was thus omitted from further investigations.

3.1.1.2 Construction of marker cassettes expressing a nuclear targeted Td-Tomato under the control of selected constitutive promoters

Promoter and Td-Tomato coding sequence were removed by *Xho*I / *Bam*HI digest from Sharina_P_{368}_td-tomato_NLS_T_{OCS} to generate the vector backbone. To allow the specific insertion of promoter sequences, *Xho*I/*Bam*HI CaMV35S promotor fragment was obtained from Sharina1 (Nehls unpublished) and was integrated in the vector backbone. This construct obtained unique restriction sites for *Eco*RI and *Hpa*I upstream of the *Bam*HI site (**Figure 5 A**). This strategy allows the directed integration of the nuclear targeted Td-Tomato coding sequence into *Sma*I and *Bam*HI sites (**Figure 5 B**). Therefore, a *td-tomato*_NLS fragment was PCR amplified from pPLV11 with primers containing *Sma*I and *Bam*HI sites respectively and cloned into the entry vector pJET1.2 (**Sup. Figure 3**). The resulting construct allows the directed exchange of promoter sequences by *Xho*I / *Eco*RI sites according to **Figure 5 C**, which was used to generate ubiquitin and NOS promoter reporter constructs in the next step.

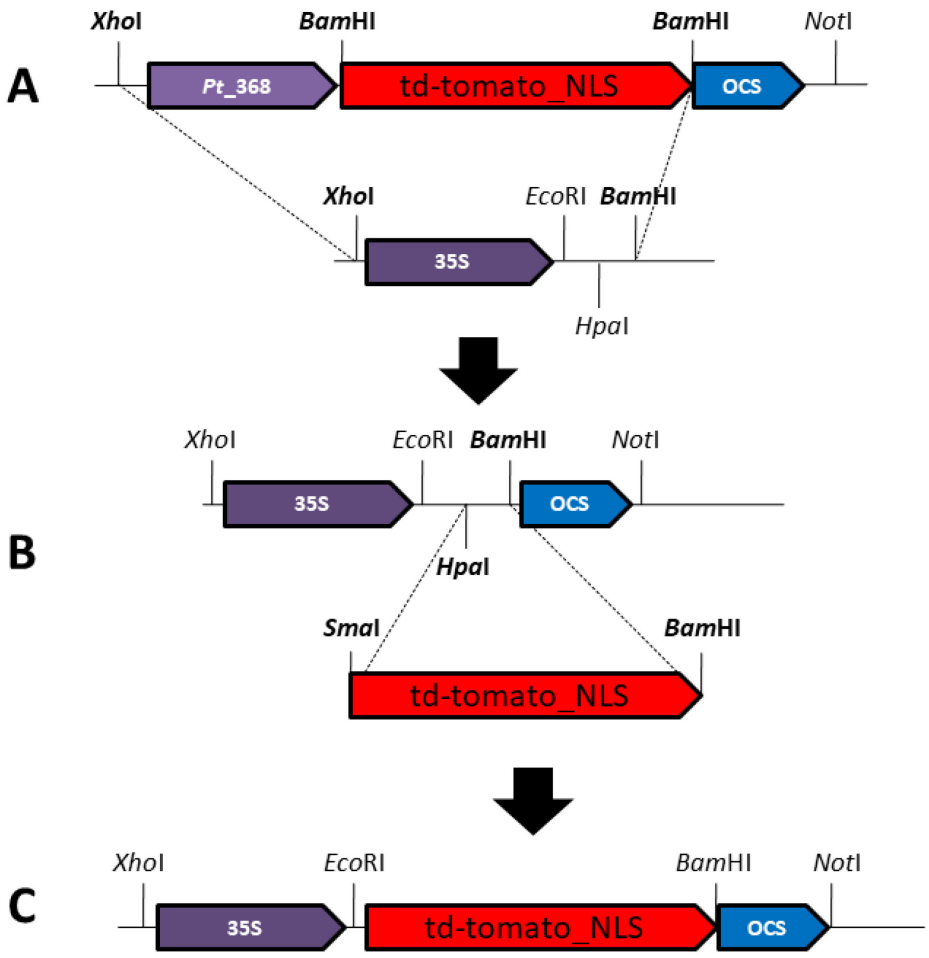

Figure 5: Construction scheme of CaMV35S promoter driven Td-Tomato_*NLS* expression cassette. The scheme presents the cloning steps which were performed to clone an expression cassette driven by the 35S cauliflower mosaic virus promoter. As marker Td-Tomato with nuclear localization signal (NLS) was used. Transcription is terminated by the octopine synthase terminator (OCS). A) The restriction enzymes *Xho*I and *Bam*HI were used to integrate the CaMV35S promoter with two additional restriction sites *Eco*RI and *Hpa*I. B) In the next step Td-Tomato_NLS coding sequence fragment was generated with *Sma*I and *Bam*HI and cloned into the *Hpa*I and *Bam*HI sites of the pPLV vector. In C the completed marker construct is shown.

A compatible UBQ10 promoter fragment was PCR amplified from pBIN19_hygII_P_{UBQ10} (Neb, RWTH Aachen, Germany) with primers containing additional *Xho*I / *Eco*RI sites. Amplification and cloning into pJET1.2 was performed by a lab rotation master student Paulina Mendosa (AG Nehls). The NOS promoter sequence was amplified from pBinCM_GRX1-roGFP2 (Gutscher *et al.* 2008) with primers containing additional *Xho*I / *Eco*RI sites and cloned into pJET1.2 (**Sup. Figure 4**). The obtained promoter fragment was released by *Xho*I / *Eco*RI digest and used for a promoter exchange together with pPLV_$P_{CaMV35S}$_td-tomato_NLS_T_{OCS} generating pPLV_P_{UBQ10}_td-tomato_NLS_T_{OCS} and pPLV_P_{NOS}_td-tomato_NLS_T_{OCS} (**Figure 6 A 1, 2, 3**). The generated constructs were confirmed by restriction analysis with *Xho*I / *Eco*RI and *Nco*I (**Figure 6 B**).

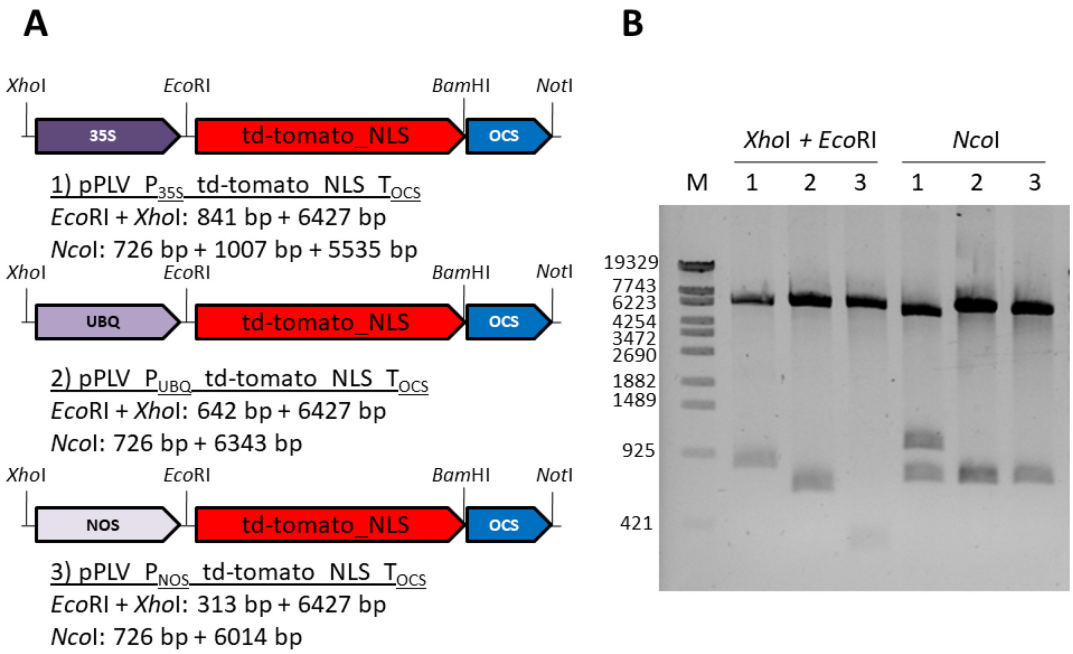

Figure 6: Scheme of the *td-tomato* expression cassettes and verification of promoter constructs. A) The constructs named are shown as scheme at the left site. In addition the expected fragment sizes for restriction analysis with *Eco*RI / *Xho*I and *Nco*I are given. B) Digested DNA fragments were separated on a 1 % agarose gel. As marker 3 µL of Phage Lambda DNA/*Sty*I marker were used. The numbers stand for the three different constructs, which are given in A.

3.1.1.3 Functional analysis of nuclear targeted Td-Tomato constructs in *N. benthamiana* leaf cells and *P. tremula x alba* roots

For *in planta* testing of the generated constructs, the respective vectors were transformed into *Agrobacteria*. For this purpose *A. rhizogenes* K599 was chosen, since it was successfully used for generation of *P. tremula x alba* composite plants (Neb *et al.* 2017), as well was transient expression in *N. benthamiana* leaves in previous studies. However, transformation of *A. rhizogenes* K599 with the designed pPLV plasmids failed. Chemical transformations as well as electroporation with different batches of competent cells were tried out without success. However, transformation of the same bacterial cell batches with the plasmids pCXUN and pBi121 harboring different backbone origin was successful. In literature it was postulated that pPLV based plasmids can replicate in *A. rhizogenes* K599 (Cevallos *et al.* 2008). In our hand, however, successful transformation of A. rhizogenes K599 was only possible when bacteria harbored the helper plasmid pSOUP as previously descripted for *A. tumefaciens* strains (Hellens *et al.* 2000). This result was obtained in collaboration with Anneke Immor and Jana Müller (AG Nehls). Functional analysis of the designed pPLV plasmids was therefore performed using an *A. rhizogenes* K599 strain harboring pSOUP.

The result of the *in planta* functionality of the designed marker cassettes was firstly tested in *N. benthamiana* leaves. *N. benthamiana* leaf infiltration was chosen as it gives results already after two to three days, while transgenic root formation by composite poplar formation lasts at least four weeks. Red fluorescent nuclei were observed for all three constructs for transient expression in *N. benthamiana* leaves as well as stable transformation of poplar roots (**Figure 7**). The CaMV35S promotor driven construct gave the strongest signal, followed by signals generated by the NOS promoter, while the lowest signal was observed under control of the UBQ10 promoter (**Figure 7 compare a, b, c**).

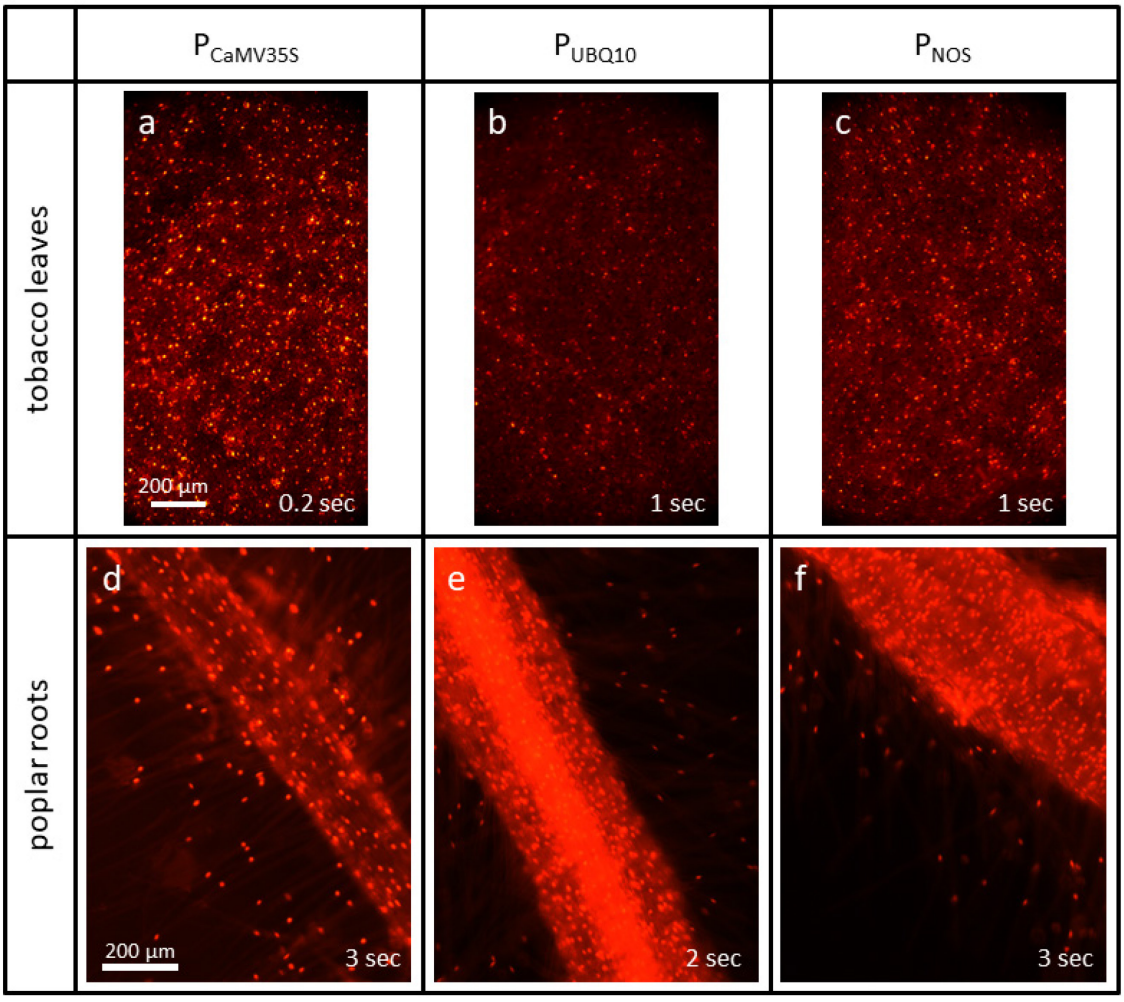

Figure 7: Detection of Td-Tomato signals in nuclei of *N. benthamiana* leaves and *P. tremula x alba* roots. The expression strength of molecular encoded Td-Tomato_NLS was compared for three different plant promoters; the cauliflower mosaic virus promoter ($P_{CaMV35S}$) (a + d), the *Arabidopsis* ubiquitin promoter 10 (P_{UBQ10}) (b + e) and the *Arabidopsis* nopaline synthase promoter (P_{NOS}) (c + f) in *N. benthamiana* leaves (a - c) and *P. tremula x alba* roots (d - f). *N. benthamiana* leaves were infiltrated with transgenic *A. rhizogenes K599* pSOUP and results were analyzed after 3 days using a binocular Mz10F (Leica Microsystems) (a, b, c). Roots of composite *P. tremula x alba* were analyzed after 5 weeks with the same equipment (d, e, f). The exposure times are given in the pictures. Excitation window was between 510 – 560 nm and the emission window between 590 – 650 nm (for technical details see 2.2.9.2).

Typical pictures of *P. tremula x alba* roots expressing nuclear localized Td-Tomato after transformation with respective constructs are shown (**Figure 7**). The highest signal intensity was obtained with the UBQ10 promoter in cortical root cells, while only weak signals were detectable in root hairs with this promoter, which was reproducible (**Figure 7 e**). Signal intensity obtained with CaMV35S promotor (**Figure 7 d**) and NOS promoter (**Figure 7 f**) were comparable and equally distributed in cortex and root hairs, but lower as in cortical cells expressing Td-Tomato under control of P_{UBQ} (**Figure 7 e**). The differences in signal intensities between the three promoters were, however, much smaller as in *N. benthamiana* leaves.

3.1.2 Expression of the tandem marker system in *N. benthamiana* leaf cells and *P. tremula x alba* roots

Next to the constitutive expressed Td-Tomato marker cassette, the presence of a second, marker cassette for the investigation of foreign promoters needed to be established. A peroxisomal targeted sYFP has been successfully used in previous experiments in poplar roots (Neb 2017). For a first test whether such a tandem cassette would works in general, a Td-Tomato cassette driven by NOS promoter, was integrated downstream of CaMV35S promotor driven peroxisomal targeted sYFP (provided by Jana Müller, AG Nehls). The Td-Tomato containing marker cassette was amplified with primers containing additional *Not*I / *Sac*I restriction sites that allowed integration into the pPLV vector harboring an analytical sYFP cassette. The obtained PCR products were firstly cloned into pJET1.2 and verified by restriction analysis and Sanger sequencing (**Sup. Figure 6**).

A first *in planta* test of this double marker construct was performed in *N. benthamiana* leaves. The infiltrated leaves showed fluorescence signals in structures of the size of peroxisomes in the YFP channel (**Figure 8 a**) and a signal in the RFP channel within the size range of a nucleus (**Figure 8 b**), which shows that the tandem cassette principle works in *N. benthamiana* leaf cells.

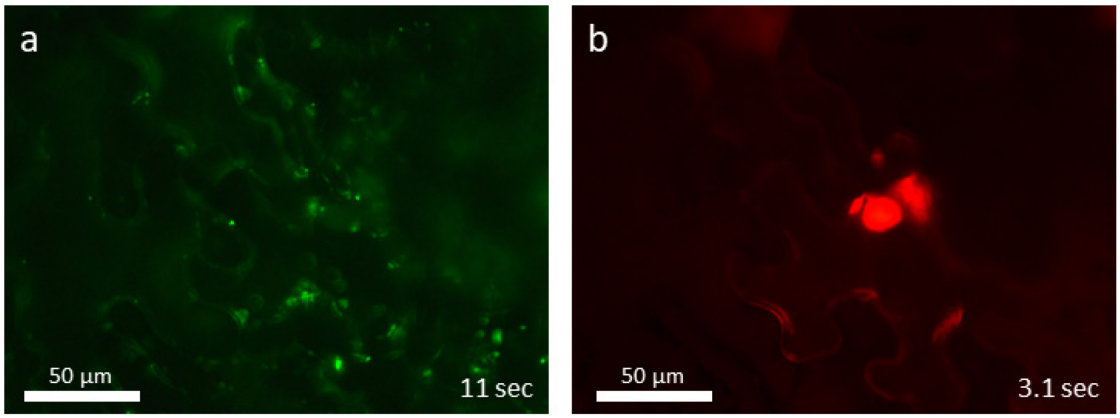

Figure 8: *Nicotiana benthamiana* leaf cells harboring a double fluorescence marker construct. Leaves were infiltrated using *A. rhizogenes* K599 pSOUP pPLV_$P_{CaMV35S}$_sYFP_SNL_T_{NOS}_P_{NOS}_td-tomato_NLS_T_{OCS}. After 3 days leaf cutting were prepared and samples were analyzed using a Leica DMRB Microscope. a) YFP channel: excitation 490-510 nm emission 520-550 nm. b) RFP channel: excitation 540-580 nm emission 595-635 nm. Illumination times are given in the pictures.

Furthermore the construct was tested in composite *P. tremula x alba*. Roots showed sYFP and Td-Tomato signals as *N. benthamiana* leaves. The signal maxima of sYFP and Td-Tomato could be detected separately (**Figure 9**), indicating a working tandem marker principle also in *P. tremula x alba* roots. In this first analysis composite poplars revealed, only a small number of transgenic roots containing the biT-DNA. The proportion of fluorescent roots on all formed roots was defined as transformation efficiency and was below 30 %, which made an optimization of the transformation procedure necessary.

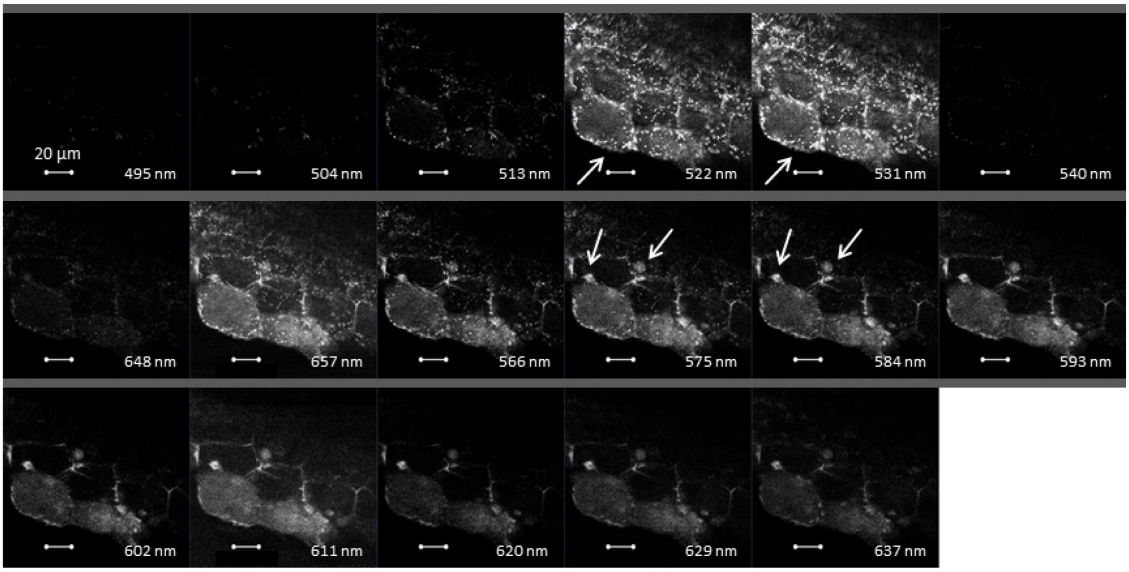

Figure 9: Analysis of *P. tremula x alba* roots harboring pPLV_$P_{CaMV35S}$_sYFP_SNL_T_{NOS}_P_{NOS}_td-tomato_NLS_T_{OCS}. Composite *P. tremula x alba* were analyzed 5 weeks after transformation. Roots expressed peroxisomal sYFP under control of CaMV35S promoter and nuclear localized Td-Tomato driven by nopaline synthase promoter. A lambda scan was performed (excitation at 488 nm, argon laser 2.4 % laser intensity and 543 nm helium neon laser 2.5 % laser intensity, window size 9 nm, cLSM, 880, Zeiss). The analysis was performed in collaboration with Uwe Nehls.

3.1.3 Optimization of transformation efficiencies of composite *P. tremula x alba*

Transformation efficiency was calculated as percentage of fluorescent roots in relation to the total number of formed roots after 6 weeks. The transformation efficiencies of composite *P. tremula x alba* were only around 30 % in the first experiments and needed to be optimize to allow an efficient analysis of time consuming mycorrhization experiments.

3.1.3.1 Optimization of bacterial growth conditions to improve transformation efficiency

During the activation procedure of transgenic *Agrobacteria* it was observed that *A. rhizogenes* K599 pSOUP grew only poorly on activation plates containing 5 mg/L tetracycline. Therefore trials with reduced tetracycline concentrations (1 – 5 mg/L) were performed. When bacteria were cultivated for 72 h at 28 °C on activation plates, a concentration of 2.5 mg/L tetracycline revealed improved growth compared to other concentrations (**Sup. Figure 5**).

To test whether improved bacterial growth would result in higher root transformation rates with *P. tremula x alba* cuttings, composite plant formation was performed with transgenic bacteria pre-grown at different tetracycline concentrations. Two experiments were performed using independent cultivated plant batches with 10 plants each and transformation efficiencies were documented after 6 weeks (**Figure 10**). With bacteria cultivated on activation plates containing 1 or 5 mg/L tetracycline transformation efficiencies of 27 % and 28 % were achieved, respectively. Only 4 % transformation efficiency was obtained using bacteria pre-grown on activation plates containing 2.5 mg/L tetracycline, which was in contrast to the improved bacterial growth for this tetracycline concentration. An improvement of the plant root transformation rates by variation of the tetracycline concentration in activation plates was therefore not achieved.

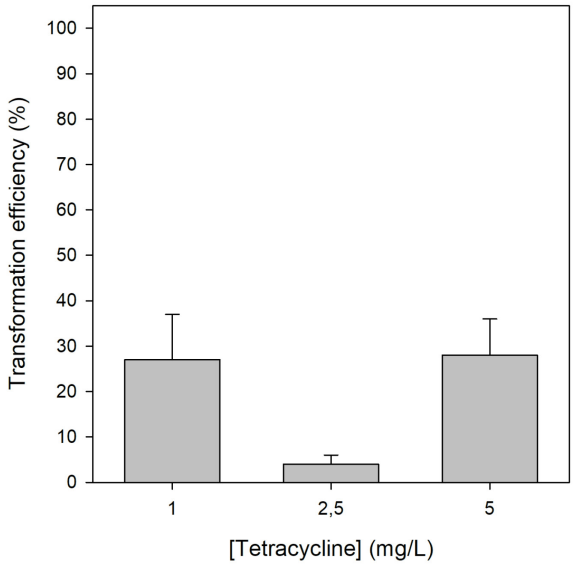

Figure 10: Effect of selected tetracycline concentrations on root transformation efficiency. Composite *P. tremula x alba* formation was performed using *A. rhizogenes* K599 pPLV_$P_{CaMV35S}$_td-tomato_NLS_T_{OCS} pre-grown on activation plates with 1-5 mg/L tetracycline. Roots were counted after 6 weeks and transformation efficiencies were calculated as percentage of fluorescent roots. The experiment was performed in two independent approaches with 10 plants per approach for each concentration, shown is the average of both experiments giving similar results.

3.1.3.2 Root transformation efficiencies are dependent on the vector background

Since the transformation efficiency using pPLV as binary vector system was only around 30 %, other binary vector systems were tested. Initial test by Anneke Immor (AG Nehls) revealed much higher transformation efficiencies using pCXUN vector based on the pCAMBIA background.

Therefore a comparative transformation approach was performed with three different plant transformation vector lines: pPLV, pBi121 and pCXUN. The same marker, a nuclear targeted Td-Tomato driven by UBQ10 promoter was integrated into the different vectors (construct origins this thesis, cloning not shown) and transgenic *A. rhizogenes* K599 were used to generate composite poplar. The experiment was performed three times with independent plant batches and 10 plants each per vector. With the vector background pPLV a transformation efficiency of 36 % was achieved (**Figure 11**), which is similar high than previous experiments. Formation of composite *P. tremula x alba* with pBi121 showed a transformation efficiency of 35 % and was thus comparable high as pPLV (**Figure 11**). In content, the transformation efficiency was much higher with the vector system pCXUN resulting in about 73 % double transgenic roots (**Figure 11**). The highest transformation efficiency was therefore achieved with pCXUN, which was significant with $p<0.01$ to the comparable results of pPLV and pBi121 (**Figure 11**). Because of this result pCXUN was used as vector backbone for all other experiments.

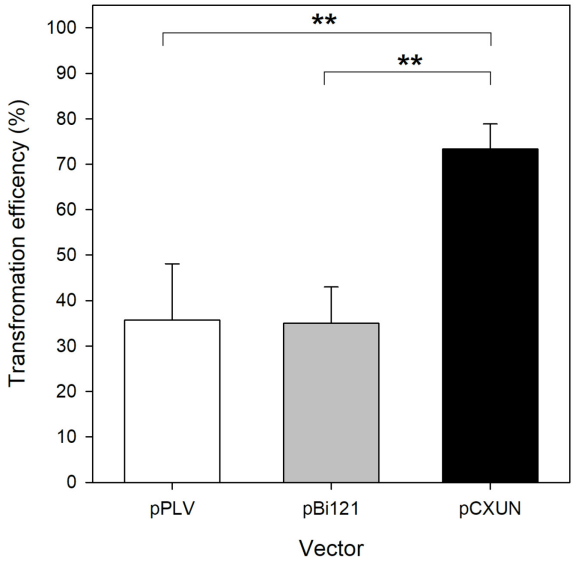

Figure 11: Transformation efficiencies of selected binary plant vectors. Composite *P. tremula x alba* cuttings were transformed using *A. rhizogenes K599* harboring pPLV, pBi121 and pCXUN. As marker a nuclear targeted Td-Tomato under control of the ubiquitin promoter from *Arabidopsis* was used. All formed roots and fluorescent roots were counted after 6 weeks and transformation efficiencies were calculated as percentage of fluorescent roots. The experiment was performed 3 times with 10 plants each per vector and batch. Statistics were calculated using the software GraphPad InStat version 3.10 with $p<0.01$ (**).

3.1.4 Construction of a tandem marker system in the pCXUN vector

Due to its small size, cloning was further performed in pPLV if feasible and final cassettes were than cloned into pCXUN.

3.1.4.1 Assembly of tandem marker cassettes in pPLV

Previously constructed *td-tomato* marker cassettes were amplified from pPLV_$P_{CaMV35S}$_td-tomato_NLS_T_{OCS}, pPLV_P_{UBQ10}_td-tomato_NLS_T_{OCS} and pPLV_P_{NOS}_td-tomato_NLS_T_{OCS} with primers containing additional *Not*I / *Sac*I restriction sites and cloned into the entry vector pJET1.2 (**Sup. Figure 6**). The fragments were extracted from pJET1.2 and integrated into *Not*I / *Sac*I sites of pPLV06 (De Rybel *et al.* 2011), which contains a sYFP tagged to the nucleus (**Figure 12 A**). Using this strategy a series of pPLV06 vectors was generated where *td-tomato* expression is controlled by different promoters that allow distinct constitutive expression levels of the marker gene in poplar roots (**Figure 12 B**). The constructs were verified by restriction analysis using *Nco*I, cleaving two times in the pPLV vector backbone and *Bam*HI, cleaving within the marker cassettes. The analysis resulted in the expected fragment pattern (**Figure 12 compare C + D**).

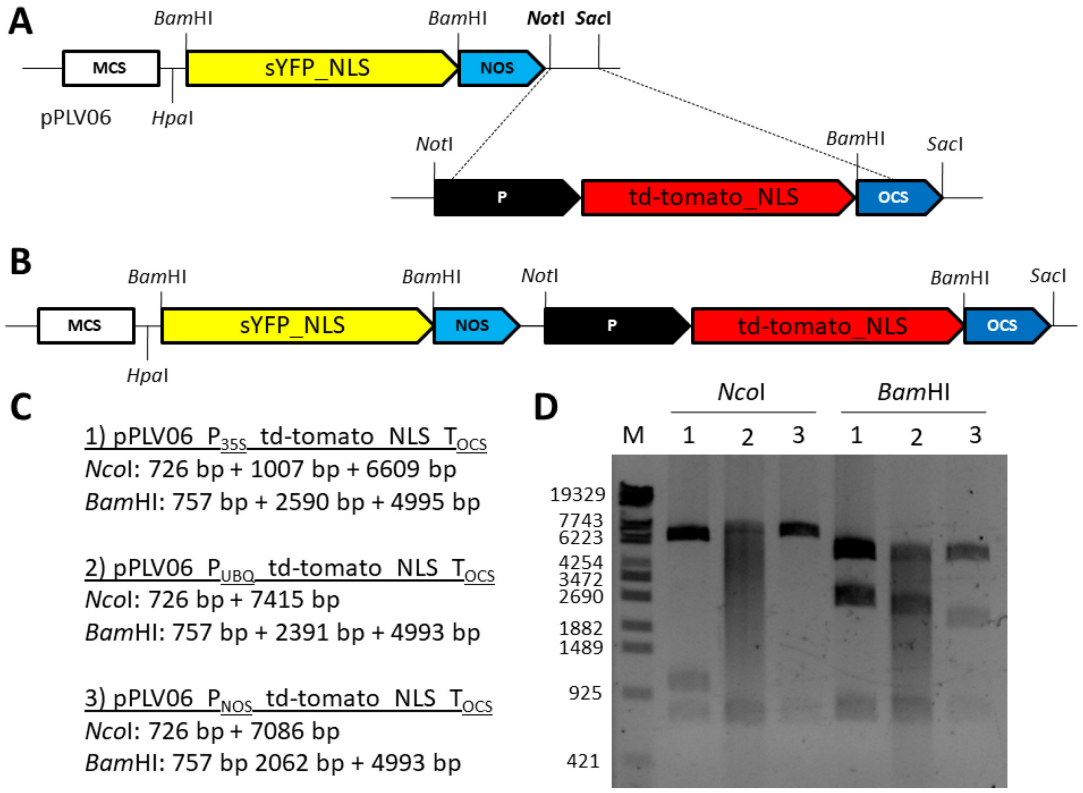

Figure 12: Integration of Td-Tomato marker cassettes into pPLV06. The cloning strategy and the verification of the cloned constructs are shown. A) The integration of the marker cassette is performed using the restriction sites *Not*I and *Sac*I. B) The construct contained a multiple cloning site (MCS), a nuclear localized super yellow florescent protein (sYFP_NLS), a nopaline synthase terminator (NOS) obtained from pPLV, and Td-Tomato cassette composed out of, one out of three promoters (P), a Td-Tomato coding sequence with nuclear localization signal (NLS) and a octopine synthase terminator (OCS). C) The expected fragment sizes for restriction analysis with *Nco*I and *Bam*HI together with the construct names and numbers are given. D) DNA fragments from restriction analysis were separated on 1 % agarose gel. As marker *Sty*I digested Phage Lambda DNA was used. Lanes were labeled with the construct numbers given in C.

3.1.4.2 Integration of Td-Tomato cassettes into the pCXUN backbone

To integrate the Td-Tomato cassettes into the vector backbone pCXUN, pCXUN-FLAG (Chen *et al.* 2009) (**Figure 13 A**) had to be modified. As a first cloning step, a *Pvu*II fragment of pPLV06 (De Rybel *et al.* 2011) (**Figure 13 B**) was integrated into a single *Pvu*II site of pCXUN-FLAG. This strategy allowed a directed integration of the Td-Tomato cassette into pCXUN in a second step.

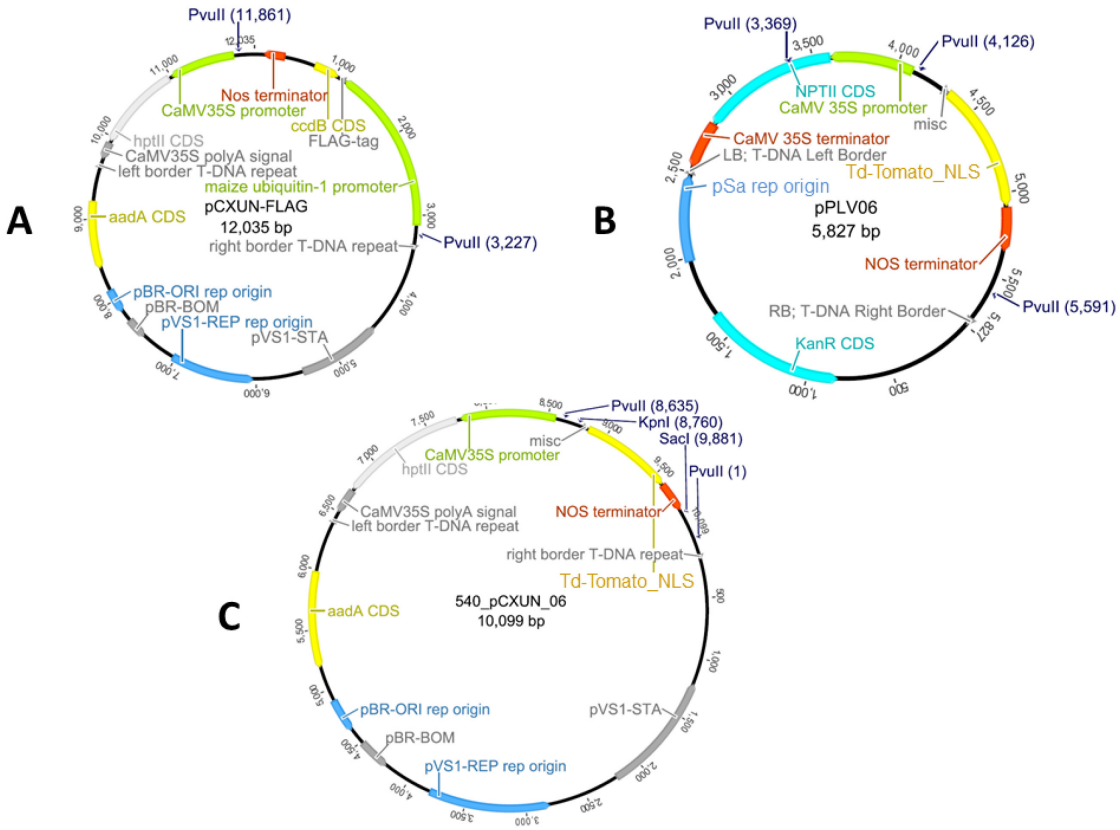

Figure 13: Construct maps of pCXUN-FLAG, pPLV06 and the new vector pCXUN06. The construct maps of the starting constructs pCXUN-FLAG (A) and pPLV (B) are shown. The vector backbone of pCXUN-FLAG and a part of the T-DNA region of pPLV06 were combined to the new vector pCXUN06 (C) by using a unique *Pvu*II site. The T-DNA insert can integrate in two different orientations, but only the counter-rotating localization of the plant resistance marker to the tandem marker cassette was used. The *Pvu*II site used for cloning is indicated in the maps. The marker cassette part of the pCXUN06 can be exchanged in a directional way using the indicated sites *Kpn*I and *Sac*I.

The vector pCXUN06 vector was verified by restriction analysis according to **Figure 14 A**. All enzyme reactions showed the expected fragment pattern after gel electrophoresis (**Figure 14 B**). The orientation of the T-DNA resulted in a counter-rotating localization of the plant resistance marker to the tandem marker cassette (**Figure 14 B**).

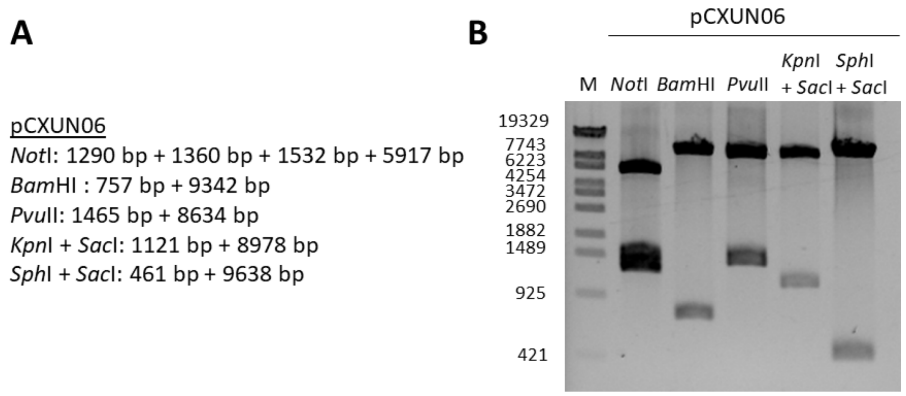

Figure 14: Restriction analysis of pCXUN06. For the restriction analysis of pCXUN06 different restriction enzymes were used. A) The excepted DNA fragment sizes for pCXUN06 are shown. The *Not*I site is present multiple times in the backbone of pCXUN and therefore verifies the backbone. With *Bam*HI the correct size of the sYFP_NLS was verified and *Pvu*II was used to see the correct size of the inserted T-DNA region. The digest with *Kpn*I and *Sac*I was performed to test the functionality of the restriction enzymes, which will be need in the following cloning steps. *Sph*I and *Sac*I were used to verify the orientation of the T-DNA fragment, since the integration could have been in both orientations. B) DNA fragments were separated on 1% agarose gel with 3 µL of Phage Lambda DNA/*Sty*I marker.

For the integration of the T-DNA regions from pPLV into pCXUN06 the restriction enzymes *Kpn*I / *Sac*I were used. The marker cassettes descripted in chapter 3.1.4.1 were transferred to the pCXUN06. The constructs named pCXUN0635S, pCXUN06UBQ and pCXUN06NOS were verified by restriction analysis with *Pvu*II and *Bam*HI. The expected fragment pattern (**Figure 15 A**) was detected for all three constructs (**Figure 15 B**).

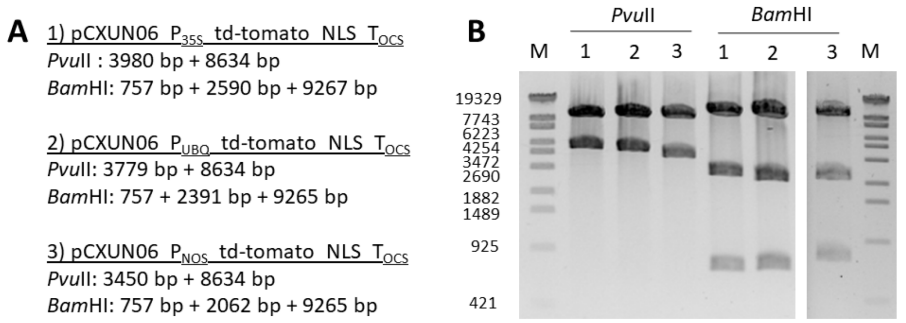

Figure 15: Restriction analysis of pCXUN06_X. Three different constructs were analyzed. A) Construct names and the expected fragment sizes for restriction analysis with *Pvu*II or *Bam*HI. B) DNA fragments were separated on 1% agarose gel. As marker 3 µL of Phage Lambda DNA/*Sty*I marker was used.

3.1.5 Functional analysis of pCXUN06NOS

Visual analysis of CaMV35S, UBQ10 and NOS promoter (**Figure 7**) showed strongest signal intensity of Td-Tomato under control of the UBQ10 promoter in cortical cells, but lower signals in root hairs. The CaMV35S and NOS promoter showed an equal distribution of signal intensity, so they were preferred over the UBQ10 promoter. CaMV35 is known to be related to secondary effects as artificial localization within the cells, which was observed in

leaves of *N. benthamiana*. Even if, those effects were not observed in roots of *P. tremula x alba* expressing Td-Tomato under control of CaMV35S, the tandem construct harboring the NOS to drive Td-Tomato expression was firstly tested as most promising candidate.

To generate a first double marker vector, a CaMV35S promoter was integrated into the multiple cloning sites of pCXUN06NOS by *Kpn*I / *Hpa*I. The resulting plasmid pCXUN06NOS_$P_{CaMV35S}$ was verified by restriction analysis (**Sup. Figure 7**) and was functionally analyzed *in planta*.

3.1.5.1 Functional analysis of pCXUN06NOS_$P_{CaMV35S}$ in *N. benthamiana* leaves

Leaves were infiltrated with *A. rhizogenes* K599 carrying pCXUN06NOS_$P_{CaMV35S}$ and as negative control pCXUN06NOS. PCXUN06NOS_$P_{CaMV35S}$ transformed cells showed weak signals in both the YFP and the RFP channel (**Figure 16 A + B**), while cells transformed with pCXUN06NOS showed no signal in the YFP (**Figure 16 C**), but a strong signal in the RFP channel (**Figure 16 D**). To obtain a clearly visible RFP signal, leaf cells expressing pCXUN06NOS_$P_{CaMV35S}$ needed an illumination time of 2 sec, while only 0.5 sec were requested for pCXUN06NOS transgenes. The strong background fluorescence in **Figure 16 B** compared to **Figure 16 D** can be explained by a longer illumination time leading to detectable chlorophyll autofluorescence.

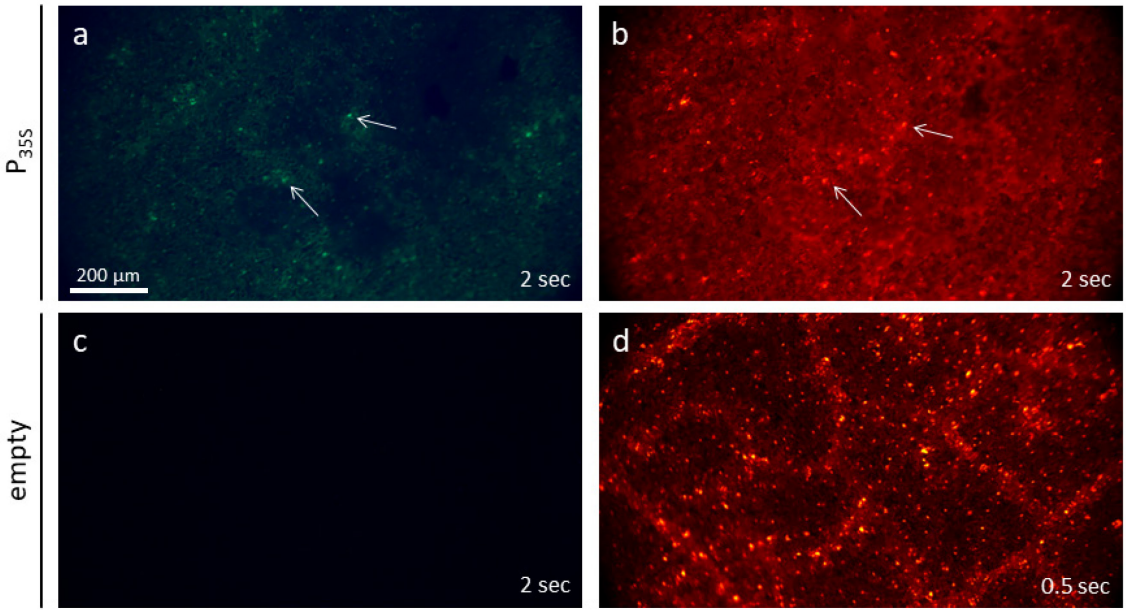

Figure 16: Functional analysis of pCXUN06NOS in *N. benthamiana* leaves. Leaves were infiltrated with *A. rhizogenes* K599 carrying pCXUN06NOS or pCXUN06NOS_$P_{CaMV35S}$. Results were analyzed 3 days after infiltration. pCXUN06NOS harbor the coding sequence of a nuclear targeted Td-Tomato driven by nopaline synthase promoter and a non-expressed sYFP coding sequence. In pCXUN06NOS_$P_{CaMV35S}$ the sYFP is under control of the cauliflower mosaic virus promoter 35S (CaM35S) and is expected to be expressed as well. Pictures were taken using a binocular (MSV269, Leica). a + c) YFP channel, b + d) RFP channel (for filter details see 2.2.9.2).

Signal intensity and specify of the sYFP signal were also analyzed using cLSM. The result showed two partial overlapping signal peaks with maxima between 522 nm and 531 nm and 557 nm and 575 nm (**Figure 17 A**). According to the expected signal peaks were around 524 nm for sYFP and 581 nm for Td-Tomato (**Figure 17 B**), which indicates a slight shift of the fluorescence spectrum of Td-Tomato *in vivo* (**Figure 17 A**). Furthermore it is shown, that the emission signals of sYFP and Td-Tomato overlap (**Figure 17 B**). Nevertheless the signal maxima are clearly separate.

In addition to the nuclear located fluorescence signals, signals were also detected in the cytoplasm for sYFP as well as Td-Tomato (**Figure 17**). The sYFP is a single fluorophore of app. 27 kDa and can pass the nuclear pore by diffusion due to its small size. Since the Td-Tomato is a dimer, with app. double the size of sYFP (54 kDa vs 27 kDa), the effect of passive nuclear efflux is expected to be much smaller and in agreement, less signal is detected in the cytoplasm compared to sYFP signal (**Figure 17 A**).

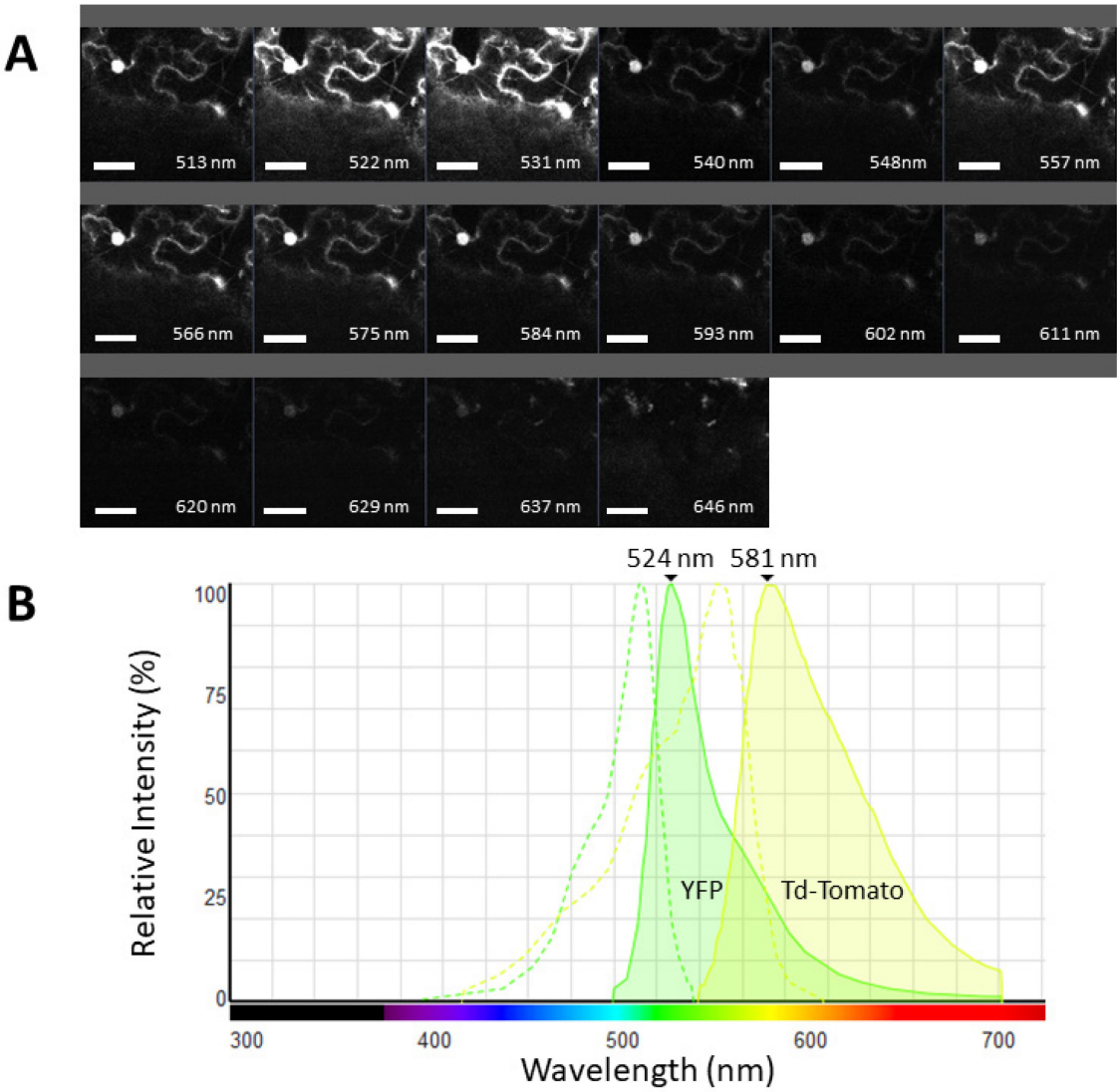

Figure 17: Emission characteristics of YFP and Td-Tomato co-expressed in *N. benthamiana* leaf cells. A) Leaves were infiltrated with transgenic *A. rhizogenes* K599 pCXUN06NOS_$P_{CaMV35S}$. Expressing a sYFP under control of cauliflower mosaic virus 35S (CaMV35S) promoter and a Td-Tomato driven by nopaline synthase promoter (NOS). The infiltrated leaves were investigated after 3 days of incubation using the argon laser at 488 nm for exitation (880, Zeiss). Shown is a lambda scan of 9 nm wide emission windows, which was performed in collaboration with Uwe Nehls. B) As reference spectrum data from the Fluorescence SpectraViewer (Thermo Fisher) are shown (graphic is modified).

3.1.5.2 Functional analysis of pCXUN06NOS in *P. tremula x alba* roots

As next step the construct was transformed into *P. tremula x alba* to generate composite plants. For microscopical analysis of the YFP signal the GFP filter set was used, as it turned out to be more suitable for fluorescence visualization in an organ revealing a strong autofluorescence background as *P. tremula x alba* roots. In transgenic *N. benthamiana* leaf cells, YFP fluorescent nuclei were only visible with pCXUN06_$P_{CaMV35S}$, but not with pCXUN06NOS transformed *P. tremula x alba* roots (**Figure 18 a + c**), while red fluorescent nuclei were clearly detectable for all transgenic roots (**Figure 18 b + d**). In

pCXUN06NOS_$P_{CaMV35S}$ transgenic roots YFP signal intensity was much lower than that of Td-Tomato.

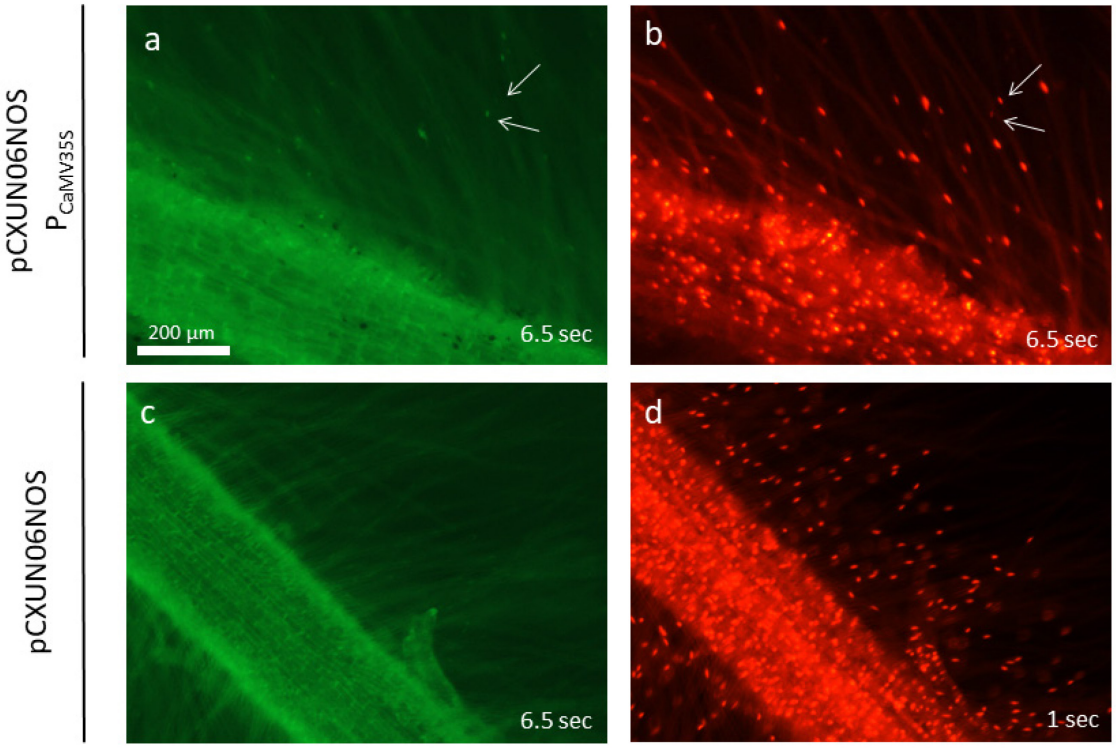

Figure 18: Functional analysis of pCXUN06NOS in *P. tremula x alba* roots. Roots from composite *P. tremula x alba* that were transformed with pCXUN06NOS_$P_{CaMV35S}$ (a + b) or pCXUN06NOS (c + d) were analyzed 5 weeks after infection. pCXUN06NOS_$P_{CaMV35S}$ harbor a sYFP coding sequence under control of the cauliflower mosaic virus promoter 35S (CaMV35S), while in pCXUN06NOS a promoter-less sYFP. Pictures were taken using a binocular (MSV269, Leica). a + c) GFP channel, b + d) RFP channel (for filter details see 2.2.9.2). Illumination times are given in the pictures.

Next to epi-fluorescence microscopy, cLSM was performed. Results of lambda scan are shown in **Figure 19**. The emission maximum of sYFP was as before detected 522 nm to 531 nm (**Figure 19**), while the Td-Tomato signal was a bit shifted (575 nm to 593 nm) to longer wavelength as in tobacco leaves (**Figure 18 b + Figure 19**). Since the NOS promoter controlled Td-Tomato expression, which was easy detectable in poplar roots, none of the other promoters was tested as tandem marker.

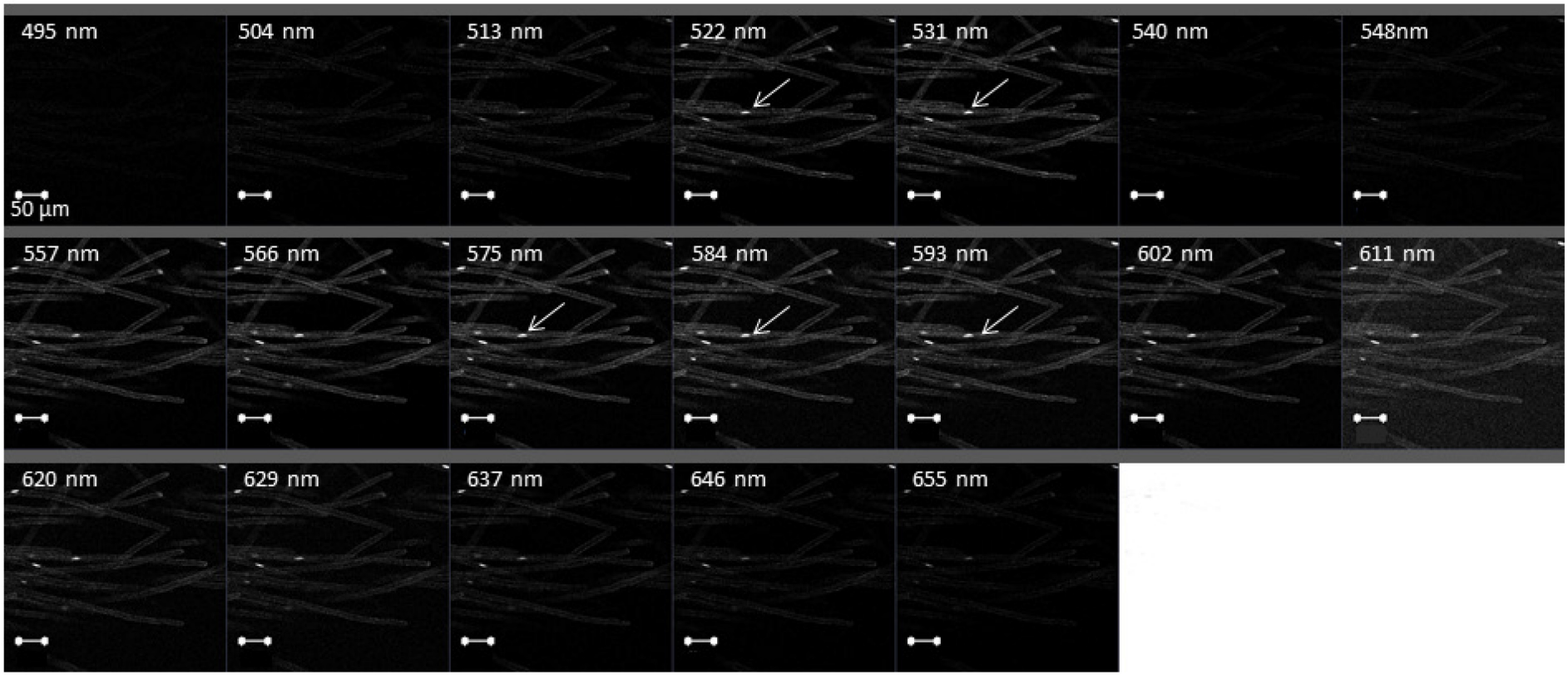

Figure 19: Lambda scan of *P. tremula x alba* plants containing pCXUN06NOS_$P_{CaMV35S}$. Roots of composite *P. tremula x alba* pCXUN06NOS_$P_{CaMV35S}$ were analyzed 5 weeks after transformation. Roots expressed sYFP under control of cauliflower mosaic virus 35S (CaMV35S) promoter and Td-Tomato driven by nopaline synthase promoter (NOS). Analysis was performed with cLSM (880, Zeiss). For illumination an argon laser with 488 nm and an intensity of 0.6 % was used. Shown is a series of 9 nm wide emission windows. The lambda scan was performed in collaboration with Uwe Nehls.

In parallel, experiments with a nuclear targeted double GFP (dGFP) instead of a nuclear targeted sYFP were performed by Jana Müller (AG Nehls). The signal intensity achieved with the dGFP was higher and only very weak signals were detected in cytoplasm. Therefore, the dGFP was used in further experiments.

3.1.6 Validation of pCXUN04NOS

The vector pCXUN04NOS was assembled by combining parts of pCXUN06 (this thesis), the NOS promoter driven Td-Tomato expression cassette (this thesis), a part of the pPLV04 T-DNA containing a dGFP, driven by a UBQ10 promoter provided by Jana Müller (AG Nehls). To show its functionality and determine detection limitations of the vector, *in planta* expression experiments were performed with *N. benthamiana* leaves and *P. tremula x alba* roots.

3.1.6.1 Functionality test of pCXUN04NOS in *N. benthamiana* leaves

As first functionality test the transient expression in *N. benthamiana* leaves was used. Nuclear dGFP signals were easily detected in leaves expressing pCXUN04NOS_P_{UBQ10} after illumination for 1 sec (**Figure 20 a**). For the detection of the Td-Tomato signal much longer illumination time of 13.4 sec was necessary (**Figure 20 b**). In contrast, an illumination time of 2 sec was already sufficient to detect clear signals in leaves expressing pCXUN04NOS (**Figure 20 d**). No specific signals were detected when leaves expressing pCXUN04NOS were illuminated for 13.4 sec using a GFP filter (**Figure 20 d**).

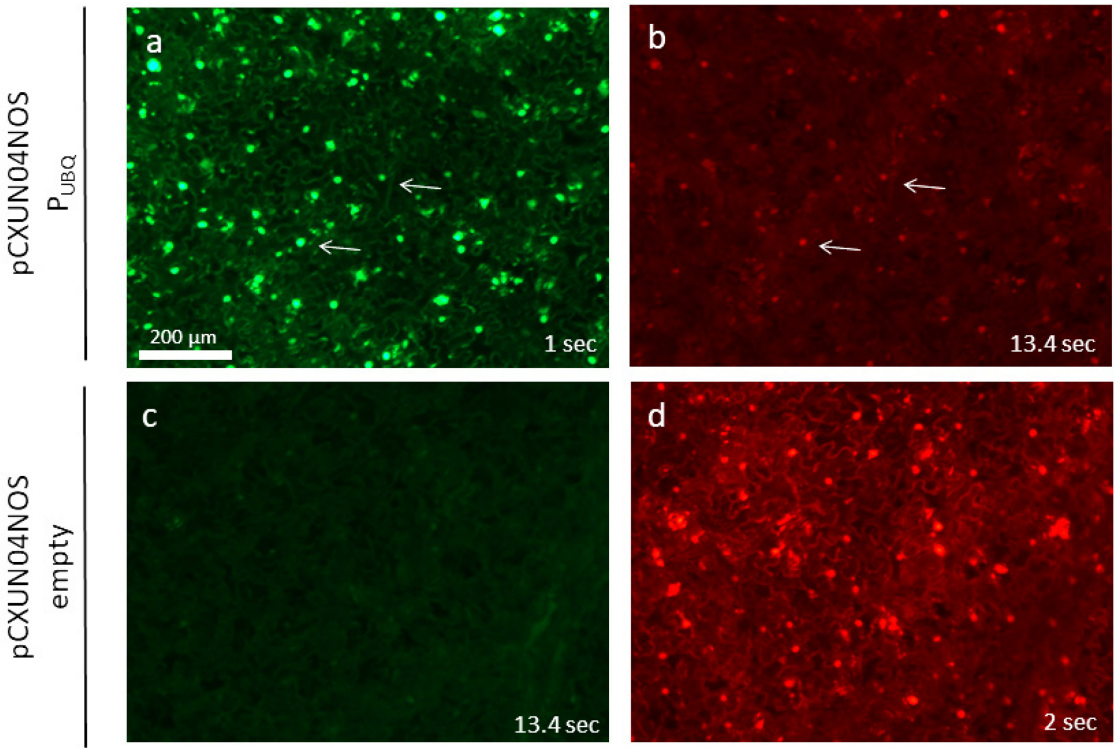

Figure 20: Functional analysis of pCXUN04NOS in *N. benthamiana* leaves. Leaves were infiltrated with *A. rhizogenes* K599 carrying pCXUN04NOS_P_{UBQ10} or pCXUN04NOS. Results were analyzed 3 days after infiltration. pCXUN04NOS harbor the coding sequence of a nuclear targeted Td-Tomato driven by nopaline synthase promoter and a non-expressed dGFP coding sequence. In pCXUN04NOS_P_{UBQ10} the dGFP is under control of the ubiquitin 10 promoter and is expected to be expressed as well. Pictures were taken using a binocular (MSV269, Leica). a + c) GFP channel, b + d) RFP channel (for filter details see 2.2.9.2).

3.1.6.2 Analysis of pCXUN04NOS in roots of *P. tremula x alba* composite plants

Composite poplar plants were analyzed using epi-fluorescence microscopy. Clear signals in the GFP as well as in the RFP channel were detected for pCXUN04NOS_P_{UBQ10} (**Figure 21 a + b**), while for pCXUN04NOS only the expected Td-Tomato fluorescence was observed (**Figure 21 c + d**). In contrast to the results obtained by transient expression in leaves *N. benthamiana* (**Figure 20**) the same illumination time of 2 sec were needed to document similar signal intensities for Td-Tomato for both constructs (**Figure 21 b + d**).

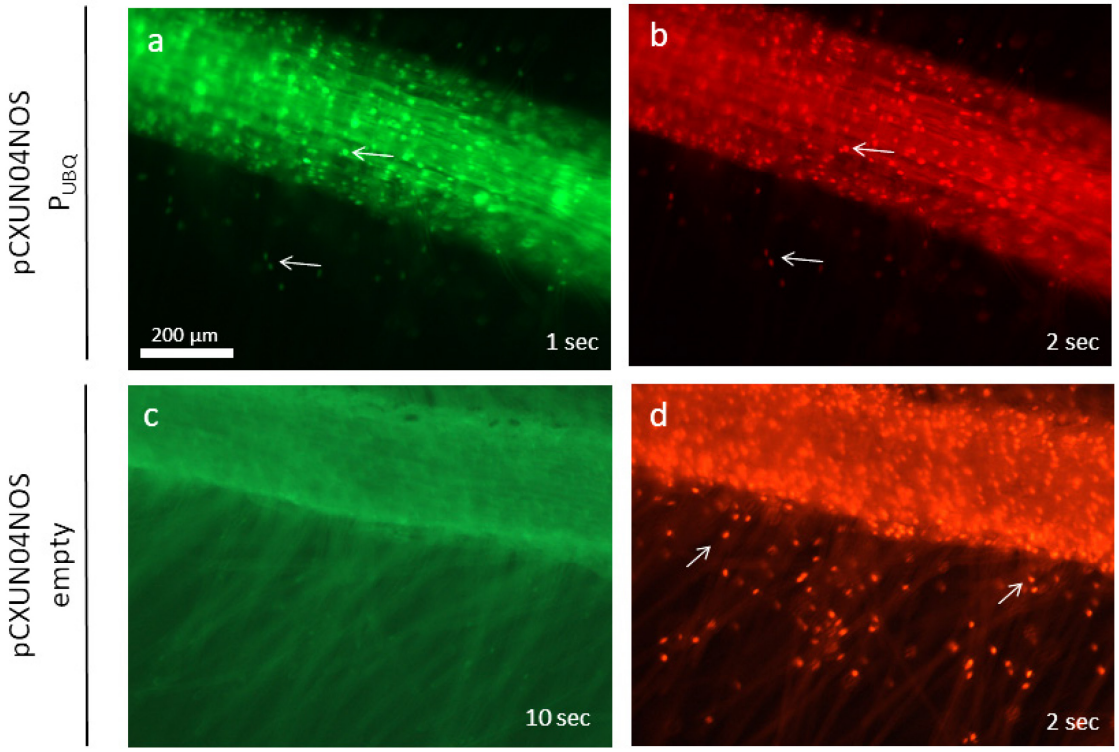

Figure 21: Analysis of pCXUN04NOS in *P. tremula x alba* roots. Roots from composite *P. tremula x alba* pCXUN04NOS_P_{UBQ10} (a + b) or pCXUN04NOS (c + d) were analyzed 5 weeks after transformation with *A. rhizogenes* K599. pCXUN04NOS_P_{UBQ10} harbor a dGFP coding sequence under control of the ubiquitin 10 promoter, while pCXUN04NOS is promoter-less. A second Td-Tomato expression cassette is under control of the nopaline synthase promoter. Pictures were taken using a binocular (MSV269, Leica). a + c) GFP channel, b + d) RFP channel (for filter details see 2.2.9.2).The used illumination times are given in the pictures.

Furthermore, transgenic roots expressing pCXUN04NOS_P_{UBQ10} were inspected using cLSM. A lambda scan revealed similar signal maxima of dGFP (504-513 nm) and Td-Tomato (575-585 nm) as observed in leaves (**Figure 22**).

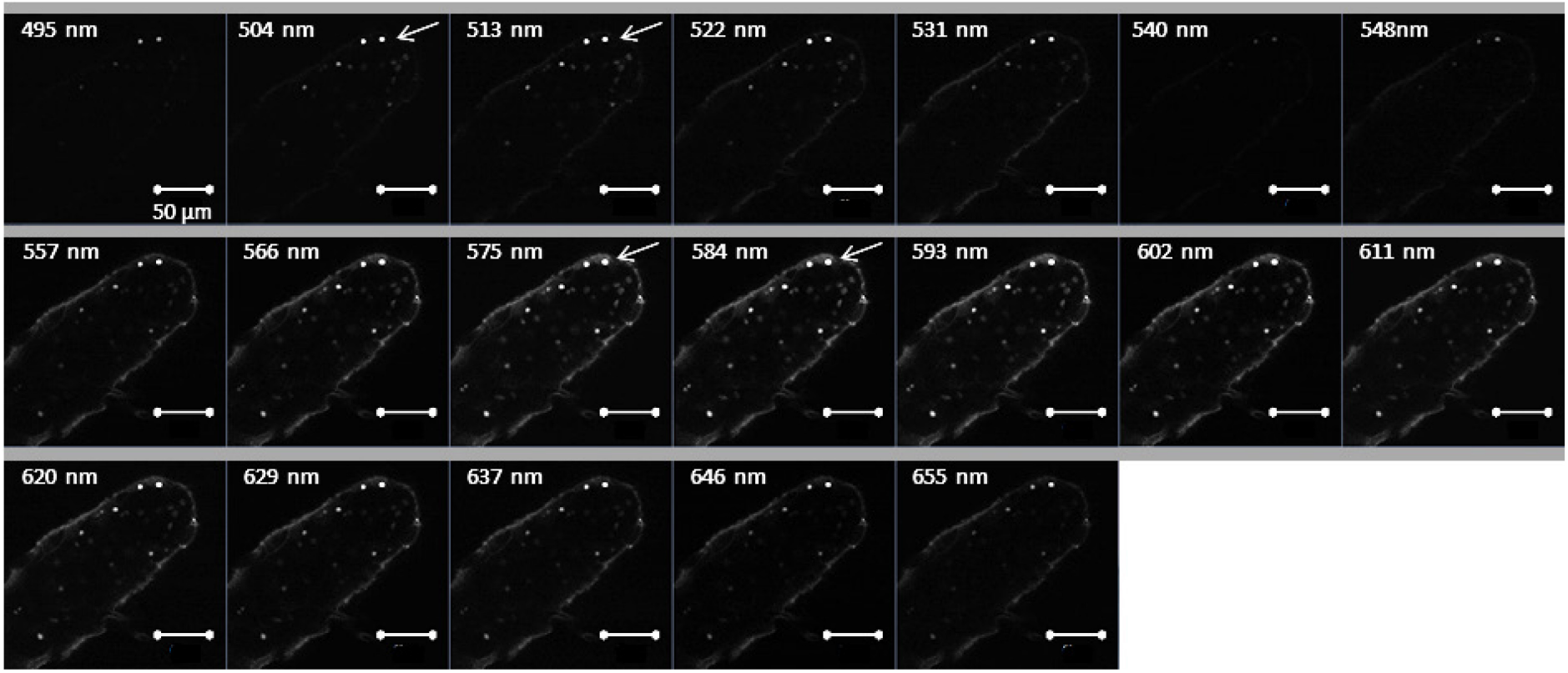

Figure 22: Lambda scan of *P. tremula x alba* root tip expressing pCXUN04NOS_P_{UBQ10}. Composite *P. tremula x alba* containing pCXUN04NOS_P_{UBQ10} were analyzed 5 weeks after transformation. Roots expressed dGFP under control of ubiquitin 10 promoter and Td-Tomato driven by nopaline synthase promoter. Analysis was performed with cLSM (880, Zeiss). For illumination an argon laser line at (488 nm) with 0.2 % intensity and a helium neon laser (543 nm) with 2.4 % intensity were used. Shown is a series of 9 nm wide emission windows. The lambda scan was performed in collaboration with Uwe Nehls.

3.2 *In planta* analysis of two promoter fragments of ectomycorrhiza induced genes from *P. tremula x tremuloides*

For promoter analysis, the previously descripted vector pCXUN04NOS (AG Nehls unpublished) harboring a promoter-less nuclear targeted dGFP and a NOS promoter driven Td-Tomato cassette was used. As positive control pCXUN04NOS_P_{UBQ10} was used. Promoter fragments of two ECM induced genes (Nehls *et al.* unpublished) were cloned upstream of the dGFP. The activity of the promoter fragments was investigated in *N. benthamiana* as well as in *P. tremula x alba* leaves and in roots of composite *P. tremula x alba*.

3.2.1 Establishing of a transient expression system in *P. tremula x alba* leaves

Even if the genes are expressed in mycorrhized roots the activity was also studied in leaf tissues, since truncated promoter sequences can show activity also in leaf tissue (Neb 2017). Transient expression analysis *in planta* is commonly performed in *Nicotiana benthamiana* leaf cells, since *N. benthamiana* leaf infiltration is a robust method. *N. benthamiana* leaves show weak auto fluorescence and can be easily handled. However, *N. benthamiana* belongs, to the asteridclade and is thus phylogenetically only distantly related to poplar that belongs to the rosids. A method for transient expression in poplar leaves was not available and was thus established in this thesis. For a transient expression analysis of promoter activity in poplar, an *Agrobacterium*-mediated transformation method was established.

3.2.1.1 Effects of leaf treatments in *Agrobacterium*-mediated transformation

Agrobacteria infect wounded plant tissue, since the cuticula of intact leaves prevents infection, thus poplar leaves were treated prior to incubation. To generate multiple entry sites for *A. tumefaciens* infection, poplar leaves were injured either by sonification in activation medium without or with transgenic *A. tumefaciens*, or vortexed with activation medium containing silicium carbide particles. Pre-treatments were followed by incubation with transgenic *Agrobacteria* (**Figure 23**). To visualize transformed plant cells, *A. tumefaciens* strain GV3101 harboring the binary vector pPLV that expressed a sYFP under control of a CaMV35S promoter were used.

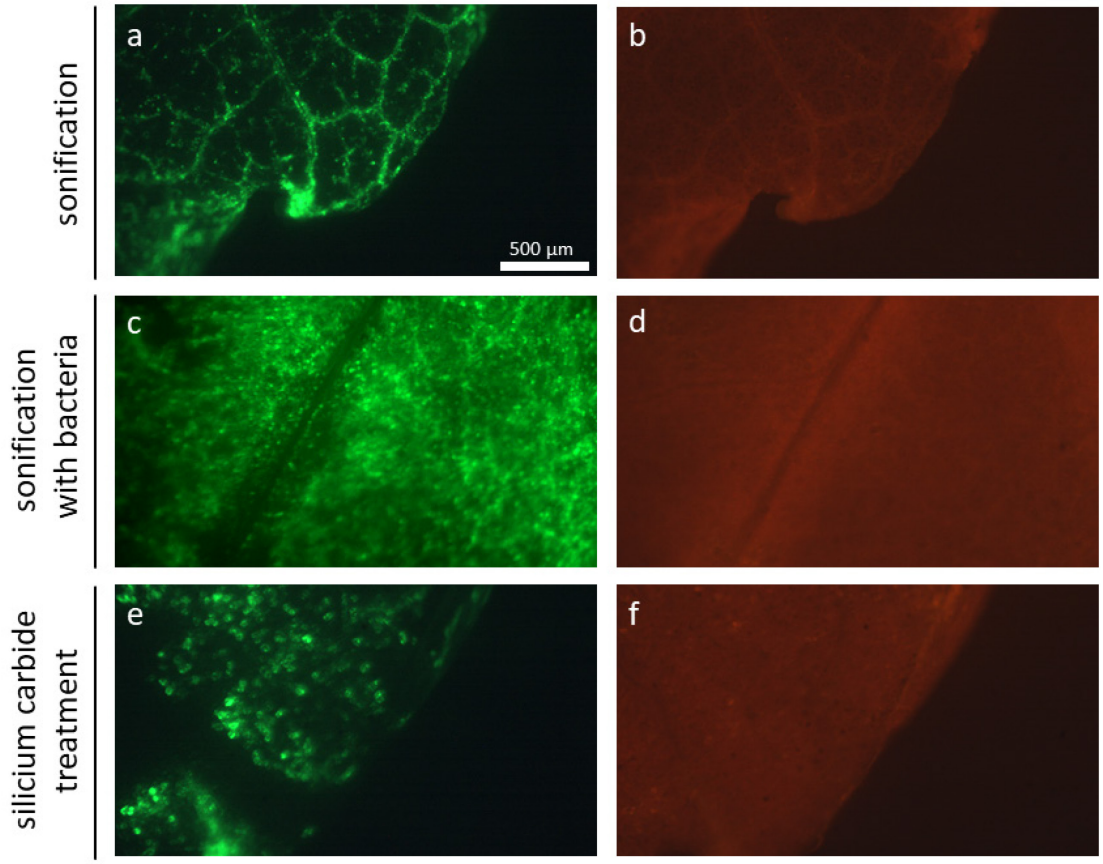

Figure 23: Impact of leaf pretreatment on *A. tumefaciens* based *P. tremula x alba* leaf transformation. *Populus tremula x alba* leaves were cut off and pre-treated either by sonification (a - d) or vortexing with silicium carbide particles (e - f) followed by incubation with transgenic *A. tumefaciens* GV3101 expressing a sYFP under control of a CaMV35S promoter for 24 h at 22 °C shaking. Leaves were transferred to MS6 agar plates containing antibiotics to stop proliferation of *A. tumefaciens* GV3101. Results were analyzed after 3 days of incubation at 22 °C using a binocular (MSV269, Leica) and the YFP (a, c, e) and RFP (b, d, f) filter sets (filter details given in 2.2.9.2).

Sonification with *A. tumefaciens* containing suspension destroyed most of the epidermal cells and led to mainly transgenic mesophyll cells (**Figure 23, c - d**). Sonification followed by incubation with transgenic *Agrobacteria* resulted in transgenic epidermal cells mainly located next to leaf vessels (**Figure 23, a - b**), while leave pre-treatment with silicium carbide particles showed transgenic epidermal cells all over the entire leaf (**Figure 23, e - f**). Transgenic mesophyll cells were observed with all leaf pretreatments. However, visualization in epidermal cells gave a much better signal to noise ratio and revealed by far less chlorophyll auto fluorescence.

3.2.1.2 Transformation of *P. tremula x alba* leaves with selected *Agrobacteria* strains

Since vortexing with silicium carbide particles followed by *A. tumefaciens* mediated transformation gave the best results, different *Agrobacteria* strains were tested. For this experiment transgenic *Agrobacteria* strains harboring the binary vector pPLV (this thesis) containing a nuclear targeted Td-Tomato expressed under control of a CaMV35S promoter was used.

While all strains were able to transform poplar leaf cells, the transformation efficiencies differed (**Figure 24**). *A. tumefaciens* C58 and *A. rhizogenes* K599 showed a much lower number of transformed leaf cells compared to *A. tumefaciens* GV3101 (**Figure 24, a, d, f**). Efficiencies achieved with *A. tumefaciens* C58 and *A. rhizogenes* K599 were too low to enable an efficient analysis of transformed leaf tissue, since successfully transformed cell cluster were very rare. *A. tumefaciens* GV3101 on the other hand turned out to be problematic in combination with an *in planta* expressed red fluorescent protein. The emission properties revealed a very strong shift of the fluorescent towards shorter wave length (**Figure 24**, **a**; details in 3.2.1.3). Instead of fluorescence in the red channel, a strong fluorescence in the YFP channel was observed.

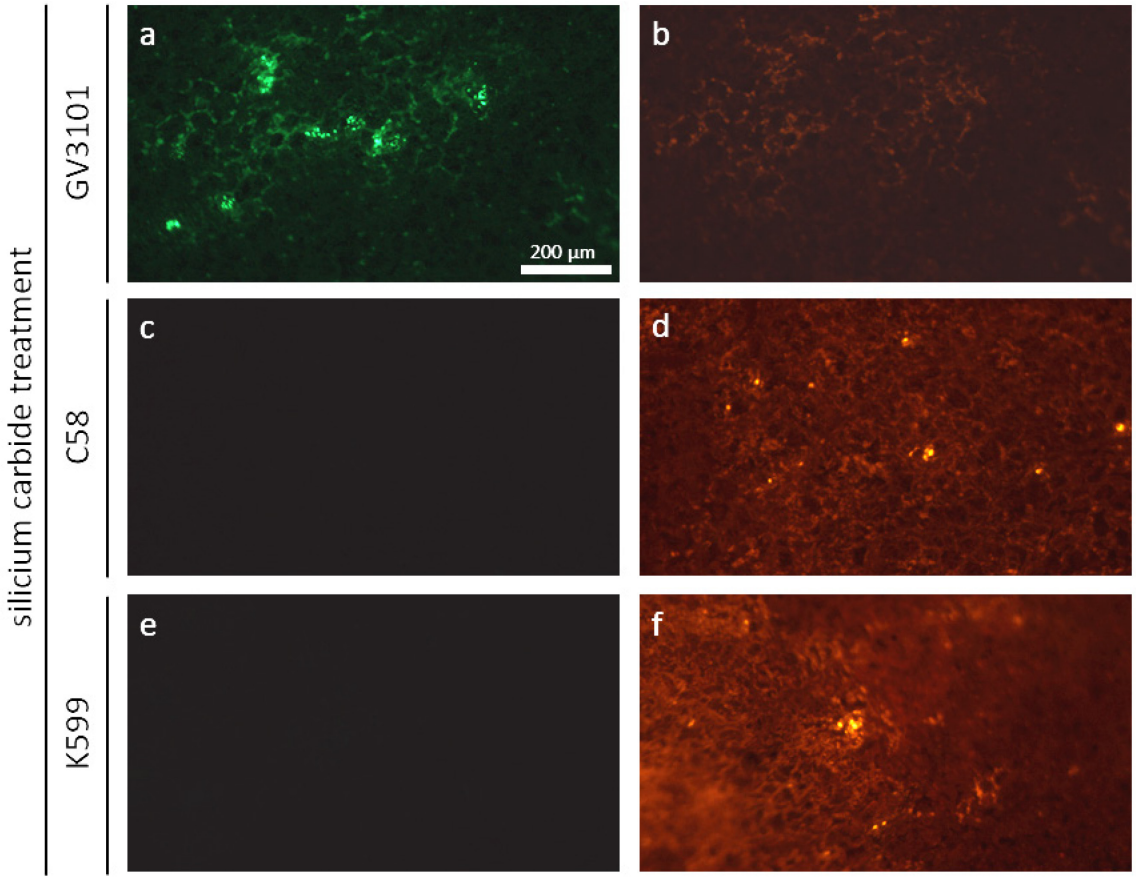

Figure 24: Transformation results of selected *Agrobacteria* strains. *P. tremula x alba* leaves were vortexed with silicium carbide particles, followed by incubation with transgenic *A. tumefaciens* strains GV3101 or C58 as well as an *A. rhizogenes* strain K599 expressing a nuclear targeted Td-Tomato under control of a CaMV35S promoter. Images were taken after 5 days of incubation using a binocular (MSV269, Leica) and the YFP (a, c, e) and RFP (b, d, f) filter sets (filter details given in 2.2.9.2).

3.2.1.3 Analysis of fluorescence emission shift of Td-Tomato by cLSM

To analyze the change in emission properties of Td-Tomato, a lambda scan was performed comparing leaf samples transformed with transgenic *A. rhizogenes* K599 (**Figure 25 a**) and *A. tumefaciens* GV3101 (**Figure 25 b**). The Td-Tomato spectrum achieved with *A. rhizogenes* K599 showed no fluorescent signal before 548 nm and a maximal signal between 575 nm – 584 nm (**Figure 25 a**). In comparison the fluorescence obtain from a leaf transformed with transgenic *A. tumefaciens* GV3101 started already at 504 nm and had the maximum between 522 nm – 531 nm (**Figure 25 b**). The fluorescence signal was not visible in the nuclei, but a number of much smaller dot like structures revealing intense fluorescence signals were visible (**Figure 25 b**). Similar results were observed also for other red fluorescence proteins (Tm-Tomato and mCherry data not shown).

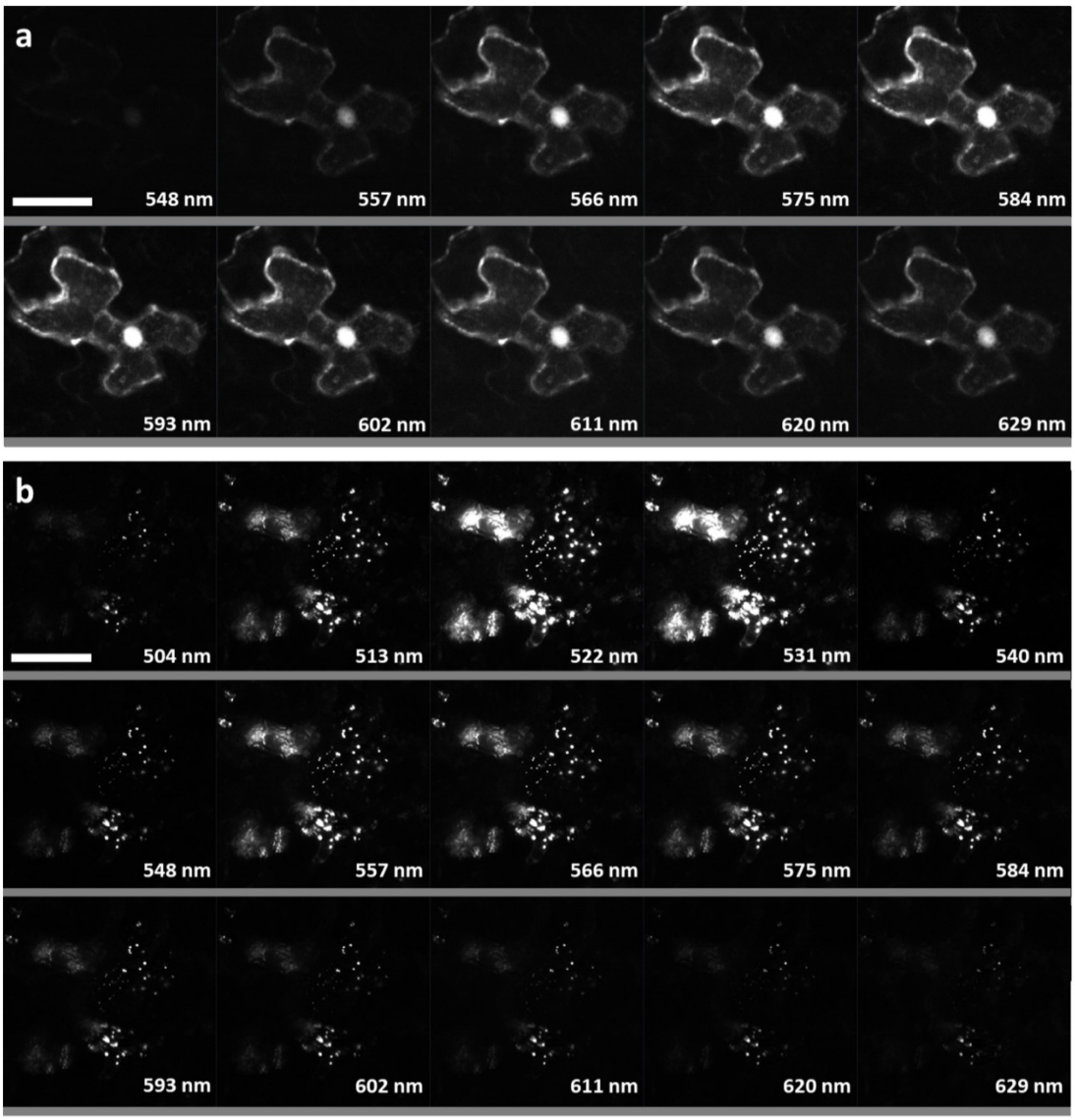

Figure 25: Impact of *A. tumefaciens* strain GV3101 on the emission spectrum of Td-Tomato. *P. tremula x alba* leaves were transformed with a) *A. rhizogenes* K599 or b) *A. tumefaciens* GV3101 expressing a nuclear-targeted Td-Tomato under control of a CaMV35S promoter. The emission spectrum properties of the Td-Tomato were analyzed by lambda scans with a cLSM (880, Zeiss) after illumination at 488 nm. Shown are series of 8 nm wide emission window. The scale bar presents a size of 50 µm. The center of the wave length windows is shown in the single images. The lambda scan was performed in collaboration with Uwe Nehls.

3.2.1.4 Leaf infiltration of *P. tremula x alba*

Additional conditions to improve poplar leaf transformation, based on *A. tumefaciens* C58 and *A. rhizogenes* K599 leaf infiltration was tried. Leaves of poplar plants grown in sterile culture are known to be easy damaged and tend to show extended senescence. Therefore, this approach was not tested in the first place. However, as the transformation efficiencies of *A. tumefaciens* C58 and *A. rhizogenes* K599 was low with the particle approach and *A. tumefaciens* GV3101 showed problematic fluorescence shift effects, the infiltration approach was tried. Surprisingly, carefully handling upon infiltration led to successful an extended leaf cell transformation.

With this approach, similar high transformation frequencies were observed for *A. tumefaciens* GV3101, C58 and *A. rhizogenes* K599 (**Figure 26**). As observed before transformation with *A. tumefaciens* GV3101 led to a shift in the fluorescence emission spectrum of Td-Tomato (details in 3.2.1.3), which was also observed for *A. tumefaciens* C58 for very few cells. However, infiltration with *A. tumefaciens* C58 and *A. rhizogenes* K599 gave specific signals and both strains can be used for transient expression. Therefore leaf infiltration turned out to be most suitable also for *P. tremula x alba* leaves (**compare Figure 24 + Figure 26**).

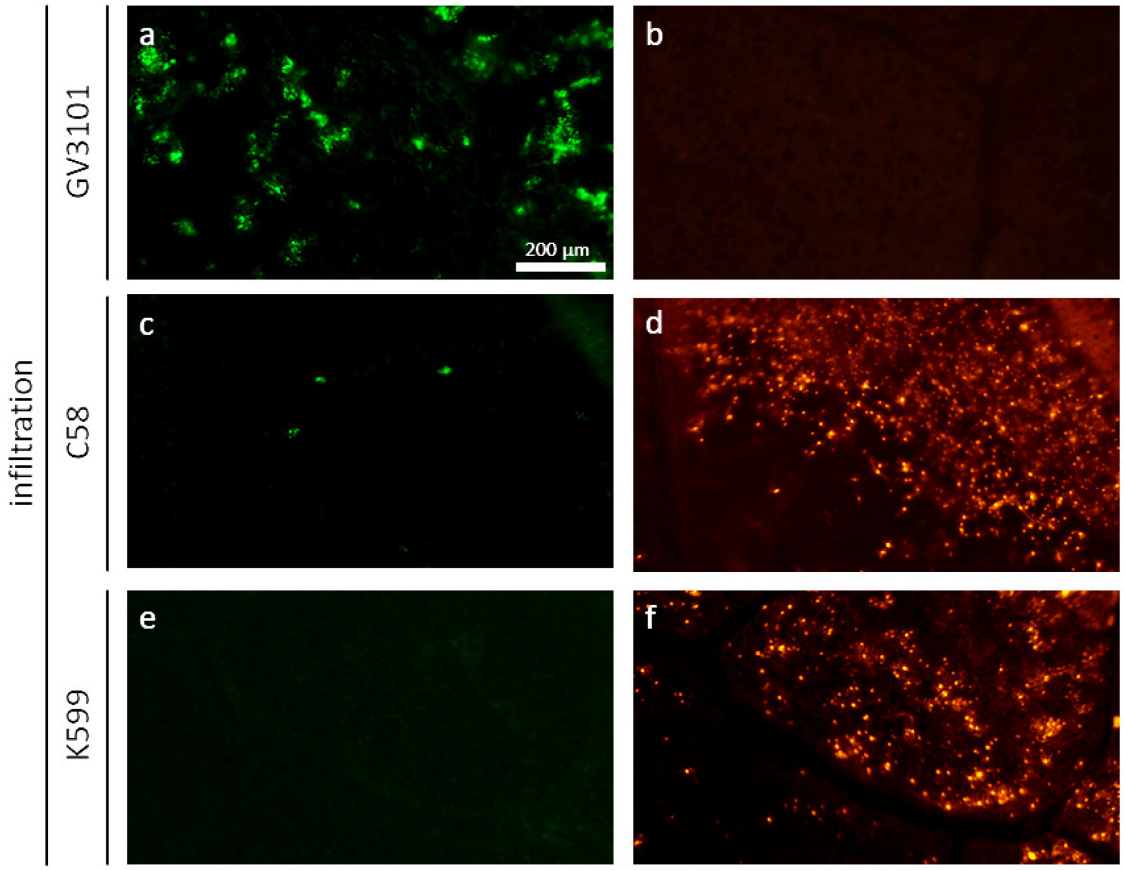

Figure 26: Transformation *P. tremula x alba* leaves with selected *Agrobacteria* strains via leaf infiltration. *P. tremula x alba* leaves were infiltrated with *A. tumefaciens* strains GV3101 or C58 as well as *A. rhizogenes K599* expressing a nuclear targeted Td- Tomato under control of a CaMV35S promoter. Images were taken after 5 days post infection, using a binocular (MSV269, Leica) and the YFP and RFP filter sets (filter details given in 2.2.9.2).

3.2.2 Analysis of a 3.2 kb long fragment of the promoter of the ectomycorrhiza induced transcription factor DREB1

The expression of the dehydration-responsive element binding factor (DREB1) is induced upon ECM formation (Nehls *et al.* unpublished). A ~3.2 kb long promoter fragment was already amplified from genomic DNA of *P. tremula x tremuloides* (Das, 2018), which was further investigated in this thesis. The final amplicon showed the highest similarity with the

genome sequences of *P. tremuloides* and covered the region from -3147 to +31 related to the predicted start ATG of the coding region (**Figure 27 A**). The start point of the longest transcript was determined via RNAseq (Nehls *et al.* unpublished) and the position of the start ATG was predicted by the *P. trichocarpa* annotation (**Figure 27 A**). The promoter fragment was released via *Kpn*I and *Hpa*I double digest from a stock based pPLV vector (Das, 2018) and cloned into the vector pCXUN04NOS to drive nuclear localized dGFP expression. The construct showed the expected fragments after restriction analysis (**Figure 27 B + C**) and was partial sequenced (**Sup. Figure 8**).

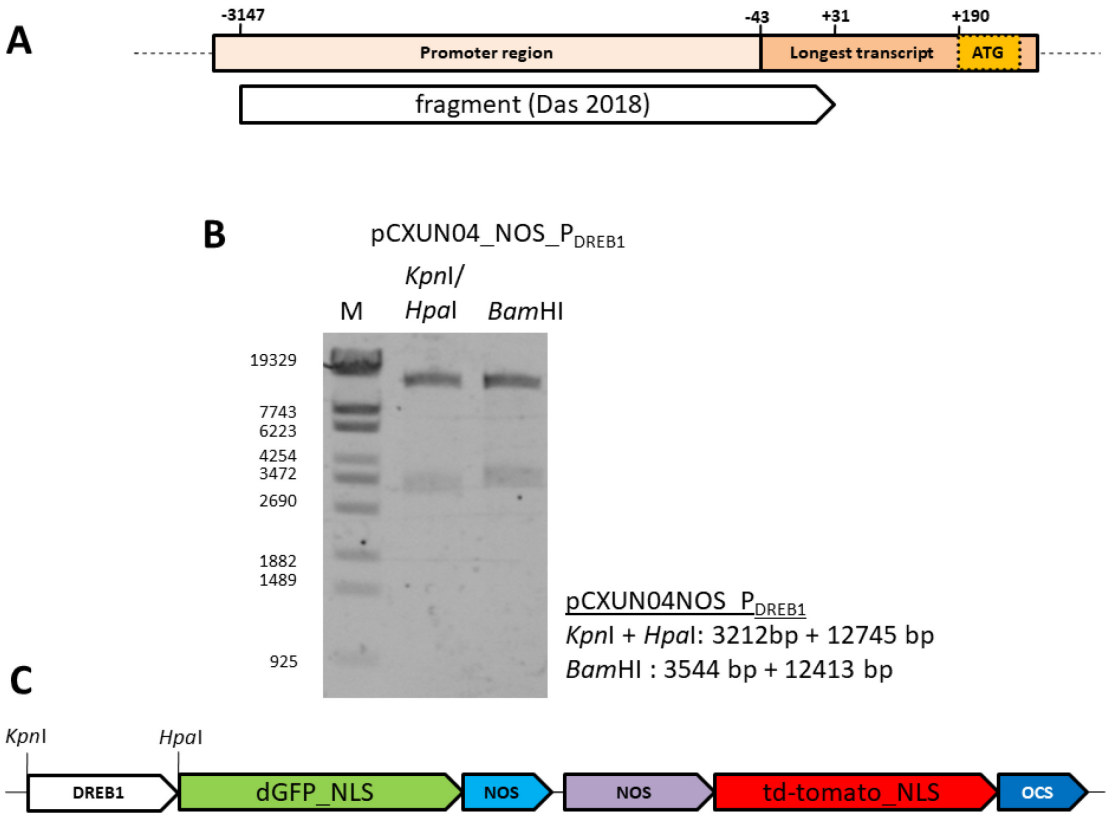

Figure 27: Cloning of DREB1 promoter region in pCXUN04NOS. A) The promoter region upstream of the ATG of the gene *DREB1* is shown as a scheme. The translational start point indicated by the ATG and the 5'-end of the longest transcript observed by RNAseq (Nehls *et al.* unpublished) are shown. B) The construct pCXUN04NOS_*DREB1* was analyzed by restriction digestion with *Kpn*I + *Hpa*I and *Bam*HI DNA. The fragments were separated on 1 % agarose gel with 3 µL of Phage Lambda DNA/*Sty*I marker as size marker (M). C) The modified T-DNA region of the vector is shown schematically.

3.2.2.1 Investigation of DREB1 promoter based gene expression in *N. benthamiana* leaves

The fluorescence intensity of DREB1 promoter driven, nuclear targeted dGFP was investigated in *N. benthamiana* leaves and compared to the dGFP fluorescence driven by the UBQ10 promoter. dGFP expression under control of the UBQ10 promoter was detected in *N. benthamiana* leaves after an illumination time of 1 sec (**Figure 28 a**). While the Td-Tomato fluorescence was rather low and only detectable after an illumination time of 13.4 sec

(**Figure 28 b**). DREB1 promoter driven dGFP expression was detected, but an illumination time of 6.5 sec was necessary to see comparable signal intensity (**Figure 28 c**). Clear Td-Tomato signals were detected for pCXUN04NOS_*DREB1* with an illumination time of only 4 sec (**Figure 28 d**).

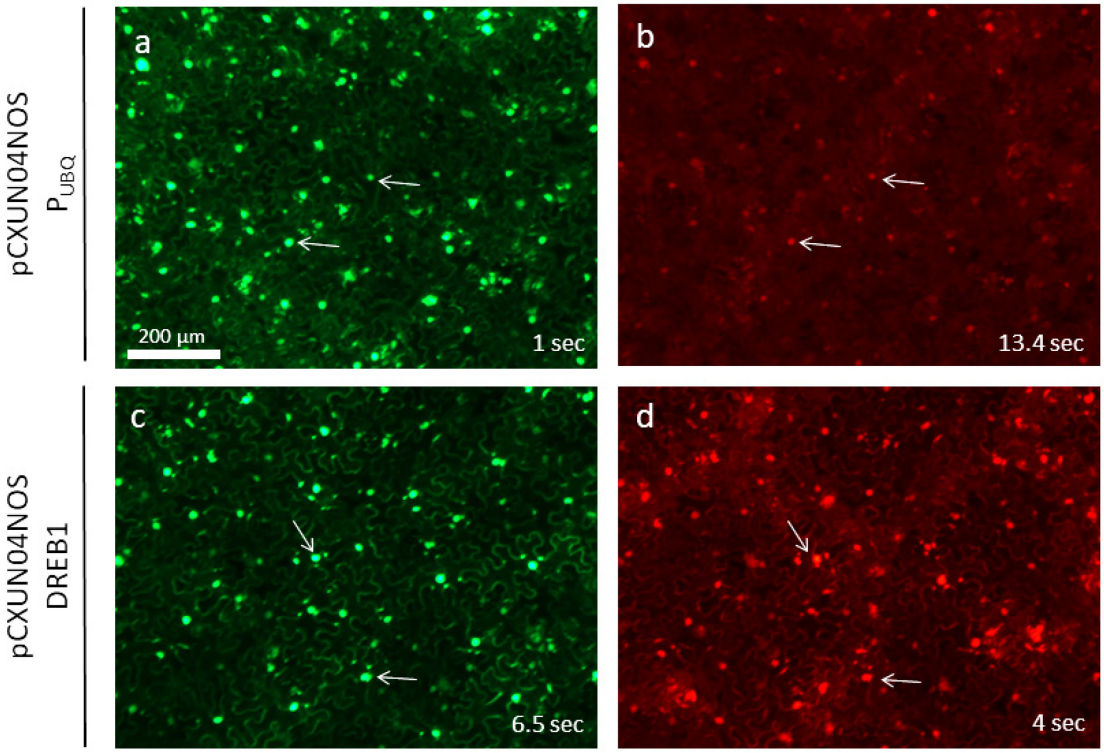

Figure 28: Expression analysis of a promoter fragment of DREB1 in *N. benthamiana* leaf cells. *N. benthamiana* leaves were infiltrated with transgenic *Agrobacterium rhizogenes* K599 and analyzed after 3 days of incubation. a) As positive control, the ubiquitin promoter 10 (UBQ10) driven expression of a nuclear localized dGFP was used. c) The activity of a promoter fragment of *DREB1* was investigated also by expression of a nuclear dGFP. b + d) A nopaline synthase promoter driving the expression of a nuclear localized Td-Tomato was used for both constructs as reference. Pictures shown in a and b are identical with a and b in **Figure 20** to allow for better comparison. For analysis a binocular (MSV269, Leica) was used. a + c GFP filter, b + d RFP filter; for filter details see 2.2.9.2.The used illumination times are given in the pictures.

3.2.2.2 Expression of DREB1 promoter in *P. tremula x alba* leaves

To validate the results obtained in *N. benthamiana* leaves, the same experimental set up was performed with *P. tremula x alba* leaves. Over all the expression in *P. tremula x alba* leaves was weaker as in *N. benthamiana* leaves (**Figure 29** + **Figure 28**). The expression of UBQ10 promoter driven dGFP was detected using an illumination time of 9.5 sec (**Figure 29 a**), while for DREB1 promoter very weak signals were detected for an illumination time of up to 13.4 sec (**Figure 29 c**). The Td-Tomato signals of pCXUN04NOSP_{UBQ10} were even with 13.4 sec of illumination time hard to detect (**Figure 29 b**), while clear signals were detected for pCXUN04NOS_*DREB1* after 6.5 sec illumination (**Figure 29 d**).

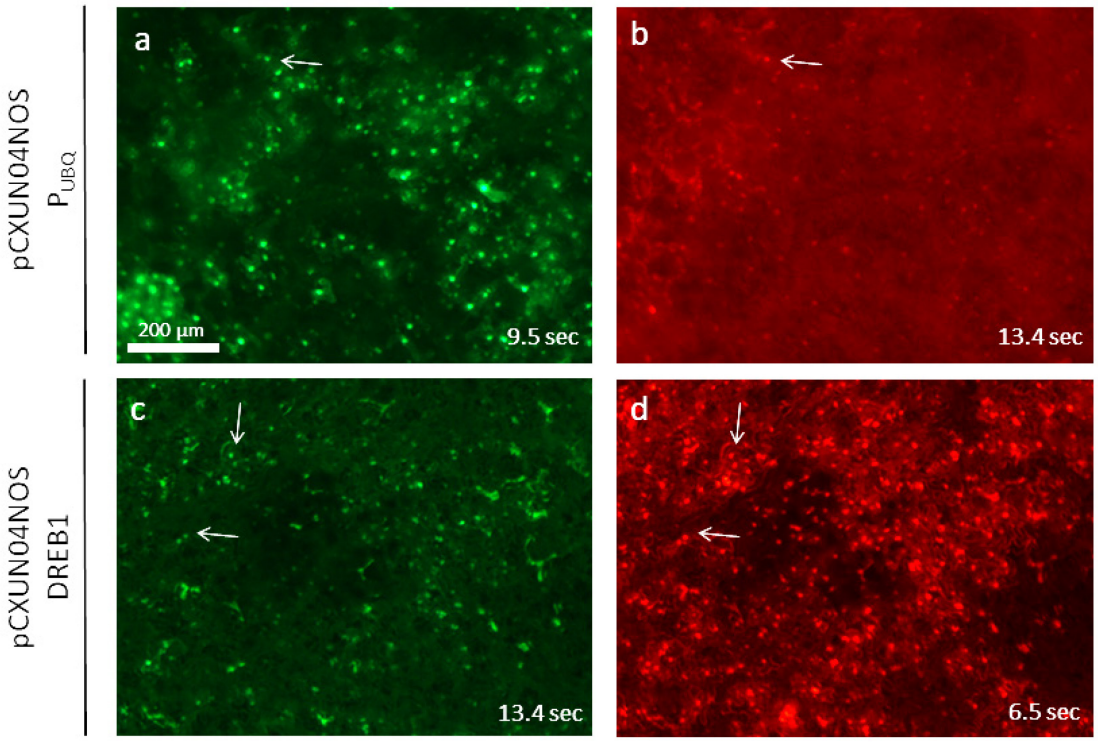

Figure 29: Promoter analysis of *DREB1* in *P. tremular x alba* leaves. Infiltration of *P. tremular x alba* leaves was performed with transgenic *A. rhizogenes* K599. Results were analyzed after 4 days of incubation. As reference a nuclear Td-Tomato is expressed under control of a nopaline synthase promoter. As positive control a nuclear dGFP is expressed under the control of an ubiquitin promoter (a). The expression of the promoter fragment of *DREB1* is shown in c. The results were documented using a binocular (MSV269, Leica). a + c GFP filter, b + d RFP filter; for filter details see 2.2.9.2.The used illumination times are given in the pictures.

The samples were furthermore analyzed using cLSM to verify the weak signals. For both constructs signals were detected for dGFP and Td-Tomato (data not shown). To sum up, the results generated in *P. tremula x alba* leaves show similar expression pattern as observed in *N. benthamiana* leaves, but much weaker signal intensities.

3.2.2.3 Expression of DREB1 promoter in non-mycorrhized *P. tremula x alba* roots

The expression of dGFP under control of the UBQ10 promoter was detected with an illumination time of 1 sec (**Figure 30 a**), while it took an exposure time of 2 sec to obtain clear Td-Tomato signals. However, the differences in signal intensities of dGFP and Td-Tomato fluorescence were much smaller in stable transgenic roots compared to transient expression in leaves. The GFP fluorescence signals detected in transgenic pCXUN04NOS_*DREB1* harboring roots were hard to see even after an illumination time of 10 sec (**Figure 30 c**). With the same time strong root autofluorescence was obtained (see 3.1.6.2, **Figure 21**). The respective roots harbor, however, the pCXUN04NOS_*DREB1* T-DNA, since Td-Tomato signals were clearly detectable (**Figure 30 d**).

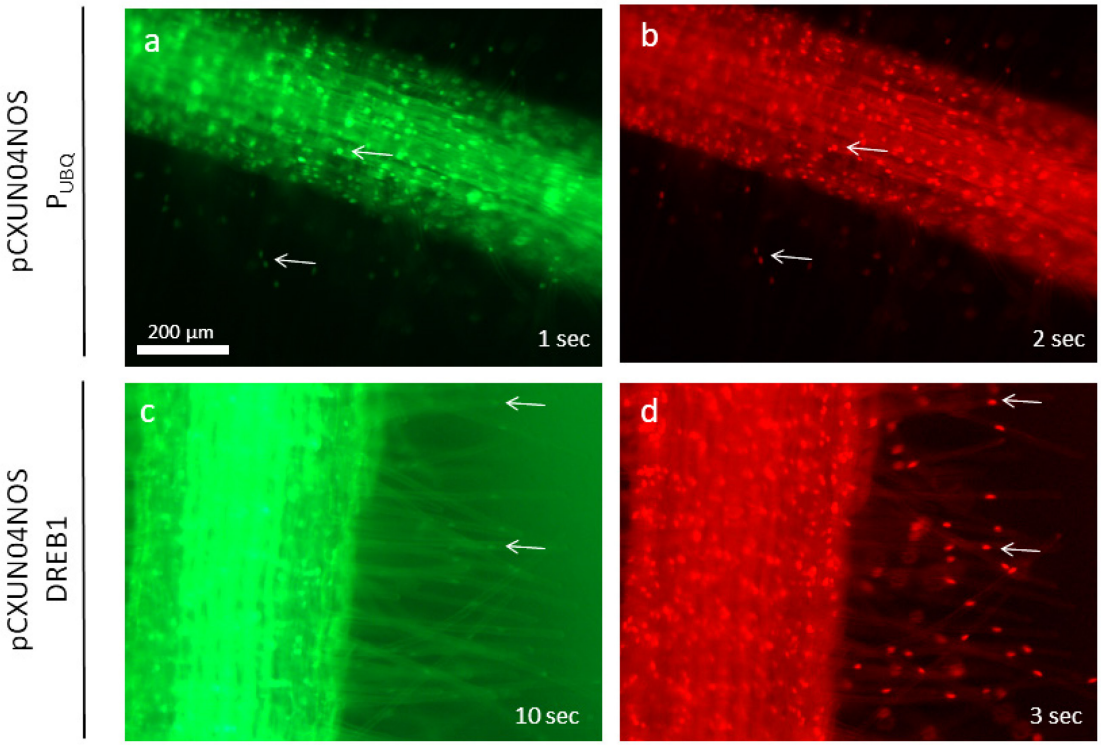

Figure 30: Expression of a DREB1 promoter fragment in non-mycorrhized *P. tremula x alba* roots. *P. tremula x alba* roots were investigated 4 weeks after transformation. As positive control, roots expressing a nuclear localized dGFP under control of the ubiquitin promoter 10 (P_{UBQ10}) (a) and nuclear localized Td-Tomato under control of a nopaline synthase (NOS) promoter (b) were used. The activity of the promoter fragment of *DREB1* was monitored by dGFP expression (c) and as internal transformation control a nuclear localized Td-Tomato is shown (d). Pictures shown in a and b are identical with a and b in **Figure 21** to allow for better comparison. The results were documented using a binocular (MSV269, Leica), a + c GFP filter, b + d RFP filter; for filter details see 2.2.9.2.The used illumination times are given in the pictures.

Since the dGFP expression under control of DREB1 promoter gave only a very weak signal in non-mycorrhized roots, the roots were also investigated by cLSM. As observed by epi-fluorescence microscopy a clear Td-Tomato signal was detectable (**Figure 30 d + Figure 31**), but only a very weak dGFP signal could be seen (**Figure 31**).

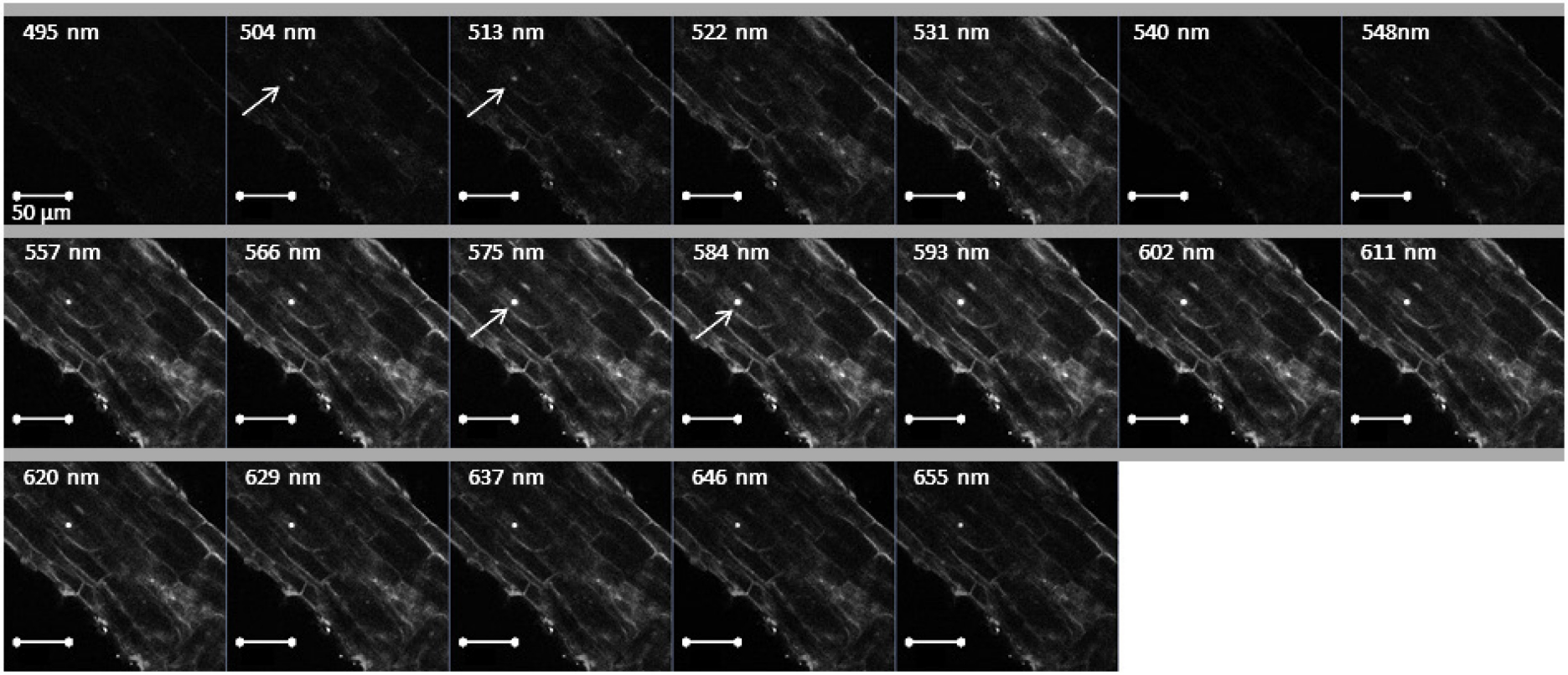

Figure 31: Non-mycorrhized *P. tremula x alba* root expressing dGFP under control of a DREB1 promoter. Composite *P. tremula x alba* were analyzed 5 weeks after transformation. Roots expressed dGFP under control of DREB1 promoter fragment and Td-Tomato driven by nopaline synthase promoter. A lambda scan was performed (excitation at 488 nm, argon laser 1 % laser intensity and 543 nm helium neon laser 5 % laser intensity, window size 9 nm, cLSM, 880, Zeiss). The analysis was performed in collaboration with Uwe Nehls.

3.2.2.4 Expression of DREB1 promoter in ectomycorrhizas

Composite plants were mycorrhized with *Pisolithus microcarpus* D2 successfully (**Figure 32 a**), while no ectomycorrhizas were obtained with *Amanita muscaria* as plant partner.

Harvested ECMs were investigated using fluorescence microscopy to selected ECMs formed on transgenic roots. Td-Tomato signals were detected in roots carrying the ECM (**Figure 32 d**). No GFP signal could be detected in the same roots (**Figure 32 c**) as it was observed before (**Figure 31**). The detection of fluorescence signals through the fungal mantle was not possible (**Figure 32 b + d**) and longitudinal sections of the structure had to be prepared.

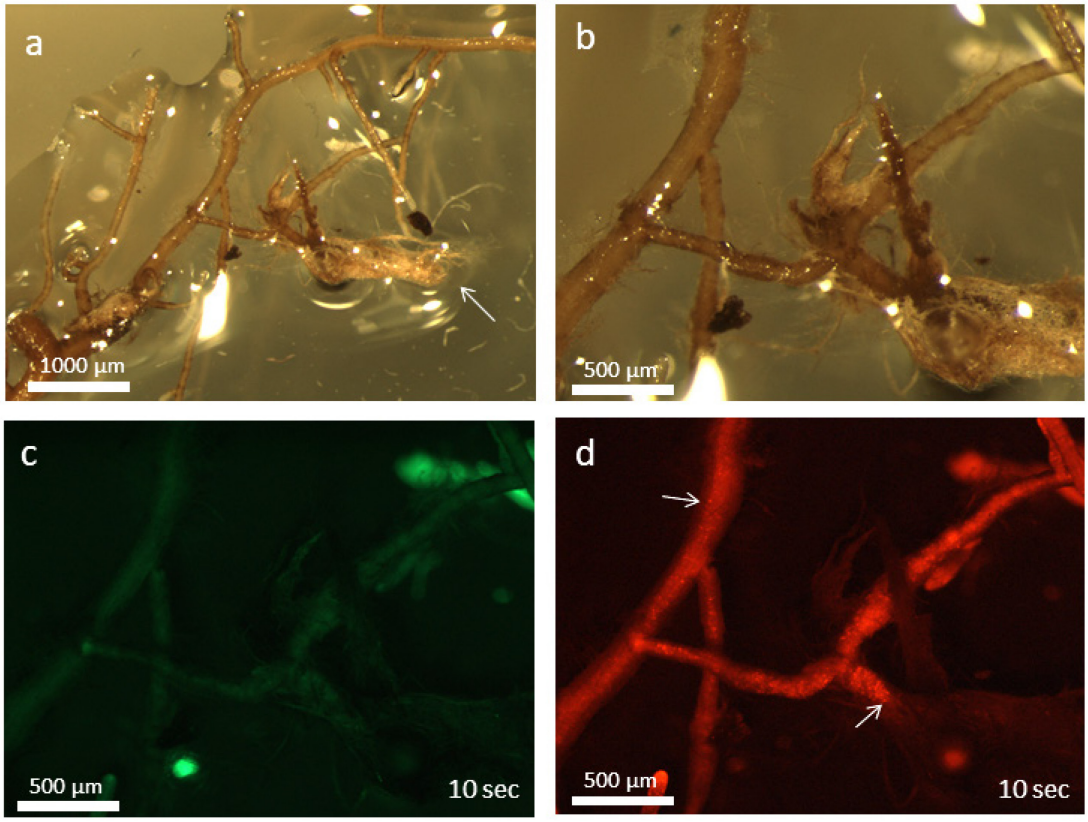

Figure 32: Transgenic ectomycorrhiza expressing dGFP under control of DREB1 promoter. Composite *P. tremula x alba* expressing dGFP under control of DREB1 promoter and Td-Tomato under control of the nopaline synthase promoter were co-cultivated with *P. microcarpus*. Analysis was performed five month after inoculation. Structures were documented after harvesting using binocular (MSV269, Leica), for filter details see 2.2.9.2. a) Bright field b) Bright field c) GFP channel d) RFP channel.

Longitudinal ectomycorrhiza sections were analyzed by cLSM (880, Zeiss), but no specific dGFP signal was detected (data not shown). Since Td-Tomato signals were clearly detectable in the respective roots, the integration of pCXUN04NOS_*DREB1* T-DNA into the root genome is proven (**Figure 32 d**).

3.2.3 Promoter analysis of the ectomycorrhiza induced *SWEET1* gene

SWEET1 expression is strongly induced in poplar ectomycorrhizas (Nehls and Bodendiek 2012). To analyze the promoter of *SWEET1* a promoter fragment was amplified by PCR. Primers were designed using the genome sequence of *P. tremula x tremuloides* as a template. The forward primer binds in position -3570 and the reverse primer 19 bp upstream of the ATG (**Figure 33 A**). The position of the supposed translational start site was predicted according to the *P. trichocarpa* sequence. The primers were designed such that they contained an additional restriction sites *Kpn*I for forward primer and *Sma*I for the reverse primer (**Figure 33 B**). The PCR product was cloned into the entry vector pJET1.2 and was partially sequenced (**Sup. Figure 9 A**). In the next step the promoter fragment was released via the introduced restriction sites *Kpn*I and *Sma*I and cloned into *Kpn*I and *Hpa*I sites of the vector pCXUN04NOS. The obtained construct was analyzed by restriction analysis (**Figure 33 C**) and partially sequenced (**Sup. Figure 9 B**). The final construct pCXUN04NOS_*SWEET1* (**Figure 33 D**) was used for *in planta* analysis.

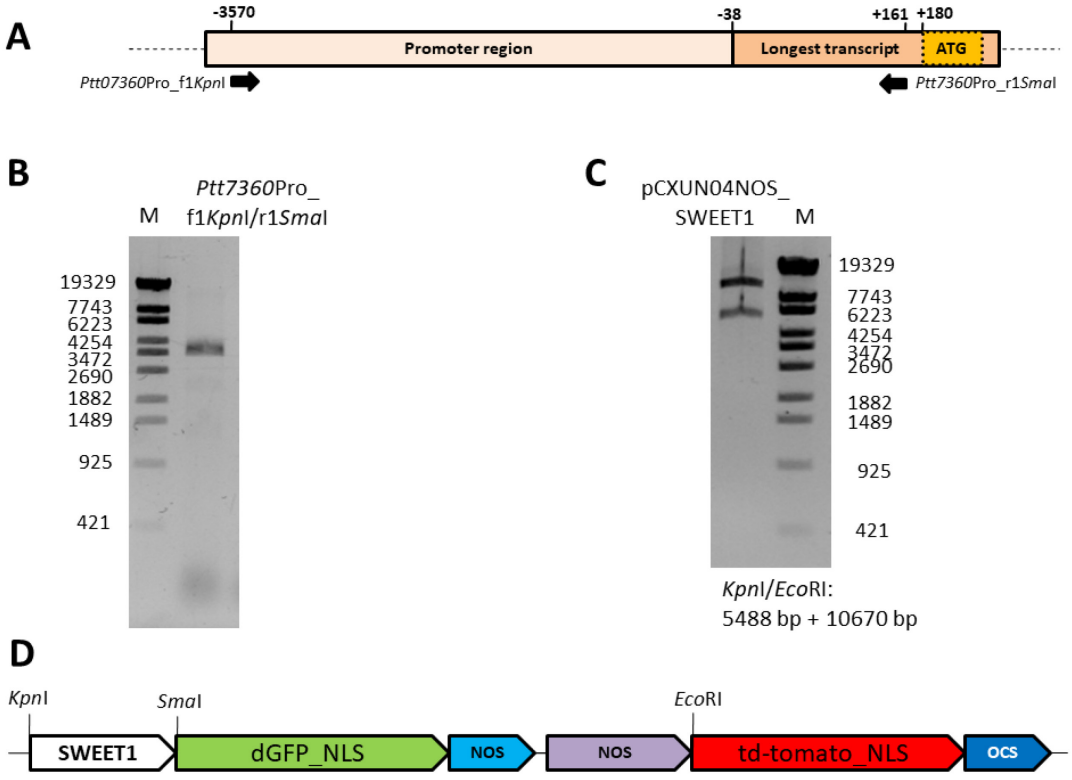

Figure 33: Cloning of a SWEET1 promoter fragment into pCXUN04NOS. A) The scheme of the region upstream of the ATG of *SWEET1* is shown. The binding positions of the designed primers and the start point of the longest transcript investigated by RNAseq (Nehls *et al.* unpublished) are shown. B) Amplification of *SWEET1* was performed using genomic DNA of *P. tremula x tremuloides* and the primer pair *Ptt07360*Pro_f1*Kpn*I and *Ptt07360*Pro_r1*Sma*I at a Tm of 61.7 °C. The 3409 bp long PCR product was controlled on a 1 % agarose gel with 3 µL of Phage Lambda DNA/*Sty*I marker as size marker (M). C) The construct pCXUN04NOS_*SWEET1* was analyzed by restriction digestion with *Kpn*I and *Eco*RI and DNA fragments were separated on 1 % agarose gel with the same marker as in B. D) The modified T-DNA region of the vector is shown schematically.

3.2.3.1 Investigation of promoter activity of the *SWEET1* promoter fragment by transient expression in *N. benthamiana* leaves

The expression strength mediated by SWEET1 promoter was compared to that of UBQ10 promoter. Both promoters induced the expression of a nuclear targeted dGFP (**Figure 34 a + c**). To document signal intensities, illumination times of 1 sec for UBQ10 promoter and 562.9 msec for SWEET1 promoter were necessary. The constitutive expressed Td-Tomato revealed lower fluorescence intensities for both constructs indicated by a much longer exposure time of 13.4 sec and 6.5 sec for pCXUN04NOSP$_{UBQ10}$ and pCXUN04NOS_*SWEET1*, respectively (**Figure 34 b + d**).

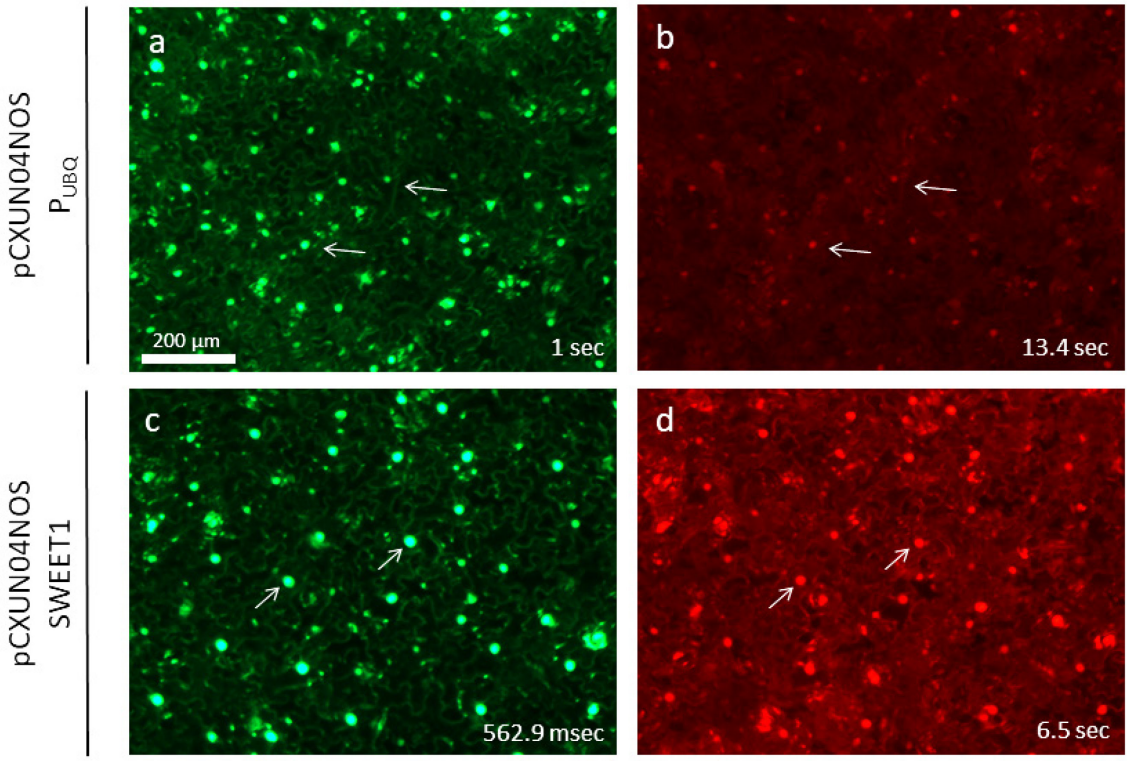

Figure 34: Activity of SWEET1 and UBQ10 promoter in *N. benthamiana* leaves. Infiltration of *N. benthamiana* leaves was performed with transgenic *A. rhizogenes* K599 strains. PCXUN04NOS_P$_{UBQ}$ transformed cells enabled dGFP under the control of the ubiquitin promoter 10 (P$_{UBQ10}$) (a) and Td-Tomato expression under control of the nopaline synthase (NOS) promoter (b). The activity of SWEET1 promoter was monitored by dGFP expression (c). Td-Tomato expression was again under control of the NOS promoter (d). All florescence proteins were targeted to the nucleus. Pictures shown in a and b are identical with a and b in **Figure 20** to allow for better comparison. The results were documented using a binocular (MSV269, Leica). a + c GFP filter, b + d RFP filter; for filter details see 2.2.9.2.The illumination times are given in the pictures.

3.2.3.2 Transient expression of *SWEET1* promoter in *P. tremula x alba* leaves

To validate the data achieved in *N. benthamiana* leaves the same experiment was performed in *P. tremula x alba* leaves. As observed before the overall expression intensity was lower in *P. tremula x alba* leaves compared to *N. benthamiana* leaves (**Figure 34** + **Figure 35**). Nevertheless distinct dGFP signals were detected with UBQ10 promoter and SWEET1

promoter (**Figure 35 a + c**), already observed in *N. benthamiana* leaves. The signal intensity obtained with SWEET1 promoter was again stronger than that of UBQ10 promoter. The Td-Tomato signals were clearly detectable for pCXUN04NOS_*SWEET1* (**Figure 35 d**), but difficult to document for pCXUN04NOSP_{UBQ10} (**Figure 35 b**).

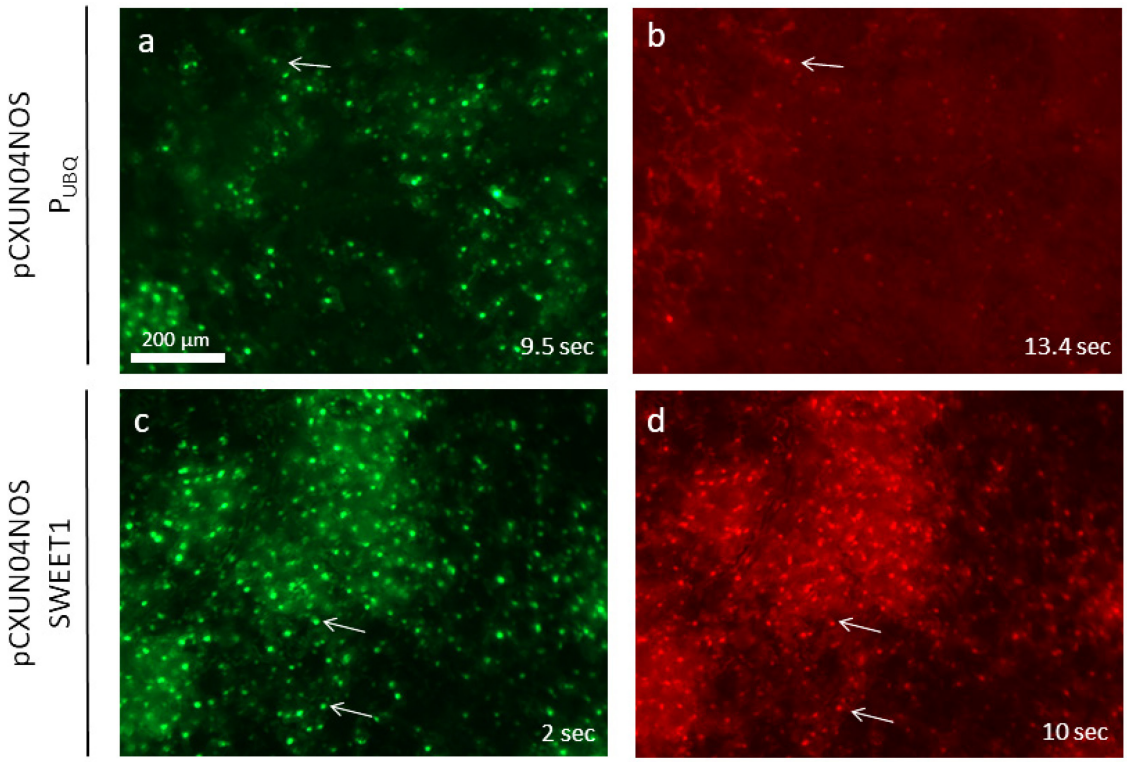

Figure 35: Activity of SWEET1 promoter in *P. tremula x alba* leaves. *P. tremula x alba* leaf infiltration was performed using transgenic *A. rhizogenes* K599 and analyzed after 4 days of incubation. The promoter activities of UBQ10 (a) and SWEET1 (c) were investigated by the nuclear located dGFP signals. In both cases a nuclear localized Td-Tomato was co-expressed under control of the nopaline synthase (NOS) promoter (b + d). Pictures shown in a and b are identical with a and b in **Figure 29** to allow for better comparison. The results were documented using a binocular (MSV269, Leica). a + c GFP filter, b + d RFP filter, for filter details see 2.2.9.2.The used illumination times are given in the pictures.

3.2.3.3 Expression of *SWEET1* promoter in non-mycorrhized *P. tremula x alba* roots

The same constructs as before were used to generate transgenic roots on composite *P. tremula x alba*. When using an illumination time of 1 sec similar fluorescence signal intensities were obtained for UBQ10 promoter and SWEET1 promoter driven dGFP signals (**Figure 36 a + c**). SWEET1 driven dGFP expression was detected in root hairs and cortex cells (**Figure 36 a).** The observed signal intensity of Td-Tomato was also comparable for transgenic roots containing both constructs (**Figure 36 b + d**). Again, the results of stable *P. tremula x alba* root transformation differed from that obtained with *N. benthamiana* leaves.

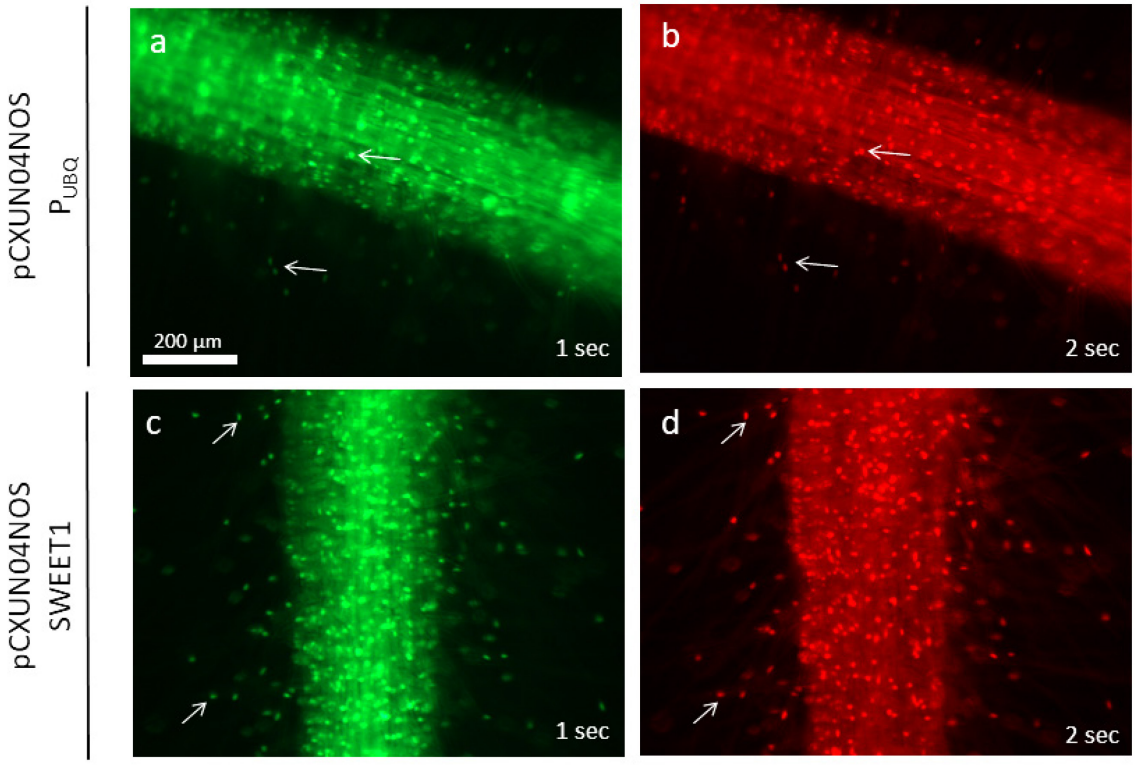

Figure 36: Promoter analysis of SWEET1 in *P. tremula x alba* roots. To analyze the expression of SWEET1 promoter composite *P. tremula x alba* plants were generated and roots were investigated after 4 weeks. The test vector expressed a nuclear localized dGFP under control of the ubiquitin promoter 10 (P_{UBQ10}) (a) or SWEET1 promoter (b). As internal transformation control the vector expressed a nuclear localized Td-Tomato under control of a nopaline synthase (NOS) promoter (b + d). Pictures shown in a and b are identical with a and b in **Figure 21** to allow for better comparison. The results were documented using a binocular (MSV269, Leica). a + c GFP filter, b + d RFP filter; for filter details see 2.2.9.2.The used illumination times are given in the pictures.

The specificity of dGFP and Td-Tomato signals in transgenic root tissue were proven by cLSM (**Figure 37**). The expected signal maxima for dGFP (504 to 513 nm) and Td-Tomato (575 to 584 nm) were confirmed the results obtain with classical fluorescence microscopy (**Figure 36 c + d**).

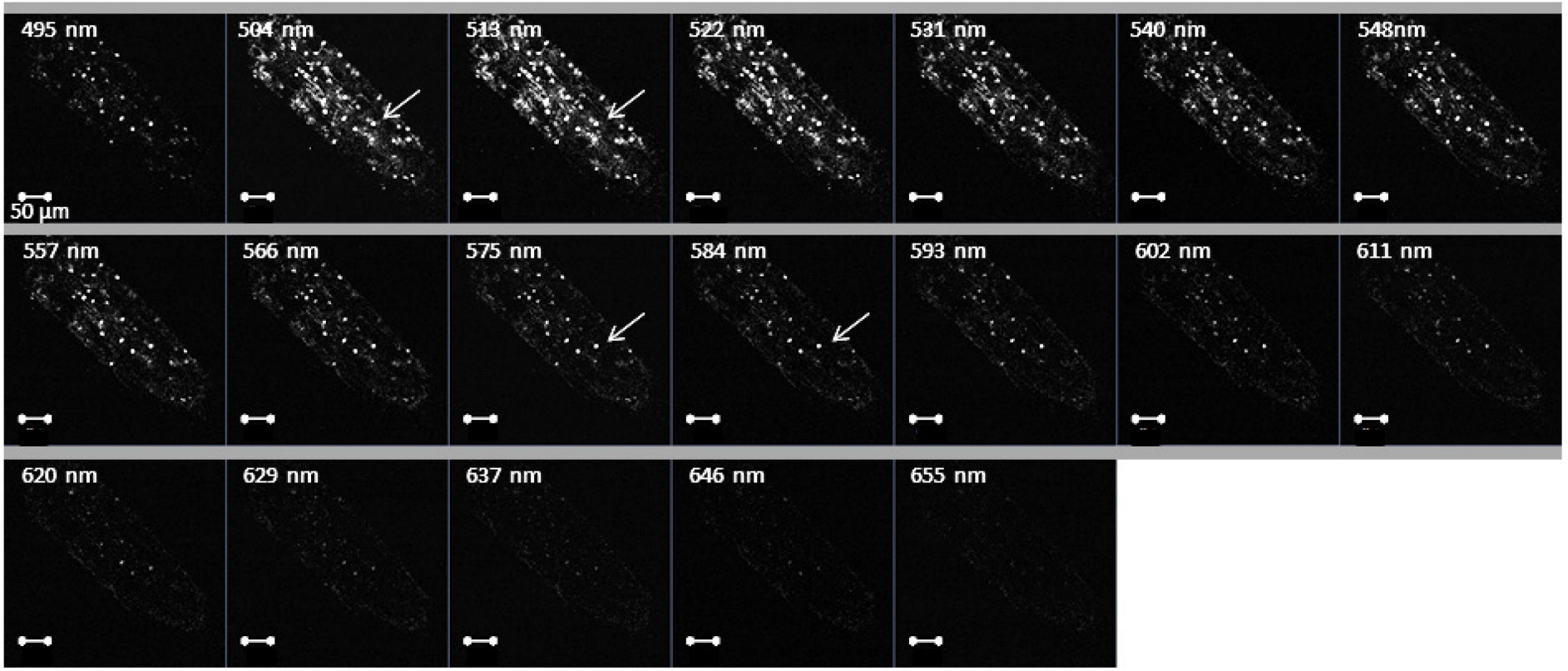

Figure 37: Analysis of *SWEET1* promoter based dGFP expression in non-mycorrhized *P. tremula x alba* roots. Composite *P. tremula x alba* were analyzed 5 weeks after transformation. Roots expressed dGFP under control of the *SWEET1* promoter fragment and Td-Tomato driven by a nopaline synthase promoter are shown. A lambda scan was performed with excitation light at 488 nm (argon laser with 0.2 % laser intensity) and 9 nm wide emission windows using a cLSM (880, Zeiss). The lambda scan was performed in collaboration with Uwe Nehls.

3.2.3.4 *SWEET1* promoter driven GFP expression in ectomycorrhizas

To investigate whether a difference in the expression intensity of SWEET1 promoter in ectomycorrhizal structures compared to non-mycorrhized roots can be observed, *P. tremula x alba* plants showing fluorescent roots were mycorrhized with *Pisolithus microcarpus* D2 and *Amanita muscaria.* While mycorrhization with *Amanita muscaria* was unsuccessful, ECM were formed by *P. tremula x alba* with *Pisolithus microcarpus*.

A typical example of a swollen root tip after fungal infection is shown in (**Figure 38 a**). Epi fluorescence microscopy indicated the selected ECMs as transgenic harboring the T-DNA of pCXUN04NOS_SWEET1. The transgenic roots showed clear dGFP and Td-Tomato signals in the nuclei (**Figure 38 c + d**). Since the visualization of fluorescence signal was not possible through the fungal mantle (**Figure 38 b + c + d)**, longitudinal sections of ectomycorrhizas were performed.

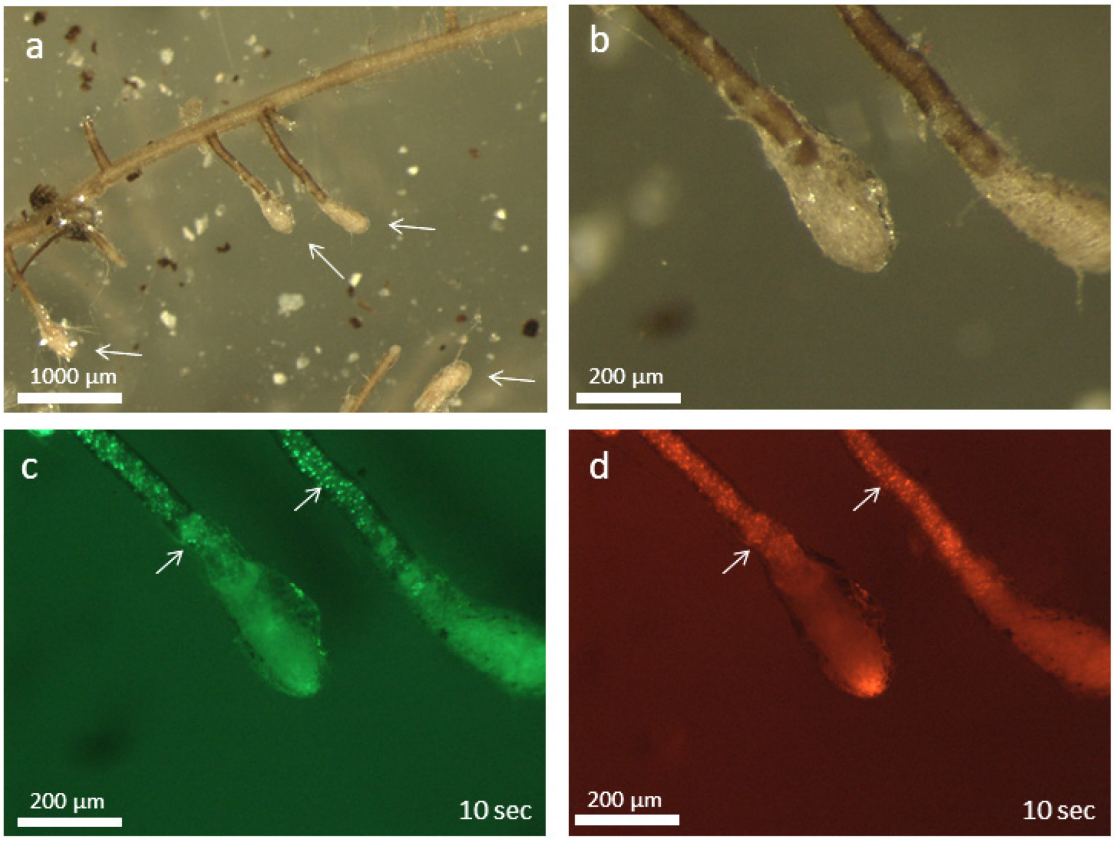

Figure 38: Ectomycorrhizas formed by transgenic roots harboring pCXUN04NOS_SWEET1. Ectomycorrhized roots of *P. tremula x alba* expressing dGFP under control of *SWEET1* promoter and Td-Tomato under control of the nopaline synthase promoter in pCXUN background were co-cultivated with *P. microcarpus*. Roots carrying ectomycorrhizas were harvested five month after inoculation. Fluorescence was visualized using a binocular (MSV269, Leica). For filter details see 2.2.9.2. Shown are images in a) Bright field b) Bright field c) GFP channel d) RFP channel.

Signals with spetral propperties of dGFP and Td-Tomato were detected in the nuclei of ECMs, but no difference in fluorescence intesity beween non-mycorrhized and mycorrhized roots were detected. Signals of dGFP and Td-Tomato were detected in nuclei of the root cortex cells (**Figure 39, 3 + 5**), while no signals were detected in rhizodermis cells (**Figure 39, 2**). In the smaller cells of the central cylinder no specific signals of dGFP or Td-Tomato could be detected (**Figure 39, 4**).

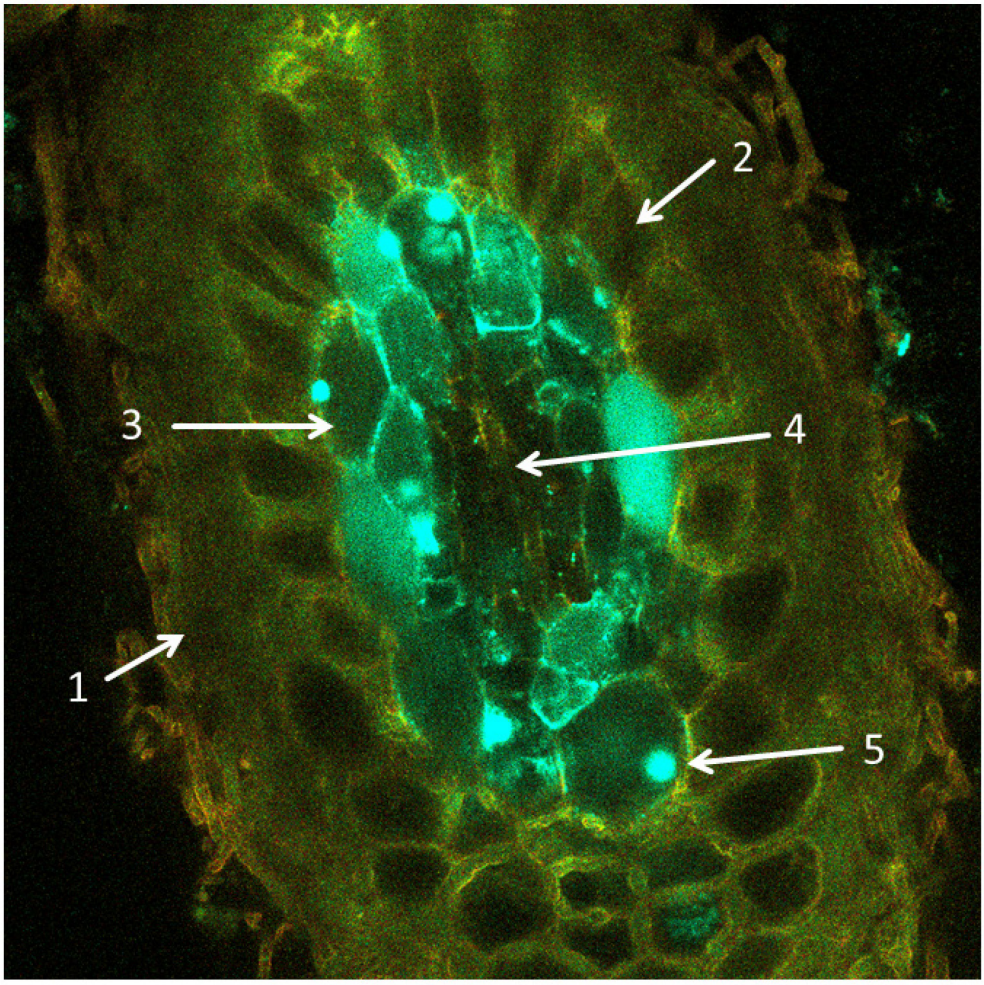

Figure 39 *In planta* promoter analysis of *SWEET1* in an longitudinal ectomycorrhiza section. The promoter of SWEET1 drove dGFP and a nopaline synthase promoter controlled a nuclear targeted Td-Tomato. 80 µm thick longitudinal sections of ectomycorrhizas were prepared and analyzed using cLSM (880, Zeiss). For illumination argon laser light (488 nm) with an intensity of 2 % was used. An overlay of 9 nm wide emission windows from 495 to 655 nm is shown. Lambda scan was performed in collaboration with Uwe Nehls. 1) Fungal mantle. 2) Rhizodermis cell. 3) Cell of the root cortex. 4) Truncated central cylinder. 5) Nucleus harboring dGFP and Td-Tomato signal.

4 Discussion

4.1 Leaf transformation: as strategy for transient expression in poplar

Since the generation of stable transformed plants takes month, the establishing of faster transformation methods is of high interest, especially in research using plants with relative low growth rates, e. g. poplar. However, the generation of composite poplar under laboratory conditions still requests six to eight weeks for the investigation of transgene expression in the root system (Neb *et al.* 2017). Transient expression in e. g. leaves generate results within days, so leaf infiltration was adopted for a large number of plant species, but manly *N. benthamiana* is usually used, since it is particular easy to handle (Wroblewski *et al.* 2005). Leaf infiltration allows promoter analysis, analysis of subcellular protein localization or construct testing within a very short time (Yang *et al.* 2000, Vaquero *et al.* 2002).

However, heterologous expression in *N. benthamiana* has a number of disadvantages. Transcription factors important for gene expression might be missing or false protein localizations could be detected due to heterologous expression (Hernandez-Garcia and Finer 2014). Some of these problems might be overcome by transient expression in leaves of the source organism, in this case, poplar. To test the suitability of such an approach, different transformation strategies were tested for transient expression in poplar leaves (**chapter 3.2.1**).

Transient expression in roots compared to leaves would be of cause the better option in ectomycorrhiza (ECM) research and could be of particular interest for promoter analysis. But in comparison to transient expression in leaves only a few *Agrobacterium*-mediated transient expression systems for roots were established. In poplar, transformation approaches like particle bombardment and incubation with transgenic *Agrobacteria* were, however not successful yet (data not shown).

4.1.1 Establishing transient gene expression in poplar leaves

Selected *Agrobacteria* strains were tested for the ability to transform leaves of *P. tremula x alba* without inducing necrotic reactions. Poplar plants in axenic culture are sensitive to humidity changes and mechanical stress (personal communication, Uwe Nehls). Therefore the more robust hybrid *P. tremula x alba* was used for the establishing of transient expression. Vortexing of leaves with silicium carbide particles followed by incubation in *Agrobacteria* cultures resulted in leaves transgenic epidermal cells in *P. tremula x alba*, but with infiltration it was possible to generate more transgenic cells as with the vortexing

approach. Against the expectations, the fragile poplar leaves could be infiltrated by *A. tumefaciens* C58 and *A. rhizogenes* K599 without severe mechanical damage. *A. rhizogenes* K599 was of greater importance, since *P. tremula x alba* leaf infiltration was designed to complement studies performed with composite plants, which are generated by transformation with *A. rhizogenes* K599. The induction of necrotic reaction by *Agrobacteria* is known especially when highly virulent strains are used (Wroblewski *et al.* 2005). The disarmed *A. tumefaciens* strain C58 as well as the *A. rhizogenes* K599 did not show any necrotic response in *P. tremula x alba* leaves.

The reason while infiltration resulted in more transgenic cells and therefore an higher transformation efficiency might be that bacterial cells get in closer contact to the plant cells, due to the application of *Agrobacteria* directly through the stomata. The closer contact could promote the attachment of *Agrobacteria* cells to the plant cells. The attachment process is not well characterized, but it can be estimated that the close contact of cell wall proteins favor the T-DNA transfer and therefore the transformation efficiency (Gelvin 2000, Zhu *et al.* 2003).

Compared to infiltration of *N. benthamiana* leaves, the main disadvantages of the established transient expression in *P. tremula x alba* leaves is the higher fragility of poplar leaves. This is resulting in less successful spreading of *Agrobacteria* culture during infiltration and lower signal intensities decreasing the sensitivity of the method compared to *N. benthamiana*. Nevertheless the great advantages of testing specific promoter activities directly in the model organism poplar, is a great option.

4.1.2 Modulated emission properties of Td-Tomato after transient expression with *A. tumefaciens* GV3101

While no obvious difference in the emission spectrum of sYFP was observed for Td-Tomato, transient expression by the *A. tumefaciens* GV3101 resulted in a shift in the emission spectrum of a nuclear targeted Td-Tomato in leaves. The highest fluorescence intensity was observed around 525 nm, while transient expression enabled by *A. tumefaciens* C58 or *A. rhizogenes* K599 showed the expected signal maximum around 584 nm. Furthermore, leaf cell transformation by *A. tumefaciens* GV3101 resulted in signals that were not localized within the nucleus, but in dot-like structures spread in the cytoplasm (**chapter 3.2.1.3**). Similar results were also observed for other red fluorescence proteins (Tm-Tomato and mCherry) and when *N. benthamiana* leaves were infiltrated with *A. tumefaciens* GV3101. Such dot-like structures might be lysosomes, which was described for GFP-like proteins in

HeLa cells by Katayama *et al.* (2007). The observed shift in the emission properties of Td-Tomato could be explained by the acidic conditions (pH 4) and the presence of proteases in lysosomes (Katayama *et al.* 2007, Burgstaller *et al.* 2019). With a pka value of 4.7, a conformational change of Td-Tomato is expected in lysosomes (Piatkevich and Verkhusha 2011). However, in comparison to green and yellow fluorescence proteins, red fluorescence proteins normally are known for a higher pH stability and changes in the environmental pH were reported to result only in fluorescence reduction, but not a shift in the emission properties (Katayama *et al.* 2007). Nevertheless the emission spectrum of Td-Tomato was clearly affected in these experiments, indicating that the combination of acidic conditions and presence of proteases do influence the stability of the Td-Tomato. The fluorescence properties of a fluorescence protein are altered by the amino acids surrounding the fluorophore (Chudakov *et al.* 2010). Therefore partial degradation of the protein in the lysosomes or incomplete protein folding, which is often related to protein aggregation and transport into lysosomes, might be reasons for the altered emission spectrum of Td-Tomato.

The described changes in Td-Tomato emission and localization were always observed when cells were transformed with *A. tumefaciens* GV3101, but rarely and when only restricted to very few transgenic leaf cells after transformation with *A. tumefaciens* C58. Very high levels of protein expression are reported to cause the formation of inclusion bodies followed by proteolytic degradation (Katayama *et al.* 2007, Grefen *et al.* 2010). Since those effects are related to high protein amount with in the cell, it can be supposed that a much higher protein amount is found. This makes it likely, that the observed artefacts after *A. tumefaciens* GV3101 based cell transformation are due to a much higher expression rate compared to *A. tumefaciens* C58 and *A. rhizogenes* K599. This hypothesis is in agreement with the much higher fluorescence intensity in *A. tumefaciens* GV3101 transformed leaf cells.

4.1.3 Gene expression properties enabled by selected promoters in *N. benthamiana* and *P. tremula x alba* leaves

Similar illumination times were necessary to visualize Td-Tomato fluorescence under control of the nopaline synthase (NOS) promoter in leaves of *P. tremula x alba* and *N. benthamiana*, when the respective gene was expressed. This indicates that this promoter is able to drive similar transient levels in both organisms. Also the *Arabidopsis* UBQ10 promoter is frequently used for heterologous expression in other plants (Peremarti *et al.* 2010). However, UBQ10 expression of dGFP resulted in quite different exposure times to obtain similar emission intensities in *N. benthamiana* (1 sec) and poplar (9.5 sec) leaves

indicating a difference in expression strength in both organisms. This finding supports the decision for the NOS promoter to drive the expression of the Td-Tomato as transformation marker in composite poplar.

Next to its function as marker for successful transformation with the T-DNA of a binary vector, nuclear Td-Tomato fluorescence should be also used to calibrate the promoter strength driving the expression of the second GFP marker cassette for promoter analysis. In this study, two poplar promoters were analyzed. RNAseq and qPCR analysis showed that the respective genes are exclusively expressed in ECMs of poplar (Nehls and Bodendiek 2012, Nehls *et al.* unpublished). Most surprisingly, the investigated promoter fragments were able to drive visible dGFP expression in both *N. benthamiana* and *P. tremula x alba* leaves (**Table 11**).

Table 11: Comparison of illumination times necessary to visualize fluorescence proteins in *N. benthamiana* and *P. tremula x alba*. The illumination times used to visualize GFP and Td-Tomato in *N. benthamiana* and *P. tremula x alba* are given in sec. Furthermore ratios between the illumination times necessary to visualize Td-Tomato and dGFP are given. The promoters of dehydration responsive element binding factor 1 (DREB1), sugar will be eventually exported transporter 1 (SWEET1) and ubiquitin 10 (UBQ10) drive expression of the GFP and Td-Tomato expression was controlled by nopaline synthase (NOS) promoter in all samples. Elements were encoded on pCXUN04NOS vector and transformed by *A. rhizogenes* K599 via infiltration.

GFP driving promoter	*N. benthamiana*			*P. tremula x alba*		
	GFP	Td-Tomato (NOS promoter)	ratio (Td-Tomato to GFP)	GFP	Td-Tomato (NOS promoter)	ratio (Td-Tomato to GFP)
DREB1	6.5 sec	4 sec	0.6	13.4 sec	6.5 sec	0.5
SWEET1	0.56 sec	6.5 sec	11.6	2 sec	10 sec	5
UBQ10	1 sec	13.4 sec	13.4	9.5 sec	13.4 sec	1.4

The illumination times were used to calculate ratios between the Td-Tomato and dGFP to normalize expression and compare the values of the different analyzed promoters. While the dehydration responsive element binding factor 1 (DREB1) promoter mediates similar expression in leaves of *N. benthamiana* (0.6) and *P. tremula x alba* (0.5), differences were detected for sugar will be eventually exported transporter 1 (SWEET1) and UBQ10 promoter (**Table 11**). For SWEET1 the expression was 11.6 times higher as expression of the NOS promoter in *N. benthamiana* and only 5 times higher in *P. tremula x alba* leaves. In case of

the UBQ10 promoter this expression difference is even higher with a ratio of 13.1 in *N. benthamiana* and 1.4 in *P. tremula x alba*.

The SWEET1 and UBQ10 promoter showed stronger expression in *N. benthamiana* compared to poplar leaves, while no difference in expression was detected for DREB1 promoter. But it cannot be ruled out that no expression difference for DREB1 was detected, since the low expression was near the detection limit of the method. In leaves of *P. tremula x alba* a higher autofluorescence was observed and therefore the sensitivity of the method is especially affected when high illumination times are used.

4.2 Establishing of a double marker system in composite poplar

To study promoter function in ECM composite *P. tremula x alba* were used in this project. During the generation of composite *P. tremula x alba* no dominant selection procedure with antibiotics can be performed as it is commonly used in stable plant transformation, since only the roots, but not the shoot would become resistant. As a consequence, transgenic and non-transgenic roots are formed by composite plants. Furthermore the transformation efficiency, defined as percentage of roots harboring the T-DNA of a binary vector in relation to the total number of formed roots, can vary batch wise. Optimization of the transformation efficiency revealed around 70 % of transgenic roots (**chapter 3.1.3 Figure 11**). Therefore, a visual selection procedure to identify roots harboring the T-DNA of a binary vector is necessary, especially for ectomycorrhizas as the formation is a time consuming process. According to RNAseq and qPCR based analysis, both genes that are analyzed in this thesis should be expressed only in ectomycorrhizas, but not in non-mycorrhized roots. As ectomycorrhizas are covered by a thick fungal mantle, detection of any fluorescence signals through the fungal mycelium is not possible. The establishing of the nuclear targeted Td-Tomato as visual selection marker in discrimination of transgenic and non-transgenic roots, that can be performed using fluorescence microscopy without taking the growing plants out of the sterile petri dish system would thus be helpful.

4.2.1 Expression of Td-Tomato in poplar roots

The expression of Td-Tomato controlled by CaMV35S, UBQ10 and NOS promoters revealed reliable signals in *N. benthamiana* leaf cells as well as roots of *P. tremula x alba*. However, the intensity pattern of these promoters differed in *N. benthamiana* leaves and poplar roots. In *N. benthamiana* the CaMV35S promoter showed the highest signal intensity followed by the NOS and the UBQ10 promoter, respectively. In contrast in poplar roots the UBQ10 promoter gave the highest signal intensity in cortical cells, while CaMV35S and NOS

promoters, enabled a similar but overall high signal intensity (**chapter 3.1.1.3 Figure 7**). The signal intensity of CaMV35S and NOS promoters was also comparable in root hairs and the root cortex, while UBQ10 showed much lower signal intensity in the root hairs compared to cortex cells. Since an equal distributed Td-Tomato signal was preferred to avoid an inconsistent fluorescent signal in different root tissues, the use of UBQ10 promoter to drive Td-Tomato expression as visual transformation control was omitted. The observation whether the UBQ10 promoter drives a higher or lower expression compared to the CaMV35S promoter is depending on the plant species and was already reported by Grefen and Collaborates 2010.

The CaMV35S promoter is described for its capability to drive gene expression in a number of different model plants (Benfey and Chua 1990). However, high expression levels enabled by the CaMV35S promoter were reported to correlate with secondary effects like gene silencing or localization artefacts (Grefen *et al.* 2010). Even if, such effects were not observed in roots of *P. tremula x alba*, localization artefacts were observed in leaf cells of *N. benthamiana*. Because no artefacts were observed using the NOS promoter in *N. benthamiana* and clear Td-Tomato signals were detected in *P. tremula x alba* roots, the NOS promoter was chosen to drive Td-Tomato expression as visual selection marker in this thesis.

4.2.2 sYFP versus dGFP to visualize promoter strength in roots of composite plants

The simultaneous expression of a nuclear targeted Td-Tomato and a nuclear targeted sYFP was feasible and both fluorescent proteins could be visualized separately. However, the fluorescence intensity of the sYFP in *P. tremula x alba* roots turned out to be rather low (**chapter 3.1.6.2 Figure 18**). Furthermore the localization of the sYFP single was not restricted to the nucleus and was also found in the cytoplasm in substantial amounts. Therefore a double GFP was tested and turned out to be the better alternative as it revealed higher signal intensities in *P. tremula x alba* roots and a distinct localization to the nucleus, due to its larger protein size.

4.2.3 Root transformation efficiency depends on the vector backbone

A general reason why the T-DNA of binary vectors is not found in roots of composite plants is that a transformation of cells with the T-DNA from the Ri-plasmid is necessary for root induction, while the T-DNA from a binary vector carrying the genes of interest is not. In the beginning of the project a pGreen based vector was used for composite poplar formation.

The reason for the use of pGreen was its small size and behavior as high copy number plasmid. However, initially only a low transformation efficiency around 30 % was obtained, making an optimization of the transformation approach necessary. Since previous work already determined the best *A. rhizogenes* strain for composite poplar formation (Neb 2017), the focus in this work was on culture conditions of *A. rhizogenes* K599. To improve fitness of *A. rhizogenes* K599 pSOUP the tetracycline concentration in the medium was altered, because of a weak growth of bacteria on CPY selection medium. While the reduction of tetracycline concentrations in culture medium improved bacterial growth, no positive effects on the root transformation efficiency was observed. Contrariwise the reduced cultivation concentration to 2.5 mg/L tetracycline further reduced the transformation efficiency (**chapter 3.1.3 Figure 10**).

Therefore other vectors (pBi121 and pCXUN), harboring a different backbone and do not need a helper plasmid to replicate in *A. rhizogenes* K599 and therefore do not need tetracycline in cultivation medium, were tested. A regular transformation efficiency of around 70 % was obtained when pCXUN was used (**chapter 3.1.3 Figure 11**), which is in the rage of a previously used vector that behaved as a low copy number plasmid in *E. coli* (Porter and Flores 1991, Neb *et al.* 2017). Gelvin (2003) showed a correlation of the copy number of the vector within *A. tumefaciens* and the transformation efficiency of *N. benthamiana*. Based on this finding it could be supposed that pCXUN is present in *A. rhizogenes* K599 in high copy numbers. However, no data regarding the copy number in *A. rhizogenes* K599 are available to validate this theory.

4.2.4 Localization of gene expression by fluorescence markers in poplar root tissues and its limitations

The tissue dependent localization of gene expression is important to suppose a potential function of a gene of interest in context of an organism or process with district localization. For example a glucose transporter could be involved in the phloem unloading processes or sugar export to an ECM fungus. By localizing gene expression within the root tissues, tissue specific function can be suggested.

For determination of expression localization complete roots can only be used to see expression in the outer layers of root tissue, rhizodermis and outer cortical cells. To determine the localization regarding all tissue layers, root cuttings need to be investigated. In case of the analysis of ectomycorrhizas, cuttings are the only option to analyze signals, since the fungal mantle covering the surface make a direct microscopic analysis impossible.

A severe problem of ectomycorrhizas is root specific autofluorescence occurring in a wide range from 500 to 650 nm, making specific signal detection difficult. The autofluorescence is especially high in cells of the vascular system and mycorrhized tissue (Neb *et al.* 2017). Additionally, the small size of cells and nuclei make the detection in the vascular system even more complicated. Targeting fluorescence proteins to a distinct cellular structure like peroxisomes or the nucleus separate the specific signal from the autofluorescence that is particular high in cell walls and allow the specific detection of even weak signals (Neb *et al.* 2017).

Root cuttings can be performed as cross or longitudinal sections. Cross sections are problematic, since root cells are prosenchymatic showing expansion in direction to the root tip. To get intact cells where nuclei are still present, cross section of 80 µm thickness need to be prepared. However, many experiments showed that even such thick cross sections were not suitable for nuclei detection. Therefore, longitudinal sections were tried and turned out to be most suitable to study nuclear detection of fluorescence proteins by confocal laser scanning microscopy analysis.

To localize gene expression also other techniques are available like *in situ* hybridization or MALDI-TOF imaging. But the preparation of cuttings is also essential for these methods and therefore not less problematic. Analysis of tissue dependent localization therefore strongly depends on the cutting quality, which should be improved in further studies. In this context, the fixation of the tissue prior to the cutting process might be helpful, to stabilize the position of the nuclei.

4.3 Investigation of ectomycorrhiza induced promoters

Promoter fragments of two ECM induced poplar genes were analyzed in this study. These genes represented two extremes in expression strength; rather low (DREB1) and rather high (SWEET1) transcriptional levels according to RNAseq (Nehls *et al.* unpublished).

The selected promoter regions were amplified from genomic DNA of the *P. tremula x tremuloides* hybrid and were analyzed in *P. tremula x alba*. The hybrid *P. tremula x alba* is more easy to handle compared to *P. tremula x tremuloides*, but ECM dependent induction of gene expression was confirmed for both hybrids with respect to *DREB1* and *SWEET1* (Nehls *et al.* unpublished). Therefore it is estimated that all regulatory factors enabling ECM specific expression are present in *P. tremula x tremuloides* as well as in *P. tremula x alba*.

Gene expression permitted by the respective promoter fragments were only analyzed by microscopic inspection of fluorescence marker in this study.

4.3.1 Expression of DREB1 in *P. tremula x alba*

The poplar gene dehydration responsive element binding factor 1 (*DREB1*) is a homolog of the transcription factor abscisic acid insensitive 4 (ABI4) in *Arabidopsis*, which was shown to be involved in regulating seed development, hormone signaling and glucose related pathways (Huijser *et al.* 2000, Söderman *et al.* 2000, Bossi *et al.* 2009, Foyer *et al.* 2012). Previous analysis in *Arabidopsis* showed that a 3 kb long promoter fragment contained all important *cis*-acting elements to perform regulatory function (Arroyo *et al.* 2003).

Therefore, a 3.2 kb long promoter fragment of *P. tremula x tremuloides* was isolated to analyze the localization of ECM induced expression of DREB1 within mycorrhized roots. Surprisingly, *DREB1* promoter fragment based dGFP expression was monitored in leaf cells of *N. benthamiana* and *P. tremula x alba* (**chapter 3.2.2**). Also in non-mycorrhized *P. tremula x alba* roots a weak fluorescence signal was observed. In *Arabidopsis* low amounts of ABI4 are regularly found and turned out to be necessary to sense inducing factors and react as positive regulator on the own expression (Bossi *et al.* 2009). However, similar weak fluorescence signals as observed in non-mycorrhized roots were also obtained in ECMs. The later observation is in clear contrast to the qPCR based gene expression in ECMs (Nehls *et al.* unpublished). This result indicates that a fragment size of 3.2 kb was not sufficient long to harbor *cis*-acting elements important for ECM control gene expression. However, gene expression determined in ECM by qPCR analysis was relatively low (Nehls *et al.* unpublished). Therefore the detection strategy might not be sensitive enough to detect ECM induction of expression of *DREB1* or elevated gene expression is observed in only very few cells and was not detected due to described technical limitations.

To analyze ECM specific gene expression, longer fragments might have to be analyzed. However, not only longer fragments in 5' direction should be taken into consideration, but also elements in the 3' region of the gene or elements within the gene itself were descripted to be involved in regulation of gene expression (Hernandez-Garcia and Finer 2014). Since no involvement of DREB1 or ABI4 in regulation of biotic interactions is reported yet, its function in ECM is only speculative. However, as ABI4 was shown to be involved in regulation of glucose related pathways in *Arabidopsis* and sugars are exposed in ECM symbiosis, sugar-based regulation by DREB1 could be supposed (Bossi *et al.* 2009, Nehls and Bodendiek 2012).

4.3.2 Localization of SWEET1 expression in ectomycorrhizas

Genes encoding sugar will be eventually exported transporters (SWEETs) were found widely spread in all kingdoms; animals, fungi, bacteria and plants. SWEET1 act as glucose transporter in *Arabidopsis* (Chen *et al.* 2010) and glucose transporting function was confirmed for a homolog from *P. trichocarpa* (Nintemann 2012). qPCR based expression analysis of *SWEET1* genes in ECMs of *P. tremula x tremuloides* and *P. tremula x alba* showed ECM specific gene induction (Nehls and Bodendiek 2012, Nehls *et al.* unpublished)

In this work a 3.4 kb long promoter fragment of *P. tremuloides* was investigated for ECM specific expression in *P. tremula x alba*. While RNAseq and qPCR based analysis revealed only barely detectable gene expression in non-mycorrhized roots (Nehls *et al.* unpublished), high dGFP expression was observed when driven by the 3.4 kb promoter fragment. Furthermore no difference in dGFP expression was observed comparing non-mycorrhized and mycorrhized roots. The observed fluorescence signal intensity was comparable to the signal intensity obtained by the *Arabidopsis* UBQ10 promoter based expression (**chapter 3.2.3.3 Figure 35**). Since the UBQ10 promoter showed very high expression rates compared to CaMV35S and NOS promoters in *P. tremula x alba* root cortex, gene expression permitted by the SWEET1 promoter fragment is rather strong in non-mycorrhized roots of *P. tremula x alba*. Similar to the situation in ectomycorrhizas, the homolog *StSWEET1b* was shown to be induced upon arbuscular mycorrhiza of *S. tuberosum.* However, in content to poplar, gene expression was also detected in non-mycorrhized tissue (Manck-Götzenberger and Requena 2016). Here, 1.3 and 2 kb long promoter fragments were sufficient to show arbuscular mycorrhiza dependent expression in *M. truncatula* and *S. tuberosum* (Manck-Götzenberger and Requena 2016, An *et al.* 2019). Since qPCR analysis of different poplar species showed an ECM specific expression, which was not observed by using the 3.4 kb promoter fragment, it can be assumed that essential *cis*-acting elements are missing in the investigated DNA fragment.

Bacterial TAL effectors are known to regulate SWEET gene expression of rice in pathogenic interaction (Chu *et al.* 2006, Yang *et al.* 2006, Chen *et al.* 2010). However, *in silico* promoter analysis could not determine TAL specific binding elements within the *PtSWEET1* promoter region (Neb 2017). In content to the result with a 3.4 kb DNA fragment from *P. tremuloides*, previous studies with a fragment of 1.3 kb in length from *P. trichocarpa* showed no expression in non-mycorrhized or mycorrhized roots (Neb 2017). Since shorter fragments revealed a potential enhancer (-1 to -200 bp) and a potential silencer (-368 to -400 bp) binding site, in that study, it was hypnotized that additional regulator binding sites

upstream of the 1.3 kb region might permit ECM dependent regulation of gene expression (Neb 2017). In content to the previous study, where only a very short *P. trichocarpa* promoter fragment revealed a strong expression of a marker gene, as the 3.4 kb fragment of *P. tremuloides* did, indicating, that the repressor binding site that was indicated in *P. trichocarpa* is missing in *P. tremuloides*. Promoter fragments of two different poplar species were analyzed in both studies. Only one SWEET1 homolog was found in the genome of *P. tremuloides*, while *P. trichocarpa* contains three SWEET1 genes, of which the coding region have high similarities and cannot be distinguished (Nehls *et al.* unpublished). Therefore it is not clear whether the same promoter region of the *P. tremuloides* SWEET1 homolog was analyzed by the previous study.

The hypothesis that the investigated promoter fragment of *P. tremuloides* does not contain all *cis*-acting elements important for native regulation of gene expression, is further supported by the strong expression of the dGFP marker induced by the 3.4 kb fragment in leaves of *N. benthamiana* and *P. tremula x alba* In qPCR based analysis no gene expression was observed in leaves (Nehls and Bodendiek 2012).

The expression of the 3.4 kb long fragment in *P. tremula x alba* ECMs was localized in cortical cells, but gene expression in the vascular system cannot be excluded (**chapter 4.2.4**). Whether this pattern is also true for ECMs is unsure as the native tissue specific expression pattern of SWEET1 was not observed with the respective promoter fragment.

4.3.3 Model of SWEET1 function in ectomycorrhiza

qPCR data reported a ECM specific induction of SWEET1 in *Populus spec.* (Nehls and Bodendiek 2012). Furthermore SWEET1 was shown to be a glucose facilitator and the localization of the protein was determined in the plasma membrane of *N. benthamiana* (Neb 2017, Nehls *et al.* unpublished). Since glucose is expected to be the main carbon source, responsible for fungal nutrition in ECM symbiosis, a key role of SWEET1 in ECM was suggested (Nehls and Bodendiek 2012). Direct involvement of MtSWEET1 in arbuscular mycorrhiza function of *M. truncatula* and the localization of MtSWEET1 to the symbiotic interface was recently published (An *et al.* 2019).

Sucrose as major photosynthetic product is transported from the leaves to the roots via the phloem (Zimmermann 1961). For active phloem loading H^+/sugar co-transporter are as well as passive loading via plasmodesmata reported. Poplar contain plasmodesmata linking mesophyll and phloem cells in high density resulting in a model for passive phloem loading (Russin and Evert 1985, Zhang *et al.* 2014). While phloem loading in poplar leaves is well

studied, relative little is known about the unloading process in the roots. Based on the estimation that the unloading is based on the same mechanism as the loading process within a plant species and a localization of MtSWEET1 at the symbiotic interface (An *et al.* 2019), it can be supposed, that PttSWEET1 is involved in sugar export to the fungal partner at the plant/fungus interface (**Figure 40**). Most likely glucose is imported from symbiotic interface by ECM fungi via monosaccharide transporters, which were also shown to be upregulated under ECM symbiosis (Nehls *et al.* 1998). Therefore, intracellular plant mediated sucrose hydrolysis must be supposed.

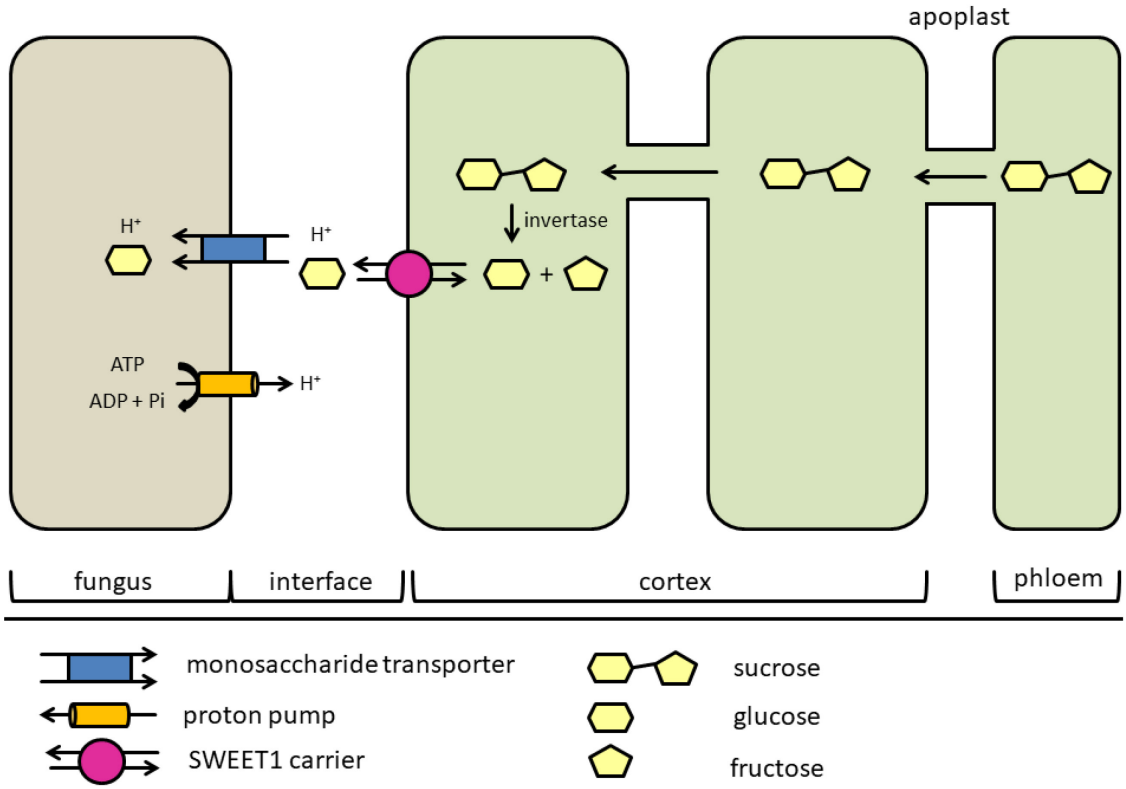

Figure 40: Hypothetic model of sugar transport to the fungal partner in ectomycorrhiza symbiosis. The photosynthetic product sucrose is transported form the leaves to the roots via the phloem vessels. Here the unloading process is shown as passive unloading via plasmodesmata. The symbiotic interface can be formed by rhizodermis and cortical cells with the fungal hyphae. This scheme shows the interface between a cortex cell and fungal hyphae. The delivered sucrose is cleaved by invertase to glucose and fructose. The glucose can be exported by the SWEET1 carrier to the symbiotic interface. The fungal cells take up glucose by proton coupled monosaccharide transporter. The proton gradient is mediated by fungal and plant proton pumps. SWEET1: sugar will be eventually exported transporter 1.

In agreement with this hypothesis is the finding that SWEET1 promoter based dGFP expression in roots and ECMs was observed in rhizodermal and cortex cells. This would fit to a potential role of SWEET1 as glucose exporter for fungal nutrition in ECM at the plant/fungus interface. However, since the expression profile of the SWEET1 promoter fragment based dGFP expression was not ECM controlled another tissue location of PttSWEET1 cannot be ruled out.

5 Outlook

The establishing of a double marker cassette within the T-DNA composed of nuclear targeted dGFP and Td-Tomato was successful. Since both fluorescence proteins are targeted to the same compartment, a visual comparison of the signal intensities of dGFP and Td-Tomato could be possible. This allows the estimation of fluorescence ratios and allows the quantification of the expression of an unknown promoter in comparison to the nopaline synthase (NOS) promoter. This technique is also solving the problem, of a sometimes strong cell wall autofluorescence of poplar roots. Variability of autofluorescence was observed in different roots, resulting in diverse background signals. Whether an exact analysis of promoter strength in comparison to the NOS promoter is possible, however needs to be further investigated. Such experiments could clarify whether the Td-Tomato can be used not only as transformation control, but as reference to compare and monitor expression intensities of other promoters, which is of particular interest for promoter truncation analysis.

To determine the detection limit of this promoter monitoring strategy, more promoters with different expression rates need to be analyzed. Prior to promoter analysis often qPCR or RNAseq are performed to identify genes differentially regulated under certain conditions. By comparing expression these values to the fluorescence intensity rates of Td-Tomato, the fluorescence protein approach can be validated. The different fluorescence values of dGFP in leaves of different species (*N. benthamiana* and *P. tremula x alba*) indicate the potential of this approach.

The investigated promoter regions of *PttDREB1* (3.2 kb) and *PttSWEET1* (3.4 kb) did not permit ectomycorrhiza (ECM) specific gene expression. Therefore longer 5' promoter regions, but also the 3' region and parts of the gene need to be tested.

The tissue-specific localization of gene expression within poplar roots and ECM is still difficult and needs improvement, by testing different fixation methods and embedding strategies. The introduction of a fixation step would also be helpful with regard to the experimental procedure, since ECM harvesting, structure documentation, embedding, cutting and microscopic analysis of the cuttings have to be performed currently at the same day. Therefore only small number of samples can be analyzed on one day and the entire procedure needs to be repeated several times. Sample fixation would overcome this problem and furthermore hopefully contribute to improved cutting quality.

6 References

Agarwal, P. and B. Jha (2010). "Transcription factors in plants and ABA dependent and independent abiotic stress signalling." Biologia Plantarum **54**(2): 201-212.

Alonso, J. M., A. N. Stepanova, R. Solano, E. Wisman, S. Ferrari, F. M. Ausubel and J. R. Ecker (2003). "Five components of the ethylene-response pathway identified in a screen for weak ethylene-insensitive mutants in Arabidopsis." Proceedings of the National Academy of Sciences **100**(5): 2992-2997.

Alpizar, E., E. Dechamp, S. Espeout, M. Royer, A.-C. Lecouls, M. Nicole, B. Bertrand, P. Lashermes and H. Etienne (2006). "Efficient production of Agrobacterium rhizogenes-transformed roots and composite plants for studying gene expression in coffee roots." Plant cell reports **25**(9): 959-967.

An, G., M. A. Costa and S.-B. Ha (1990). "Nopaline synthase promoter is wound inducible and auxin inducible." The Plant Cell **2**(3): 225-233.

An, J., T. Zeng, C. Ji, S. de Graaf, Z. Zheng, T. T. Xiao, X. Deng, S. Xiao, T. Bisseling and E. Limpens (2019). "A Medicago truncatula SWEET transporter implicated in arbuscule maintenance during arbuscular mycorrhizal symbiosis." New Phytologist **224**(1): 396-408.

Antony, G., J. Zhou, S. Huang, T. Li, B. Liu, F. White and B. Yang (2010). "Rice xa13 recessive resistance to bacterial blight is defeated by induction of the disease susceptibility gene Os-11N3." The Plant Cell: tpc. 110.078964.

Arenas-Huertero, F., A. Arroyo, L. Zhou, J. Sheen and P. León (2000). "Analysis of Arabidopsis glucose insensitive mutants, gin5 and gin6, reveals a central role of the plant hormone ABA in the regulation of plant vegetative development by sugar." Genes & Development **14**(16): 2085-2096.

Arroyo, A., F. Bossi, R. R. Finkelstein and P. León (2003). "Three genes that affect sugar sensing (abscisic acid insensitive 4, abscisic acid insensitive 5, and constitutive triple response 1) are differentially regulated by glucose in Arabidopsis." Plant Physiology **133**(1): 231-242.

Benedito, V. A., I. Torres-Jerez, J. D. Murray, A. Andriankaja, S. Allen, K. Kakar, M. Wandrey, J. Verdier, H. Zuber and T. Ott (2008). "A gene expression atlas of the model legume Medicago truncatula." The Plant Journal **55**(3): 504-513.

Benfey, P. N. and N.-H. Chua (1990). "The cauliflower mosaic virus 35S promoter: combinatorial regulation of transcription in plants." Science **250**(4983): 959-966.

Bevan, M. (1984). "Binary Agrobacterium vectors for plant transformation." Nucleic Acids Research **12**(22): 8711-8721.

Blasius, D., W. Feil, I. Kottke and F. Oberwinkler (1986). "Hartig net structure and formation in fully ensheathed ectomycorrhizas." Nordic Journal of Botany **6**(6): 837-842.

Borowicz, V. A. and S. A. Juliano (1991). "Specificity in host-fungus associations: do mutualists differ from antagonists?" Evolutionary Ecology **5**(4): 385-392.

Bossi, F., E. Cordoba, P. Dupré, M. S. Mendoza, C. S. Román and P. León (2009). "The Arabidopsis ABA-INSENSITIVE (ABI) 4 factor acts as a central transcription activator of the expression of its own gene, and for the induction of ABI5 and SBE2. 2 genes during sugar signaling." The Plant Journal **59**(3): 359-374.

Boutilier, K., R. Offringa, V. K. Sharma, H. Kieft, T. Ouellet, L. Zhang, J. Hattori, C.-M. Liu, A. A. van Lammeren and B. L. Miki (2002). "Ectopic expression of BABY BOOM triggers a conversion from vegetative to embryonic growth." The Plant Cell **14**(8): 1737-1749.

Brunner, A. M., W. H. Rottmann, L. A. Sheppard, K. Krutovskii, S. P. DiFazio, S. Leonardi and S. H. Strauss (2000). "Structure and expression of duplicate AGAMOUS orthologues in poplar." Plant Molecular Biology **44**(5): 619-634.

Bruns, T. D., M. I. Bidartondo and D. L. Taylor (2002). "Host specificity in ectomycorrhizal communities: what do the exceptions tell us?" Integrative and comparative biology **42**(2): 352-359.

Burgstaller, S., H. Bischof, T. Gensch, S. Stryeck, B. Gottschalk, J. Ramadani-Muja, E. Eroglu, R. Rost, S. Balfanz and A. Baumann (2019). "pH-Lemon, a fluorescent protein-based pH reporter for acidic compartments." ACS sensors **4**(4): 883-891.

Burley, S. and R. Roeder (1996). "Biochemistry and structural biology of transcription factor IID (TFIID)." Annual Review of Biochemistry **65**(1): 769-799.

Campbell, R. E., O. Tour, A. E. Palmer, P. A. Steinbach, G. S. Baird, D. A. Zacharias and R. Y. Tsien (2002). "A monomeric red fluorescent protein." Proceedings of the National Academy of Sciences **99**(12): 7877-7882.

Cao, P. B., S. Azar, H. SanClemente, F. Mounet, C. Dunand, G. Marque, C. Marque and C. Teulières (2015). "Genome-wide analysis of the AP2/ERF family in Eucalyptus grandis: an intriguing over-representation of stress-responsive DREB1/CBF genes." PloS one **10**(4): e0121041-e0121041.

Cevallos, M. A., R. Cervantes-Rivera and R. M. Gutiérrez-Ríos (2008). "The repABC plasmid family." Plasmid **60**(1): 19-37.

Chalfie, M., Y. Tu, G. Euskirchen, W. W. Ward and D. C. Prasher (1994). "Green fluorescent protein as a marker for gene expression." Science **263**(5148): 802-805.

Chen, L.-Q., L. S. Cheung, L. Feng, W. Tanner and W. B. Frommer (2015). "Transport of sugars." Annual Review of Biochemistry **84**.

Chen, L.-Q., B.-H. Hou, S. Lalonde, H. Takanaga, M. L. Hartung, X.-Q. Qu, W.-J. Guo, J.-G. Kim, W. Underwood and B. Chaudhuri (2010). "Sugar transporters for intercellular exchange and nutrition of pathogens." Nature **468**(7323): 527-532.

Chen, L.-Q., X.-Q. Qu, B.-H. Hou, D. Sosso, S. Osorio, A. R. Fernie and W. B. Frommer (2012). "Sucrose efflux mediated by SWEET proteins as a key step for phloem transport." Science **335**(6065): 207-211.

Chen, L. Q. (2014). "SWEET sugar transporters for phloem transport and pathogen nutrition." New Phytologist **201**(4): 1150-1155.

Chen, P.-Y., C.-K. Wang, S.-C. Soong and K.-Y. To (2003). "Complete sequence of the binary vector pBI121 and its application in cloning T-DNA insertion from transgenic plants." Molecular breeding **11**(4): 287-293.

Chen, S., P. Songkumarn, J. Liu and G.-L. Wang (2009). "A versatile zero background T-vector system for gene cloning and functional genomics." Plant Physiology **150**(3): 1111-1121.

Chen, Y., J. Yang, Z. Wang, H. Zhang, X. Mao and C. Li (2013). "Gene structures, classification, and expression models of the DREB transcription factor subfamily in Populus trichocarpa." The Scientific World Journal **2013**.

Chu, Z., B. Fu, H. Yang, C. Xu, Z. Li, A. Sanchez, Y. Park, J. Bennetzen, Q. Zhang and S. Wang (2006). "Targeting xa13, a recessive gene for bacterial blight resistance in rice." Theoretical and Applied Genetics **112**(3): 455-461.

Chuck, G., R. B. Meeley and S. Hake (1998). "The control of maize spikelet meristem fate by theAPETALA2-like gene indeterminate spikelet1." Genes & Development **12**(8): 1145-1154.

Chudakov, D. M., M. V. Matz, S. Lukyanov and K. A. Lukyanov (2010). "Fluorescent proteins and their applications in imaging living cells and tissues." Physiol Rev **90**(3): 1103-1163.

Cohn, M., R. S. Bart, M. Shybut, D. Dahlbeck, M. Gomez, R. Morbitzer, B.-H. Hou, W. B. Frommer, T. Lahaye and B. J. Staskawicz (2014). "Xanthomonas axonopodis virulence is promoted by a transcription activator-like effector–mediated induction of a SWEET sugar transporter in cassava." Molecular Plant-Microbe Interactions **27**(11): 1186-1198.

Collier, R., B. Fuchs, N. Walter, W. Kevin Lutke and C. G. Taylor (2005). "Ex vitro composite plants: an inexpensive, rapid method for root biology." The Plant Journal **43**(3): 449-457.

Cronk, Q. (2005). "Plant eco-devo: the potential of poplar as a model organism." New Phytologist **166**(1): 39-48.

Daimon, H., M. FUKAMI and M. MII (1990). "Hairy root formation in peanut by the wild type strains of Agrobacterium rhizogenes." Plant tissue culture letters **7**(1): 31-34.

Das, A. (2018). "Ectomycorrhiza development: Investigation of selected ectomycorrhiza induced poplar genes." Dissertation.

De Boever, L., D. Vansteenkiste, J. Van Acker and M. Stevens (2007). "End-use related physical and mechanical properties of selected fast-growing poplar hybrids (Populus trichocarpa× P. deltoides)." Annals of forest science **64**(6): 621-630.

De Rybel, B., W. van den Berg, A. Lokerse, C. Y. Liao, H. van Mourik, B. Moller, C. L. Peris and D. Weijers (2011). "A versatile set of ligation-independent cloning vectors for functional studies in plants." Plant Physiol **156**(3): 1292-1299.

Dickmann, D. I. (2001). "An overview of the genus Populus." Poplar culture in north America(Part A): 1e42.

Duplessis, S., P. E. Courty, D. Tagu and F. Martin (2005). "Transcript patterns associated with ectomycorrhiza development in Eucalyptus globulus and Pisolithus microcarpus." New Phytologist **165**(2): 599-611.

Ehrenberg, M. (2008). "The green fluorescent protein: discovery, expression and development." Information Department, The Royal Swedish Academy of Sciences.

Elliott, R. C., A. S. Betzner, E. Huttner, M. P. Oakes, W. Tucker, D. Gerentes, P. Perez and D. R. Smyth (1996). "AINTEGUMENTA, an APETALA2-like gene of Arabidopsis with pleiotropic roles in ovule development and floral organ growth." The Plant Cell **8**(2): 155-168.

Eom, J.-S., L.-Q. Chen, D. Sosso, B. T. Julius, I. Lin, X.-Q. Qu, D. M. Braun and W. B. Frommer (2015). "SWEETs, transporters for intracellular and intercellular sugar translocation." Current Opinion in Plant Biology **25**: 53-62.

Ferrari, S., R. Galletti, C. Denoux, G. De Lorenzo, F. M. Ausubel and J. Dewdney (2007). "Resistance to Botrytis cinerea induced in Arabidopsis by elicitors is independent of salicylic acid, ethylene, or jasmonate signaling but requires PHYTOALEXIN DEFICIENT3." Plant Physiology **144**(1): 367-379.

Fillatti, J. J., J. Sellmer, B. McCown, B. Haissig and L. Comai (1987). "Agrobacterium mediated transformation and regeneration of Populus." Molecular and General Genetics MGG **206**(2): 192-199.

Finkelstein, R. R., M. L. Wang, T. J. Lynch, S. Rao and H. M. Goodman (1998). "The Arabidopsis abscisic acid response locus ABI4 encodes an APETALA2 domain protein." The Plant Cell **10**(6): 1043-1054.

Finlay, R. and B. Söderström (1992). "Mycorrhiza and carbon flow to the soil." Mycorrhizal functioning: An integrative plant-fungal process: 134-160.

Foyer, C. H., P. I. Kerchev and R. D. Hancock (2012). "The ABA-INSENSITIVE-4 (ABI4) transcription factor links redox, hormone and sugar signaling pathways." Plant signaling & behavior **7**(2): 276-281.

Frisch, D. A., L. W. Harris-Haller, N. T. Yokubaitis, T. L. Thomas, S. H. Hardin and T. C. Hall (1995). "Complete sequence of the binary vector Bin 19." Plant Molecular Biology **27**(2): 405-409.

Fujimoto, S. Y., M. Ohta, A. Usui, H. Shinshi and M. Ohme-Takagi (2000). "Arabidopsis ethylene-responsive element binding factors act as transcriptional activators or repressors of GCC box–mediated gene expression." The Plant Cell **12**(3): 393-404.

Gelvin, S. B. (2000). "Agrobacterium and plant genes involved in T-DNA transfer and integration." Annu Rev Plant Biol **51**(1): 223-256.

Gelvin, S. B. (2003). "Agrobacterium-mediated plant transformation: the biology behind the "gene-jockeying" tool." Microbiology and molecular biology reviews **67**(1): 16-37.

Grefen, C., N. Donald, K. Hashimoto, J. Kudla, K. Schumacher and M. R. Blatt (2010). "A ubiquitin-10 promoter-based vector set for fluorescent protein tagging facilitates temporal stability and native protein distribution in transient and stable expression studies." The Plant Journal **64**(2): 355-365.

Grunze, N., M. Willmann and U. Nehls (2004). "The impact of ectomycorrhiza formation on monosaccharide transporter gene expression in poplar roots." New Phytologist **164**(1): 147-155.

Guo, W.-J., R. Nagy, H.-Y. Chen, S. Pfrunder, Y.-C. Yu, D. Santelia, W. B. Frommer and E. Martinoia (2013). "SWEET17, a facilitative transporter, mediates fructose transport across the tonoplast of Arabidopsis roots and leaves." Plant Physiology: pp. 113.232751.

Gutscher, M., A.-L. Pauleau, L. Marty, T. Brach, G. H. Wabnitz, Y. Samstag, A. J. Meyer and T. P. Dick (2008). "Real-time imaging of the intracellular glutathione redox potential." Nature methods **5**(6): 553.

Hajdukiewicz, P., Z. Svab and P. Maliga (1994). "The small, versatile pPZP family of Agrobacterium binary vectors for plant transformation." Plant Molecular Biology **25**(6): 989-994.

Hanahan, D. (1983). "Studies on transformation of Escherichia coli with plasmids." Journal of molecular biology **166**(4): 557-580.

Hansen, J., J.-E. Jørgensen, J. Stougaard and K. A. Marcker (1989). "Hairy roots—a short cut to transgenic root nodules." Plant cell reports **8**(1): 12-15.

Heim, R., A. B. Cubitt and R. Y. Tsien (1995). "Improved green fluorescence." Nature **373**(6516): 663-664.

Hellens, R. P., E. A. Edwards, N. R. Leyland, S. Bean and P. M. Mullineaux (2000). "pGreen: a versatile and flexible binary Ti vector for Agrobacterium-mediated plant transformation." Plant Molecular Biology **42**(6): 819-832.

Hernandez-Garcia, C. M. and J. J. Finer (2014). "Identification and validation of promoters and cis-acting regulatory elements." Plant Science **217**: 109-119.

Hibbett, D. S., L.-B. Gilbert and M. J. Donoghue (2000). "Evolutionary instability of ectomycorrhizal symbioses in basidiomycetes." Nature **407**(6803): 506-508.

Hirokawa, T., S. Boon-Chieng and S. Mitaku (1998). "SOSUI: classification and secondary structure prediction system for membrane proteins." Bioinformatics (Oxford, England) **14**(4): 378-379.

Hobbie, J. E. and E. A. Hobbie (2006). "15N in symbiotic fungi and plants estimates nitrogen and carbon flux rates in Arctic tundra." Ecology **87**(4): 816-822.

Högberg, M. N. and P. Högberg (2002). "Extramatrical ectomycorrhizal mycelium contributes one-third of microbial biomass and produces, together with associated roots, half the dissolved organic carbon in a forest soil." New Phytologist **154**(3): 791-795.

Holsters, M., D. De Waele, A. Depicker, E. Messens, M. Van Montagu and J. Schell (1978). "Transfection and transformation of Agrobacterium tumefaciens." Molecular and General Genetics MGG **163**(2): 181-187.

Holsters, M., B. Silva, F. Van Vliet, C. Genetello, M. De Block, P. Dhaese, A. Depicker, D. Inzé, G. Engler and R. Villarroel (1980). "The functional organization of the nopaline A. tumefaciens plasmid pTiC58." Plasmid **3**(2): 212-230.

Hooykaas, P. J. and R. A. Schilperoort (1992). "Agrobacterium and plant genetic engineering." Plant Molecular Biology **19**(1): 15-38.

Hu, B., H. Wu, W. Huang, J. Song, Y. Zhou and Y. Lin (2019). "SWEET gene family in Medicago truncatula: Genome-wide identification, expression and substrate specificity analysis." Plants **8**(9): 338.

Hu, Y. X., Y. H. Wang, X. F. Liu and J. Y. Li (2004). "Arabidopsis RAV1 is down-regulated by brassinosteroid and may act as a negative regulator during plant development." Cell research **14**(1): 8-15.

Huijser, C., A. Kortstee, J. Pego, P. Weisbeek, E. Wisman and S. Smeekens (2000). "The Arabidopsis SUCROSE UNCOUPLED-6 gene is identical to ABSCISIC ACID INSENSITIVE-4: involvement of abscisic acid in sugar responses." The Plant Journal **23**(5): 577-585.

Jefferson, R. A., T. A. Kavanagh and M. W. Bevan (1987). "GUS fusions: beta-glucuronidase as a sensitive and versatile gene fusion marker in higher plants." The EMBO journal **6**(13): 3901-3907.

Jordy, M., S. Azemar-Lorentz, A. Brun, B. Botton and J. Pargney (1998). "Cytolocalization of glycogen, starch, and other insoluble polysaccharides during ontogeny of Paxillus involutus–Betula pendula ectomycorrhizas." The New Phytologist **140**(2): 331-341.

Kanhere, A. and M. Bansal (2005). "Structural properties of promoters: similarities and differences between prokaryotes and eukaryotes." Nucleic Acids Research **33**(10): 3165-3175.

Katayama, H., A. Yamamoto, N. Mizushima, T. Yoshimori and A. Miyawaki (2007). "GFP-like proteins stably accumulate in lysosomes." Cell Structure and Function.

Kottke, I., M. Guttenberger, R. Hampp and F. Oberwinkler (1987). "An in vitro method for establishing mycorrhizae on coniferous tree seedlings." Trees **1**(3): 191-194.

Kottke, I. and F. Oberwinkler (1987). "The cellular structure of the Hartig net: coenocytic and transfer cell-like organization." Nordic Journal of Botany **7**(1): 85-95.

Koussevitzky, S., A. Nott, T. C. Mockler, F. Hong, G. Sachetto-Martins, M. Surpin, J. Lim, R. Mittler and J. Chory (2007). "Signals from chloroplasts converge to regulate nuclear gene expression." Science **316**(5825): 715-719.

Kremers, G.-J., J. Goedhart, E. B. van Munster and T. W. Gadella (2006). "Cyan and yellow super fluorescent proteins with improved brightness, protein folding, and FRET Förster radius." Biochemistry **45**(21): 6570-6580.

Kryvoruchko, I. S., S. Sinharoy, I. Torres-Jerez, D. Sosso, C. I. Pislariu, D. Guan, J. Murray, V. A. Benedito, W. B. Frommer and M. K. Udvardi (2016). "MtSWEET11, a nodule-specific sucrose transporter of Medicago truncatula." Plant Physiology **171**(1): 554-565.

Kuhn, H., H. Küster and N. Requena (2010). "Membrane steroid-binding protein 1 induced by a diffusible fungal signal is critical for mycorrhization in Medicago truncatula." New Phytologist **185**(3): 716-733.

Laby, R. J., M. S. Kincaid, D. Kim and S. I. Gibson (2000). "The Arabidopsis sugar-insensitive mutants sis4 and sis5 are defective in abscisic acid synthesis and response." The Plant Journal **23**(5): 587-596.

Lacroix, B., T. Tzfira, A. Vainstein and V. Citovsky (2006). "A case of promiscuity: Agrobacterium's endless hunt for new partners." TRENDS in Genetics **22**(1): 29-37.

Lam, E., P. N. Benfey, P. M. Gilmartin, R.-X. Fang and N.-H. Chua (1989). "Site-specific mutations alter in vitro factor binding and change promoter expression pattern in transgenic plants." Proceedings of the National Academy of Sciences **86**(20): 7890-7894.

Lata, C. and M. Prasad (2011). "Role of DREBs in regulation of abiotic stress responses in plants." J Exp Bot **62**(14): 4731-4748.

Leclercq, J., T. Szabolcs, F. Martin and P. Montoro (2015). "Development of a new pCAMBIA binary vector using Gateway® technology." Plasmid **81:** 50-54.

Lee, L.-Y. and S. B. Gelvin (2008). "T-DNA binary vectors and systems." Plant Physiology **146**(2): 325-332.

Lee, T. I. and R. A. Young (2000). "Transcription of eukaryotic protein-coding genes." Annual review of genetics **34**(1): 77-137.

Lepage, B. A., R. S. Currah, R. A. Stockey and G. W. Rothwell (1997). "Fossil ectomycorrhizae from the Middle Eocene." American journal of botany **84**(3): 410-412.

Lin, I. W., D. Sosso, L.-Q. Chen, K. Gase, S.-G. Kim, D. Kessler, P. M. Klinkenberg, M. K. Gorder, B.-H. Hou and X.-Q. Qu (2014). "Nectar secretion requires sucrose phosphate synthases and the sugar transporter SWEET9." Nature **508**(7497): 546-549.

Liu, Q., M. Kasuga, Y. Sakuma, H. Abe, S. Miura, K. Yamaguchi-Shinozaki and K. Shinozaki (1998). "Two transcription factors, DREB1 and DREB2, with an EREBP/AP2 DNA binding domain separate two cellular signal transduction pathways in drought-and low-temperature-responsive gene expression, respectively, in Arabidopsis." The Plant Cell **10**(8): 1391-1406.

Macdonald, R. and J. Westerman (1979). Fungi of south-eastern Australia, Thomas Nelson.

Manck-Götzenberger, J. and N. Requena (2016). "Arbuscular mycorrhiza Symbiosis Induces a Major Transcriptional Reprogramming of the Potato SWEET Sugar Transporter Family." Frontiers in Plant Science **7**(487).

Martin, F., J. Díez, B. Dell and C. Delaruelle (2002). "Phylogeography of the ectomycorrhizal Pisolithus species as inferred from nuclear ribosomal DNA ITS sequences." New Phytologist **153**(2): 345-357.

Martin, F., S. Duplessis, F. Ditengou, H. Lagrange, C. Voiblet and F. Lapeyrie (2001). "Developmental cross talking in the ectomycorrhizal symbiosis: signals and communication genes." New Phytologist **151**(1): 145-154.

McCullen, C. A. and A. N. Binns (2006). "Agrobacterium tumefaciens and plant cell interactions and activities required for interkingdom macromolecular transfer." Annu. Rev. Cell Dev. Biol. **22**: 101-127.

Mizoi, J., K. Shinozaki and K. Yamaguchi-Shinozaki (2012). "AP2/ERF family transcription factors in plant abiotic stress responses." Biochimica et Biophysica Acta (BBA)-Gene Regulatory Mechanisms **1819**(2): 86-96.

Molina, C. and E. Grotewold (2005). "Genome wide analysis of Arabidopsis core promoters." BMC genomics **6**(1): 25.

Morris, L. M., C. Klanke, S. Lang, F. Lim and T. Crombleholme (2010). "TdTomato and EGFP identification in histological sections: insight and alternatives." Biotechnic & Histochemistry **85**(6): 379-387.

Murashige, T. and F. Skoog (1962). "A revised medium for rapid growth and bio assays with tobacco tissue cultures." Physiologia plantarum **15**(3): 473-497.

Neb, D. (2017). "Bedeutung von SWEET-Genen für den pflanzlichen Zuckerexport in einer Ektomykorrhizasymbiose." Dissertation.

Neb, D., A. Das, A. Hintelmann and U. Nehls (2017). "Composite poplars: a novel tool for ectomycorrhizal research." Plant cell reports **36**(12): 1959-1970.

Nehls, U. (2008). "Mastering ectomycorrhizal symbiosis: the impact of carbohydrates." J Exp Bot **59**(5): 1097-1108.

Nehls, U., A. Bock and R. Hampp (2001). Differential expression of hexose-regulated fungal genes within Amanita muscaria/Populus tremula× tremuloides ectomycorrhizas. Plant Nutrition, Springer**:** 650-651.

Nehls, U. and I. Bodendiek (2012). 7 Carbohydrates Exchange Between Symbionts in Ectomycorrhizas. Fungal associations, Springer**:** 119-136.

Nehls, U., N. Grunze, M. Willmann, M. Reich and H. Küster (2007). "Sugar for my honey: Carbohydrate partitioning in ectomycorrhizal symbiosis." Phytochemistry **68**(1): 82-91.

Nehls, U., A. Hintelmann, D. Neb and D. Arpita (unpublished).

Nehls, U. and F. Martin (1995). "Changes in root gene expression in ectomycorrhiza." Biotechnology of Ectomycorrhizae: Molecular Approaches. Plenum Press, New York: 125-138.

Nehls, U., J. Wiese, M. Guttenberger and R. Hampp (1998). "Carbon allocation in ectomycorrhizas: identification and expression analysis of an Amanita muscaria monosaccharide transporter." Molecular Plant-Microbe Interactions **11**(3): 167-176.

Newell, C. A. (2000). "Plant transformation technology." Molecular biotechnology **16**(1): 53-65.

Nicolson, T. (1975). "Evolution of vesicular-arbuscular mycorrhizas." Endomycorrhizas; Proceedings of a Symposium.

Nintemann, S. (2012). "Functional analysis of mycorrhizal carbohydrate exchange in poplar." Masterthesis.

Niu, X., T. Helentjaris and N. J. Bate (2002). "Maize ABI4 binds coupling element1 in abscisic acid and sugar response genes." The Plant Cell **14**(10): 2565-2575.

Odell, J. T., F. Nagy and N.-H. Chua (1985). "Identification of DNA sequences required for activity of the cauliflower mosaic virus 35S promoter." Nature **313**(6005): 810-812.

Ohme-Takagi, M. and H. Shinshi (1995). "Ethylene-inducible DNA binding proteins that interact with an ethylene-responsive element." The Plant Cell **7**(2): 173-182.

Ow, D. W., J. R. de Wet, D. R. Helinski, S. H. HOWELL, K. V. WOOD and M. DELUCA (1986). "Transient and stable expression of the firefly luciferase gene in plant cells and transgenic plants." Science **234**(4778): 856-859.

Pakhomov, A. A. and V. I. Martynov (2008). "GFP family: structural insights into spectral tuning." Chemistry & biology **15**(8): 755-764.

Patterson, G. H., S. M. Knobel, W. D. Sharif, S. R. Kain and D. W. Piston (1997). "Use of the green fluorescent protein and its mutants in quantitative fluorescence microscopy." Biophysical journal **73**(5): 2782.

Penfield, S., Y. Li, A. D. Gilday, S. Graham and I. A. Graham (2006). "Arabidopsis ABA INSENSITIVE4 regulates lipid mobilization in the embryo and reveals repression of seed germination by the endosperm." The Plant Cell **18**(8): 1887-1899.

Peremarti, A., R. M. Twyman, S. Gómez-Galera, S. Naqvi, G. Farré, M. Sabalza, B. Miralpeix, S. Dashevskaya, D. Yuan, K. Ramessar, P. Christou, C. Zhu, L. Bassie and T. Capell (2010). "Promoter diversity in multigene transformation." Plant Molecular Biology **73**(4): 363-378.

Piatkevich, K. D. and V. V. Verkhusha (2011). "Guide to red fluorescent proteins and biosensors for flow cytometry." Methods in cell biology **102**: 431-461.

Pirozynski, K. and D. Malloch (1975). "The origin of land plants: a matter of mycotrophism." Biosystems **6**(3): 153-164.

Plett, J. M., A. Kohler, A. Khachane, K. Keniry, K. L. Plett, F. Martin and I. C. Anderson (2015). "The effect of elevated carbon dioxide on the interaction between Eucalyptus grandis and diverse isolates of Pisolithus sp. is associated with a complex shift in the root transcriptome." New Phytologist **206**(4): 1423-1436.

Porter, J. R. and H. Flores (1991). "Host range and implications of plant infection by Agrobacterium rhizogenes." Critical Reviews in Plant Sciences **10**(4): 387-421.

Riechmann, J. L. and E. M. Meyerowitz (1998). "The AP2/EREBP family of plant transcription factors." Biol Chem **379**(6): 633-646.

Robinson, R. (2010). "First record of Amanita muscaria in Western Australia." Australasian Mycologist **29**(1): 4-6.

Russin, W. A. and R. F. Evert (1985). "Studies on the leaf of Populus deltoides (Salicaceae): ultrastructure, plasmodesmatal frequency, and solute concentrations." American journal of botany **72**(8): 1232-1247.

Sakuma, Y., Q. Liu, J. G. Dubouzet, H. Abe, K. Shinozaki and K. Yamaguchi-Shinozaki (2002). "DNA-binding specificity of the ERF/AP2 domain of Arabidopsis DREBs, transcription factors involved in dehydration-and cold-inducible gene expression." Biochemical and Biophysical Research Communications **290**(3): 998-1009.

Sambrook, J., E. F. Fritsch and T. Maniatis (1989). Molecular cloning, Cold spring harbor laboratory press, New York.

Sawyer, N. A., S. M. Chambers and J. W. Cairney (2001). "Distribution and persistence of Amanita muscaria genotypes in Australian Pinus radiata plantations." Mycological Research **105**(8): 966-970.

Shahmuradov, I. A., V. V. Solovyev and A. Gammerman (2005). "Plant promoter prediction with confidence estimation." Nucleic Acids Research **33**(3): 1069-1076.

Shaner, N. C., R. E. Campbell, P. A. Steinbach, B. N. Giepmans, A. E. Palmer and R. Y. Tsien (2004). "Improved monomeric red, orange and yellow fluorescent proteins derived from Discosoma sp. red fluorescent protein." Nature biotechnology **22**(12): 1567-1572.

Shimomura, O., F. H. Johnson and Y. Saiga (1962). "Extraction, purification and properties of aequorin, a bioluminescent protein from the luminous hydromedusan, Aequorea." Journal of cellular and comparative physiology **59**(3): 223-239.

Smith, S. E. and D. J. Read (2010). Mycorrhizal symbiosis, Academic press.

Söderman, E. M., I. M. Brocard, T. J. Lynch and R. R. Finkelstein (2000). "Regulation and function of the Arabidopsis ABA-insensitive4 gene in seed and abscisic acid response signaling networks." Plant Physiology **124**(4): 1752-1765.

Sohn, K. H., S. C. Lee, H. W. Jung, J. K. Hong and B. K. Hwang (2006). "Expression and functional roles of the pepper pathogen-induced transcription factor RAV1 in bacterial disease resistance, and drought and salt stress tolerance." Plant Molecular Biology **61**(6): 897.

Streubel, J., C. Pesce, M. Hutin, R. Koebnik, J. Boch and B. Szurek (2013). "Five phylogenetically close rice SWEET genes confer TAL effector-mediated susceptibility to Xanthomonas oryzae pv. oryzae." New Phytologist **200**(3): 808-819.

Takada, S. and G. Jürgens (2007). "Transcriptional regulation of epidermal cell fate in the Arabidopsis embryo." Development **134**(6): 1141-1150.

Tedersoo, L., T. W. May and M. E. Smith (2010). "Ectomycorrhizal lifestyle in fungi: global diversity, distribution, and evolution of phylogenetic lineages." Mycorrhiza **20**(4): 217-263.

Trappe, J. M. (1962). "Fungus associates of ectotrophic mycorrhizae." The Botanical Review **28**(4): 538-606.

Tuskan, G. A., S. Difazio, S. Jansson, J. Bohlmann, I. Grigoriev, U. Hellsten, N. Putnam, S. Ralph, S. Rombauts and A. Salamov (2006). "The genome of black cottonwood, Populus trichocarpa (Torr. & Gray)." Science **313**(5793): 1596-1604.

Vaquero, C., M. Sack, F. Schuster, R. Finnern, J. Drossard, D. Schumann, A. Reimann and R. Fischer (2002). "A carcinoembryonic antigen-specific diabody produced in tobacco." The FASEB journal **16**(3): 408-410.

Vaucheret, H., C. Béclin, T. Elmayan, F. Feuerbach, C. Godon, J. B. Morel, P. Mourrain, J. C. Palauqui and S. Vernhettes (1998). "Transgene-induced gene silencing in plants." The Plant Journal **16**(6): 651-659.

Veena, V. and C. G. Taylor (2007). "Agrobacterium rhizogenes: recent developments and promising applications." In Vitro Cellular & Developmental Biology-Plant **43**(5): 383-403.

Vodnik, D. and N. Gogala (1994). "Seasonal fluctuations of photosynthesis and its pigments in 1-year mycorrhized spruce seedlings." Mycorrhiza **4**(6): 277-281.

Wainwright, M. (1993). "Oligotrophic growth of fungi: stress or natural state?" Mycology series.

Wang, X., X. Chen, Y. Liu, H. Gao, Z. Wang and G. Sun (2011). "CkDREB gene in Caragana korshinskii is involved in the regulation of stress response to multiple abiotic stresses as an AP2/EREBP transcription factor." Molecular biology reports **38**(4): 2801-2811.

Wood, D. W., J. C. Setubal, R. Kaul, D. E. Monks, J. P. Kitajima, V. K. Okura, Y. Zhou, L. Chen, G. E. Wood and N. F. Almeida (2001). "The genome of the natural genetic engineer Agrobacterium tumefaciens C58." Science **294**(5550): 2317-2323.

Wright, D., J. Scholes, D. Read and S. Rolfe (2000). "Changes in carbon allocation and expression of carbon transporter genes in Betula pendula Roth. colonized by the ectomycorrhizal fungus Paxillus involutus (Batsch) Fr." Plant, Cell & Environment **23**(1): 39-49.

Wroblewski, T., A. Tomczak and R. Michelmore (2005). "Optimization of Agrobacterium-mediated transient assays of gene expression in lettuce, tomato and Arabidopsis." Plant Biotechnology Journal **3**(2): 259-273.

Xuan, Y. H., Y. B. Hu, L.-Q. Chen, D. Sosso, D. C. Ducat, B.-H. Hou and W. B. Frommer (2013). "Functional role of oligomerization for bacterial and plant SWEET sugar transporter family." Proceedings of the National Academy of Sciences **110**(39): E3685-E3694.

Yang, B., A. Sugio and F. F. White (2006). "Os8N3 is a host disease-susceptibility gene for bacterial blight of rice." Proceedings of the National Academy of Sciences **103**(27): 10503-10508.

Yang, Y., R. Li and M. Qi (2000). "In vivo analysis of plant promoters and transcription factors by agroinfiltration of tobacco leaves." The Plant Journal **22**(6): 543-551.

Zhang, C., R. Hampp and U. Nehls (2005). "Investigation of horizontal gene transfer in poplar/Amanita muscaria ectomycorrhizas." Environmental Biosafety Research **4**(4): 235-242.

Zhang, C., L. Han, T. L. Slewinski, J. Sun, J. Zhang, Z.-Y. Wang and R. Turgeon (2014). "Symplastic phloem loading in poplar." Plant Physiology **166**(1): 306-313.

Zhao, S., A. Chen, C. Chen, C. Li, R. Xia and X. Wang (2019). "Transcriptomic analysis reveals the possible roles of sugar metabolism and export for positive mycorrhizal growth responses in soybean." Physiologia plantarum **166**(3): 712-728.

Zhu, Y., J. Nam, J. M. Humara, K. S. Mysore, L.-Y. Lee, H. Cao, L. Valentine, J. Li, A. D. Kaiser and A. L. Kopecky (2003). "Identification of Arabidopsis rat mutants." Plant Physiology **132**(2): 494-505.

Zimmermann, M. H. (1961). "Movement of organic substances in trees." Science **133**(3446): 73-79.

Zuo, Y.-C. and Q.-Z. Li (2011). "Identification of TATA and TATA-less promoters in plant genomes by integrating diversity measure, GC-Skew and DNA geometric flexibility." Genomics **97**(2): 112-120.

7 Abbreviations

Abbreviation	Meaning
aa	Amino acid
ABA	Abscisic acid
ABI4	Abscisic acid insensitive-4
AP2/EREBP	APETALA 2/ethylene responsive element binding protein
AP2/ERF	APETALA 2/ethylene responsive factor
app.	approximately
biT-DNA	Binary vector transfer DNA
CaMV35S	Cauliflower mosaic virus
cLSM	Confocal laser scanning microscope
CRT	C-repeat
dGFP	Double green fluorescence protein
DNA	Deoxyribonucleic acid
dNTP	Deoxyribonucleotide
DPE	Downstream promoter element
DRE	Dehydration-responsive element
DREB	Dehydration-responsive element-binding
ECM	Ectomycorrhiza
EGFP	Enhanced green fluorescence protein
GFP	Green fluorescent protein
Inr	Inducing region
kDa	kilo Dalton
MALDI-TOF	Matrix-assisted laser desorption/ionization-time-of-flight
MCS	Multiple cloning site
MCS	Multiple cloning site
NLS	Nuclear localization signal
NOS	Nopaline synthase
NPTII	Gene for Kanamycin resistance
OCS	Octopine synthase
ori	Origin of replication
P	Promoter

PCR	Polymerase chain reaction
pERF	Putative transcription factor
RAV	Related to ABI3/VP1
Ri	Root inducing
riT-DNA	Root inducing transfer-DNA
ri-transgenic roots	Roots containing only root inducing transfer DNA
RNAseq	Ribonucleic acid sequencing
rol-genes	Root inducing genes
Sup.	Supplemented
SWEET	Sugar will eventually be exported transporter
sYFP	Super yellow fluorescent protein
T	Terminator
TAL	Transcriptional activator like
T-DNA	Transfer-DNA
Td-Tomato	Tandem dimer tomato
TF	Transcription factor
Ti	Tumor inducing
Tm	Melting temperature
TMD	Transmembrane domain
TMD	Transmembrane domain
TSS	Transcriptional start site
UBQ10	Ubiquitin10
vir-genes	Virulence genes

8 Versicherung an Eides Statt

Ich, Jana Schnakenberg, Schönauenstraße 6, 28357 Bremen

versichere an Eides Statt durch meine Unterschrift, dass ich die vorstehende Arbeit selbständig und ohne fremde Hilfe angefertigt und alle Stellen, die ich wörtlich dem Sinne nach aus Veröffentlichungen entnommen habe, als solche kenntlich gemacht habe, mich auch keiner anderen als der angegebenen Literatur oder sonstiger Hilfsmittel bedient habe.

Ich versichere an Eides Statt, dass ich die vorgenannten Angaben nach bestem Wissen und Gewissen gemacht habe und dass die Angaben der Wahrheit entsprechen und ich nichts verschwiegen habe.

Die Strafbarkeit einer falschen eidesstattlichen Versicherung ist mir bekannt, namentlich die Strafandrohung gemäß § 156 StGB bis zu drei Jahren Freiheitsstrafe oder Geldstrafe bei vorsätzlicher Begehung der Tat bzw. gemäß § 161 Abs. 1 StGB bis zu einem Jahr Freiheitsstrafe oder Geldstrafe bei fahrlässiger Begehung.

_____ _____

Ort, Datum Unterschrift

9 Supplemented data

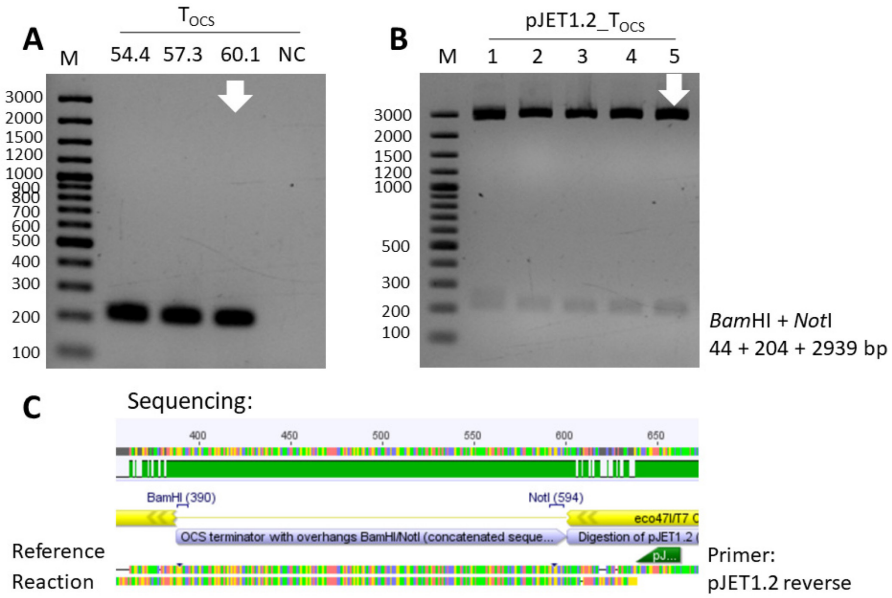

Sup. Figure 1: Cloning of the OCS termination (T_{OCS}). A) The TOCS was amplified from pBinCM_GRX1-roGFP2 with Tm from 54.4 to 60.1 °C. Negative control (NC) was a no template control. B) The PCR product of 204 bp generated with Tm 60.1 C° was used for cloning into pJET1.2 and construct was verified with *Bam*HI and *Not*I digest. 2 % agarose gels were used with 3 µL Gene Ruler 100 bp plus DNA ladder (Thermo Fisher Scientific, Waltham, Massachusetts). C) Sanger sequencing was performed by Macrogen (Amsterdam, Netherlands) and results were analyzed using geneious 6.1.8.

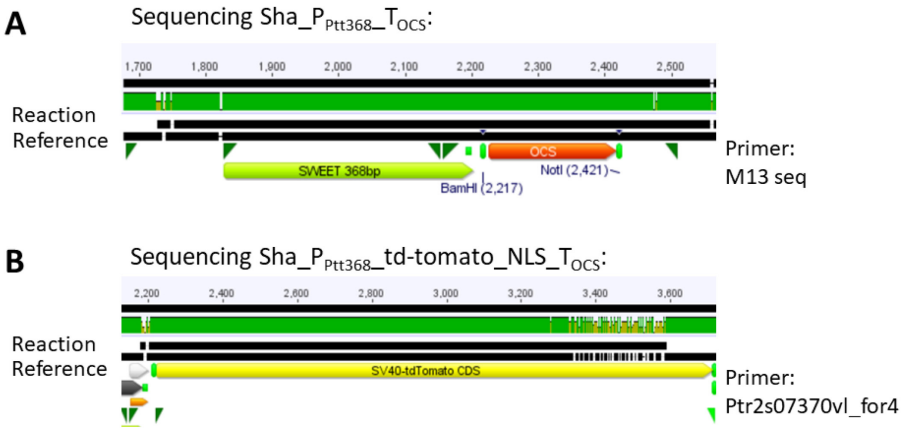

Sup. Figure 2: Sequencing of Sha_P_{Ptt368}_Tocs and Sha_P_{Ptt368}_td-tomato_NLS_Tocs. Sequencing reactions were performed by Macrogen (Amsterdam, Netherlands). The results were analyzed using geneious 6.1.8.

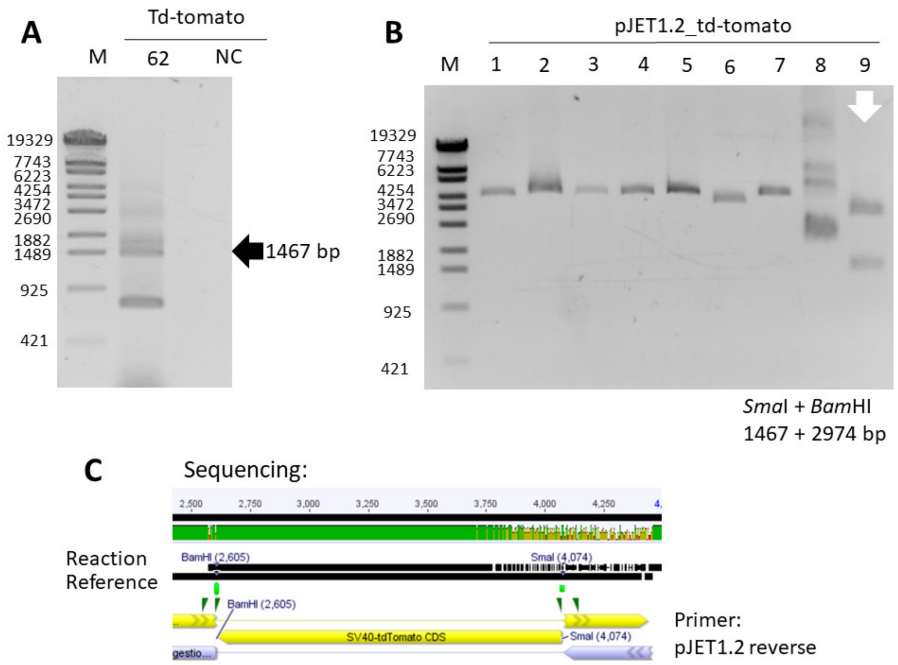

Sup. Figure 3: Cloning of the *td-tomato*_NLS. A) The *td-tomato*_NLS was amplified from pPLV11 with a Tm of 62 °C. B) The PCR product of 1467 bp was cloned into pJET1.2 and the construct was verified by *Sma*I / *Bam*HI digest. DNA fragments were separated on 1 % agarose gel and 3 µL Phage Lambda DNA/*Sty*I marker (Bioron, Ludwigshafen am Rhein, Germany). C) Sequencing of the sample was performed by Macrogen (Amsterdam, Netherlands) and results were analyzed using geneious 6.1.8.

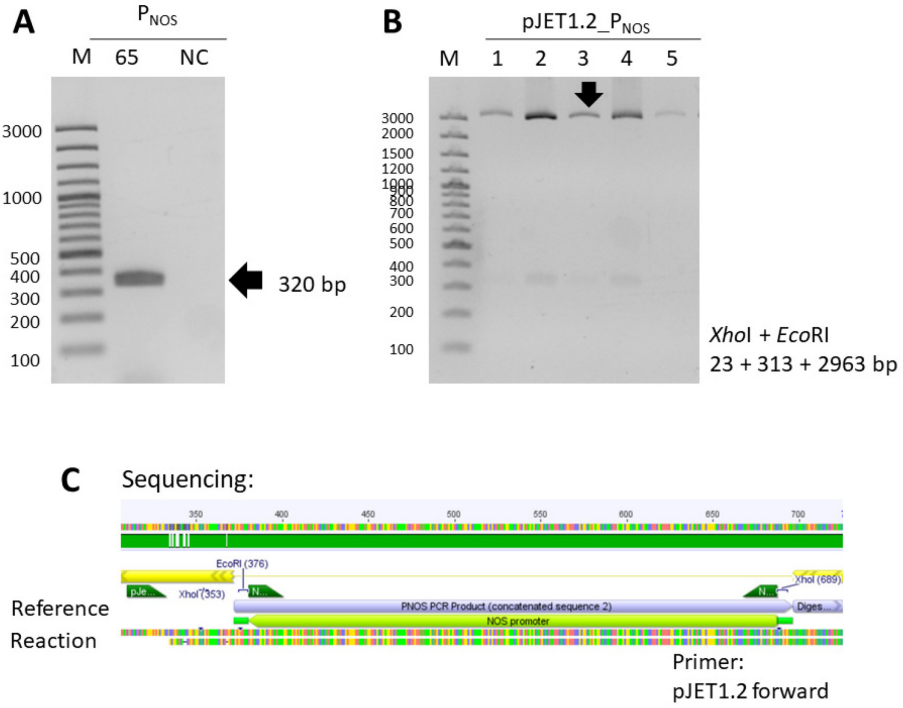

Sup. Figure 4: Cloning of the NOS promoter (P_{NOS}). A) The P_{NOS} was amplified from pBinCM_GRX1-roGFP2 with Tm 65 °C. Negative control (NC) was a no template control. B) The PCR product was cloned into pJET1.2 and the resultion construct was verified by restriction analysis with *Xho*I and *Eco*RI. 2 % agarose gels were used with 3 µL Gene Ruler 100 bp plus DNA ladder (Thermo Fisher Scientific, Waltham, Massachusetts) for separation of the DNA fragments. C) Sanger sequencing was performed by Macrogen (Amsterdam, Netherlands) and results were analyzed using geneious 6.1.8.

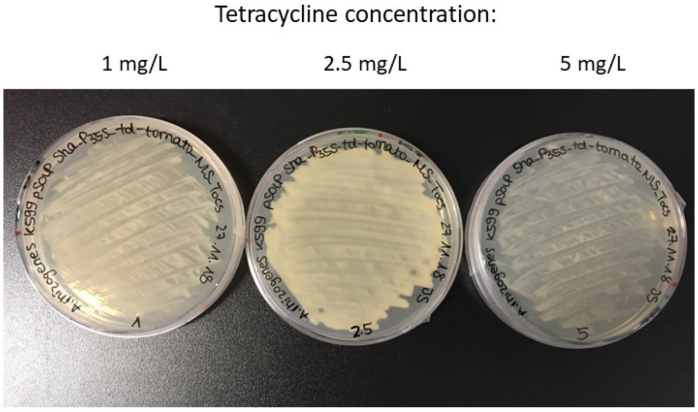

Sup. Figure 5: Growth of *A. rhizogenes* K599 pSOUP on different tetracycline concentrations. Strain A. rhizogenes K599 pSOUP pPLV_P_{35S}_td-tomato_NLS_T_{OCS} is grown on CPY agar plates containing 200 µM acetoseringone, 50 mg/L kanamycin and indicated tetracycline concentrations. Plates were incubated 72 h at 28 °C.

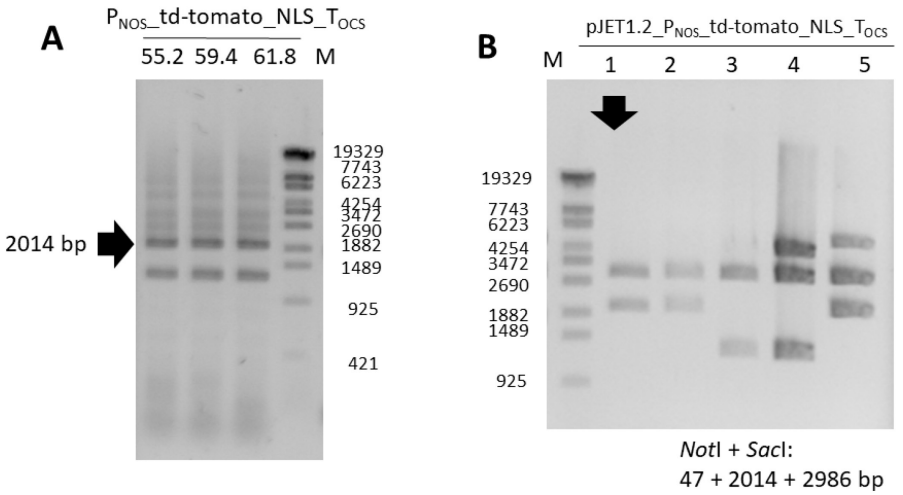
A
P_NOS_td-tomato_NLS_T_OCS
55.2 59.4 61.8 M
2014 bp
19329
7743
6223
4254
3472
2690
1882
1489
925
421
B
pJET1.2_P_NOS_td-tomato_NLS_T_OCS
M 1 2 3 4 5
19329
7743
6223
4254
3472
2690
1882
1489
925
NotI + SacI:
47 + 2014 + 2986 bp

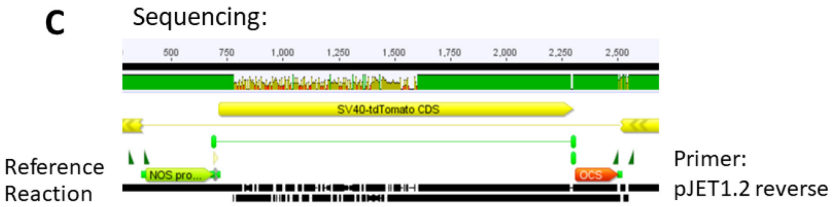
C
Sequencing:
SV40-tdTomato CDS
NOS pro...
OCS
Reference Reaction
Primer:
pJET1.2 reverse

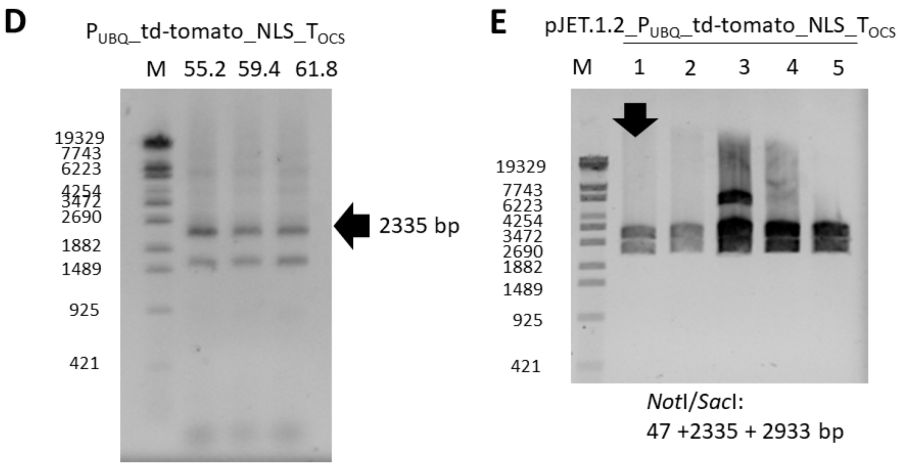
D
P_UBQ_td-tomato_NLS_T_OCS
M 55.2 59.4 61.8
19329
7743
6223
4254
3472
2690
1882
1489
925
421
2335 bp
E
pJET.1.2_P_UBQ_td-tomato_NLS_T_OCS
M 1 2 3 4 5
19329
7743
6223
4254
3472
2690
1882
1489
925
421
NotI/SacI:
47 +2335 + 2933 bp

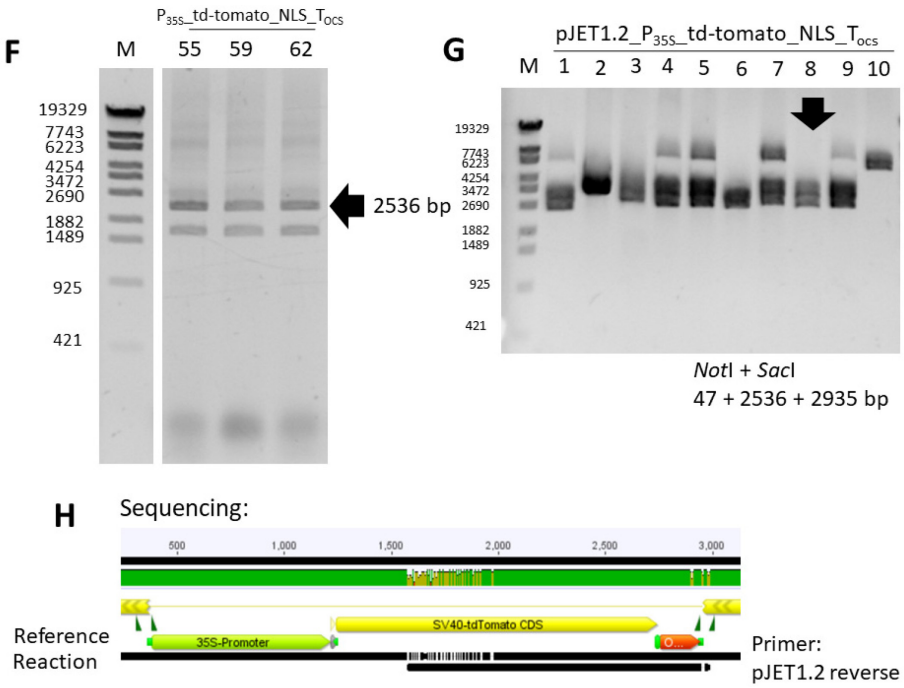

Sup. Figure 6: Verification of Td-Tomato expression cassettes in pJET1.2. A-C) Shows data for P_{NOS}_td-tomato_NLS_T_{OCS}. D-E) Shows data for P_{UBQ}_td-tomato_NLS_T_{OCS}. F-H) Shows data for P_{35S}_td-tomato_NLS_T_{OCS}. A, D, F) The designed cassettes were amplified with *Not*I / *Sac*I restriction sites from the respective pPLV constructs with indicated Tm values. B, E, G) The PCR products were cloned into the entry vector pJET1.2. The resulting constructs were analyzed by *Not*I / *Sac*I double digestion. DNA fragments were analyzed on 1 % agarose gels and 3 µL of Phage Lambda DNA/*Sty*I marker (Bioron, Ludwigshafen am Rhein, Germany). C, H) Furthermore constructs were verified by Sanger sequencing reaction performed by Macrogen (Amsterdam, Netherlands) and results were analyzed using geneious 6.1.8.

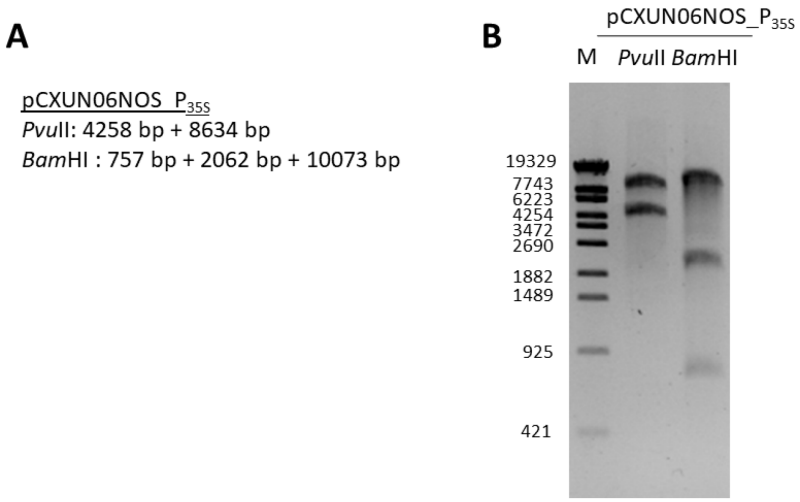

Sup. Figure 7: Restriction analysis of pCXUN06NOS_P_{35S}. A) The expected fragment sizes for *Pvu*II and *Bam*HI are shown. B) Fragments of pCXUN06NOS_P_{35S} were separated on 1 % agarose gel with 3 µL of Phage Lambda DNA/*Sty*I marker (Bioron, Ludwigshafen am Rhein, Germany) as size reference.

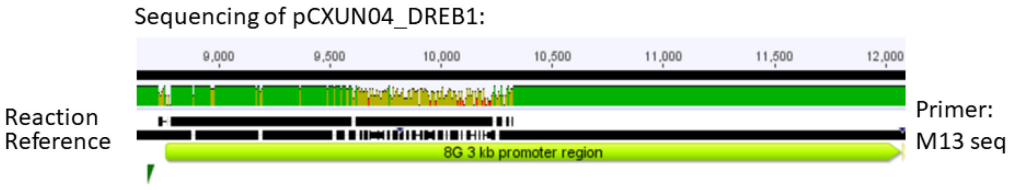

Sup. Figure 8: Sequencing results of *DREB1* promoter in pCXUN04NOS. Promoter region of *DREB1* was taken from pPLV construct of Das 2018 and sup-cloned into pCXUN04NOS. The final construct pCXUN04NOS_DREB1 was sequenced only from one site using the M13 seq primer. Sanger sequencing was performed by Macrogen (Amsterdam, Netherlands) and results were analyzed using geneious 6.1.8.

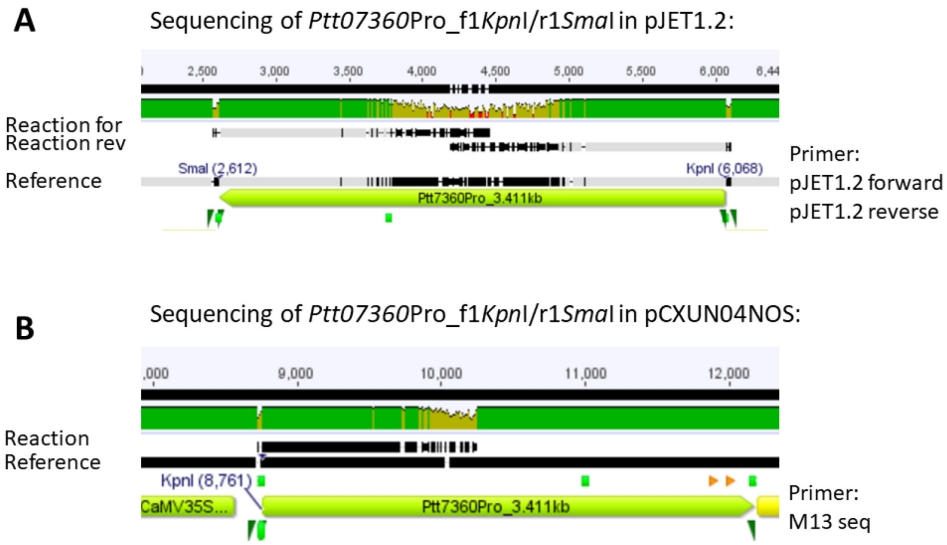

Sup. Figure 9: Sequencing results of *SWEET1* promoter in Jet1.2 and pCXUN04NOS. Promoter region of *SWEET1* was amplified from genomic DNA of *P. tremolus x tremuloides*. The amplified fragment was cloned into pJET1.2 as entry vector and pCXUN04NOS. pJET1.2_ *Ptt07360*Pro_f1*Kpn*I/r1*Sma*I was sequenced from forward and reverse site (A) and pCXUN04NOS_ *SWEET1* was sequenced only from one site (B). Sanger sequencing was performed by Macrogen (Amsterdam, Netherlands) and results were analyzed using geneious 6.1.8.